International journal
for science, technics and
innovations for the industry

MACHINES TECHNOLOGIES MATERIALS

YEAR XII Issue 9 / 2018 ISSN PRINT 1313-0226
ISSN WEB 1314-507X



Published by
Scientific technical
Union of Mechanical Engineering

MACHINES. TECHNOLOGIES. MATERIALS

INTERNATIONAL SCIENTIFIC JOURNAL

PUBLISHER

SCIENTIFIC TECHNICAL UNION OF MECHANICAL ENGINEERING "INDUSTRY 4.0"

108, Rakovski Str., 1000 Sofia, Bulgaria
tel. (+359 2) 987 72 90,
tel./fax (+359 2) 986 22 40,
office@stumejournals.com
www.stumejournals.com

ISSN PRINT 1313-0226, ISSN WEB 1314-507X, YEAR XII, ISSUE 9 / 2018

EDITOR-IN-CHIEF

Prof. D.Sc. DHC Georgi Popov,
President of Bulgarian Scientific and Technical Union of Mechanical Engineering

EDITORIAL BOARD

MEMBERS	SCIENTIFIC COMPETENCE
Prof. Dimitar Damyanov	Automatisation of production
Prof. Dimitar Karaivanov	Mechanics of machines
Prof. Dimitar Stavrev	Technologies and materials
Prof. Dimitar Yonchev	National and industrial security
Prof. Galina Nikolcheva	Machines tools and technologies
Prof. Hristo Shehtov	Automatisation of production
Prof. Idilija Bachkova	Automatisation of production
Prof. Ivan Kralov	Mechanics of machines
Prof. Ivan Parshorov	Technologies and materials
Prof. Ivan Yanchev	Machines and technologies
Prof. Ivo Malakov	Automatisation of production
Prof. Kiril Angelov	Industrial Management
Prof. Lilo Kunchev	Transport Equipment and Technology
Prof. Lubomir Dimitrov	Machines and technologies
Prof. Miho Mihov	Agricultural machinery
Prof. Miroslav Denchev	Ergonomics and design
Prof. Mladen Velev	Economics and Marketing
Prof. Nikolay Diulgerov	Technologies and materials
Prof. Ognyan Andreev	Production management
Prof. Petar Kolev	Transport Equipment and Technology
Prof. Roman Zahariev	Robotics
Prof. Sasho Guergov	Robotic systems and technology
Prof. Tsanka Dikova	Technologies and materials
Prof. Vitan Galabov	Mechanics of machines

MACHINES. TECHNOLOGIES. MATERIALS

INTERNATIONAL SCIENTIFIC JOURNAL

ISSN PRINT 1313-0226, ISSN WEB 1314-507X, YEAR XII, ISSUE 9 / 2018

EDITORIAL BOARD FOREIGN MEMBERS			
Prof. Adel Mahmoud	IQ	Prof. Marian Tolnay	SK
Prof. Ahmet Ertas	TR	Prof. Mark Easton	AU
Prof. Andonaq Londo	AL	Prof. Mart Tamre	EE
Prof. Andrei Firsov	RU	Prof. Maryam Ehteshamzade	IR
Prof. Andrzej Golabczak	PL	Prof. Michael Evan Goodsite	DK
Prof. Anita Jansone	LV	Prof. Mihail Aurel Titu	RO
Prof. Aude Billard	CH	Prof. Movlazade Vagif Zahid	AZ
Prof. Bojan Dolšak	SI	Prof. Natasa Naprstkova	CZ
Prof. Christian Marxt	LI	Prof. Oana Dodun	RO
Prof. Dale Carnegie	NZ	Prof. Oleg Sharkov	RU
Prof. Emilia Abadjieva	BG	Prof. Páll Jensson	IS
Prof. Ernest Nazarian	AM	Prof. Patrick Anderson	NL
Prof. Esam Husein	KW	Prof. Paul Heuschling	LU
Prof. Ewa Gunnarsson	SW	Prof. Pavel Kovac	RS
Prof. Filipe Samuel Silva	PT	Prof. Per Skjerpe	NO
Prof. Francisco Martinez Perez	CU	Prof. Péter Korondi	HU
Prof. Franz Haas	AT	Prof. Peter Kostal	SK
Prof. Genadii Bagliuk	UA	Prof. Juan Alberto Montano	MX
Prof. Georg Frey	DE	Prof. Raul Turmanidze	GE
Prof. Gregory Gurevich	IL	Prof. Renato Goulart	BR
Prof. Haydar Odinaev	TJ	Prof. Roumen Petrov	BE
Prof. Hiroyuki Moriyama	JP	Prof. Rubén Darío Vásquez Salazar	CO
Prof. Dr. Ilir Doci	Ko	Prof. Safet Isić	BA
Prof. Iryna Charniak	BY	Prof. Sean Leen	IE
Prof. Ivan Svarc	CZ	Prof. ShI Xiaowei	CN
Prof. Ivica Veza	HR	Prof. Shoirdzan Karimov	UZ
Prof. Jae-Young Kim	KR	Prof. Sreten Savićević	ME
Prof. Jerzy Jedzejewski	PL	Prof. Stefan Dimov	UK
Prof. Jean-Emmanuel Broquin	FR	Prof. Svetlana Gubenko	UA
Prof. Jordi Romeu Garbi	ES	Prof. Sveto Cvetkovski	MK
Prof. Jukka Tuhkuri	FI	Prof. Tamaz Megrelidze	GE
Prof. Katia Vutova	BG	Prof. Tashtanbay Sartov	KG
Prof. Kazimieras Juzėnas	LT	Prof. Teimuraz Kochadze	GE
Prof. Krasimir Marchev	USA	Prof. Thorsten Schmidt	DE
Prof. Krzysztof Rokosz	PL	Prof. Tonci Mikac	HR
Prof. Leon Kukielka	PL	Prof. Vasile Cartofeanu	MD
Prof. Mahmoud El Gammal	EG	Prof. Yasar Pancar	TR
Prof. Manolakos Dimitrios	GR	Prof. Yurij Kuznetsov	UA
Prof. Marat Ibatov	KZ	Prof. Wei Hua Ho	ZA
Prof. Marco Bocciolone	IT	Prof. Wu Kaiming	CN

C O N T E N T S

MACHINES

THE CONCEPT OF SYNTHESIS OF MOBILE ROBOTS
Prof. Dr. Kuznetsov Yu.N., Assoc. Prof. Polishchuk M.N. 344

IMPACT OF THE SPEED OF SLIDING OF FRICTION LINING ON THE TRIBOLOGICAL PARAMETERS OF FRICTION CLUTCHES OF MOTOR VEHICLES
M.Sc. Sasko Milev, PhD. Simeon Simeonov, PhD.Nikola Avramov, PhD.P.Simonovski, M.Sc.Gorgi Duskov, Eng. Elica Simeonova 348

TECHNOLOGIES

EMBEDDED MICROPROCESSORY SCADA SYSTEM FOR SUPERVISORY, CONTROL AND DATA ACQUISITION IN THE PROCESS OF PURIFICATION OF GASSES IN FERRO-NICKEL FACTORY.
Engineer Iliev Dejan., Ph.D Goce Stefanov 351

THE CONCEPT OF KNOWLEDGE MANAGEMENT IN THE REGION AS A BASIS OF ESTIMATION OF CONDITIONS OF INNOVATIVE ACTIVITY
Prof. dr. Zaborovskaia O., Babskova O. PhD Student 355

USING PATTERNS IN ARCHITECTURE OF SOFTWARE ENGINEERING
M.Sc. Ivanova Milka 358

CALCULATION OF PARAMETERS OF TENSELY DEFORMED STATE OF DISK PIEZOELEMENTS WITH SURFACES PARTIALLY COVERED BY ELECTRODES
Dr. Bazilo C. PhD. 362

KNOWLEDGE, CREATIVITY AND INNOVATION IN KNOWLEDGE SOCIETY FORMATION
Zhavoronkova G., Doctor of Economic Sciences, Professor, Zavalko K. Doctor of Pedagogical Sciences, Professor,
Zhavoronkov V., PhD (Economics), Associate Professor 367

MATERIALS

SUPERPARAMAGNETIC PROPERTIES IN LANTHANUM STRONTIUM MANGANITES DOPED WITH ZINC
Prof. Eremina R. Dr., Yatsyk I. PhD., Seidov Z. PhD., Badelin A. PhD. Prof. Krug von Nidda H.-A. Dr. 371

CALCULATION OF TEMPERATURE DEPENDENCES OF THERMAL EFFECTS AT COOLING OF METAL ALLOYS
Ass. Prof., Dr. Eng. Khristenko V., Omelko L., Ass. Prof., Dr. Eng. Donii O. 374

RULE-BASED MAMDANI-TYPE FUZZY MODELING OF PERFORMANCE OF HYDROXY (HHO) DRY CELL WITH 12x12 PLATE COMBINATION
Assist. Prof. Dr..Ali Serhat E., Assist. Prof. Dr. Yusuf Y., Mech. Engineer..Burak Buğra Ç., Mech. Engineer ..Taylan P.,
Assoc.. Prof. Dr..Kevser D. 378

ADHESION AND PHYSICO-MECHANICAL CHARACTERISTICS OF COATINGS OF CHROMIUM CARBONITRIDE, GENERATED ON STEEL SUBSTRATES
Phd Chekan N.M., Ass.prof, dr.Eng. Auchynnikau Y.V., Phd Akula I.P., Ass.prof. Phd Eisymont Y.I., Pinchuk T.I. 382

THE CONCEPT OF SYNTHESIS OF MOBILE ROBOTS

КОНЦЕПЦИЯ СИНТЕЗА МОБИЛЬНЫХ РОБОТОВ

Prof. Dr. Kuznetsov Yu.N.[1], Assoc. Prof. Polishchuk M.N.[2]
Professor of the Department of Machine Tool Design and Machines[1], Associate Professor at the Department of Technical Cybernetics[2] – National Technical University of Ukraine "Igor Sikorsky Kyiv Polytechnic Institute", Kyiv, Ukraine

Abstract: The paper proposes three basic principles for the synthesis of mobile robots: the accumulation and conversion of energy, the integration of motion drives and the use of a generator of reactive pneumatic traction. These technical solutions allow robots to navigate on surfaces of arbitrary orientation in different coordinate systems. The implementation of these principles contributes to reducing the total power of the drives and increasing the reliability of holding robots on the surface of arbitrary orientation in the technological space. The results of mathematical modelling of constructive and technological parameters of mobile robots are described.
KEYWORDS: *MOBILE ROBOTS, WALKING MECHANISMS, ROBOTS OF VERTICAL MOVEMENT, CLIMBING ROBOTS*

1. Introduction

The evolution of technical systems in the field of engineering science, as a rule, led to the emergence of new means of production. In the twentieth century scientific and technical thought created sufficiently reliable means of overcoming the gravitational force in the form of flying and reactive equipment. These funds are used as a reliable transport. However, up to the present time there are no industrial samples of equipment for performing contact technological operations while simultaneously overcoming the forces of gravity.

Mobile robots of arbitrary orientation are known in publications as robots of vertical movement or in international publications – under the term Climber Robot, are a new modification of mobile robots. These robots are equipped with means of fixation on the surface of arbitrary orientation relative to the horizon of the technological space. The creation of this kind of robotics is at the initial stage and is dictated by the need to perform technological operations in such areas of industrial activity as monitoring of industrial facilities, installation and dismantling of building structures, repair and prevention of their components. In the context of the fourth industrial revolution, "Industry 4.0" [1], with the focus on the use of robotic systems, information and communication tools, and the use of these robots becomes especially urgent in the extreme conditions of man-made disasters that are dangerous and even unacceptable for human presence.

2. Prerequisites and means for solving the problem

The problem of creating this type of robots is the lack of a methodology for synthesizing the robot subsystems that compensate or overcome the gravitational load in order to ensure that the robot is held on an arbitrarily oriented surface during the execution of technological operations. Therefore, the purpose of this research is to develop principles for the synthesis of mobile robots and the introduction of modern computer modeling tools for the transition to the design and manufacture of prototypes of mobile robots.

Theoretical and experimental studies on the creation of robots of arbitrary orientation in the technological space began in the last decade of the twentieth century in the countries of Western Europe, Japan, the United States, Korea, China and Russia. To date, there are mainly experimental samples of such robots.

Mobile works [2-5] are equipped with devices to fix the robot on surfaces of arbitrary orientation, and in studies [6, 7] hybrid drives are proposed that can improve the energy efficiency of mobile robots. Technical solutions [8-11] allow the robot to move on surfaces oriented at different angles to the horizon, but only in 2D space, that is, in a plane. In the general case, the variations of the constructions of the above-mentioned robots restrict their movement only in the Cartesian coordinate system.

Unlike the aforementioned technical solutions, the robot model [12] allows servicing objects in the cylindrical coordinate system, in particular, objects such as trees, but with a soft porous surface for the movement of the robot, which limits the technological capabilities of mobile robots. At a time when there are objects facilities that are also close to the cylindrical coordinate system, for example, electric grid posts, columns, pipes of thermal power plants and the like. In addition, the mobile robot should also work in a system of angular coordinates, which is typical for humans. The development of systems for connecting the robot to the surface of motion is a technical solution [13], which uses adhesion technology. However, current implementations of this technology are characterized by an extremely low speed of movement of the robot due to the effect of slow adhesion. This property still prevents the industrial use of adhesion as a method of fixing the robot to a surface of arbitrary orientation.

Thus, the problem of synthesizing mobile robots capable of performing technological operations in a space of arbitrary orientation is topical.

3. Solution of the problem under consideration

In contrast to the above, the concept of improving robots of arbitrary orientation based on three fundamental principles of the synthesis of mobile robot designs is proposed:

1. Accumulation of potential energy at each previous step of the robot's movement and subsequent conversion to kinetic energy at the next step of the movement.

2. Integration of drives of longitudinal, vertical displacement, and also drives of change of orientation of the robot according to the set route.

3. The use of traction generators (aerodynamic lift forces) as a means of counteracting the gravitational force to increase the technological load while simultaneously reducing the power of clutch drives and the movement of robots.

As technical means of implementing these principles of synthesis, consider the corresponding models of robots of arbitrary orientation. In Fig. 1 shows a mobile robot [14] realizing the first of the above mentioned principles, namely having the ability to accumulate potential energy at each previous step and converting it into kinetic energy of motion at each subsequent step of displacement.

On the robot body 1 are mounted rotary pneumatic actuators 2 connected through a gear train 10 with running mechanisms 3. When the elastic members 4 are compressed due to the rotation of the legs of the robot, the potential energy is accumulated during the first half of the step, and in the second half of the step, these elements convert the potential compression energy in the kinetic energy of the robot's motion [15, 16]. To implement a plane-parallel motion along the vertical, the robot is equipped with parallelograms 5. The latter connect pedipulators with vacuum grippers 6 that hold the robot on a surface of arbitrary orientation. Also, the robot is equipped with a control unit 7 and a power supply module 8. To overcome obstacles on the moving surface, the robot is additionally equipped with rolling bearings 9.

Volumes of the potential and kinetic energy of the robot motion at different stages of displacement can be determined using Lagrangian equations of the second kind.

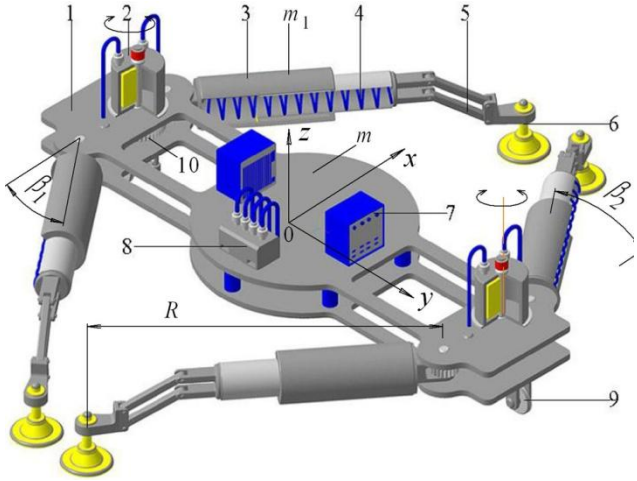


Fig.1. *The robot model of arbitrary orientation with the accumulation and transformation of energy*

The kinetic energy T_1 of the robot's foot free from adhesion to the moving surface will be

$$T_1 = \frac{1}{2}\int (V_{x1}^2 + V_{y1}^2)dm\,, \qquad (1)$$

where: V_{x1}, V_{y1} – the velocity projections on the coordinate axis 0xyz; m – the mass of the robot.

Pedipulator of the robot, whose grips are engaged with the surface, performs a rotary motion with angular velocity $\dot{\beta}_1$. The expression for the kinetic energy of a supporting leg of mass m_1 and radius R can be obtained from expression (1) after integrating it, substituting the velocity of the translational motion of the robot $V = 0$ and the angular velocities of the pedipulators $\dot{\beta}_2 = \dot{\beta}_1$:

$$T_2 = \frac{m_1 R^2}{6}(\dot{\beta}_1)^2\ . \qquad (2)$$

Thus, the movement of the robot at each second half of the cycle occurs due to the energy accumulated at each first half of the travel step. This allows 40% ... 45% to reduce energy costs for the movement of the robot and to direct the resulting energy reserve for the execution of technological operations.

Pedipulators work with elastic elements (Fig.1, pos.4), which perform the function of accumulation of potential energy during the first half of the cycle of displacement.

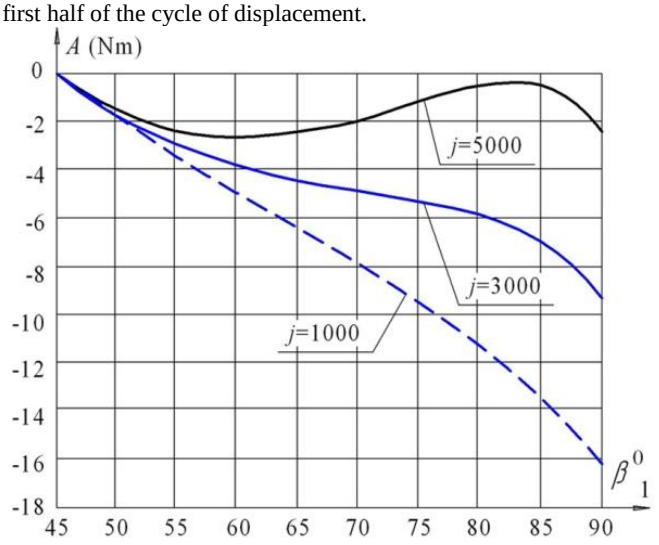


Fig.2. *The effect of the elastic element j (N/m) on the work performed in the step $\beta_1 > 45^o$ of the robot movement*

The main characteristic of elastic elements is their rigidity *j* – parameter, which determines the force of compression of these elements, and hence the value of the accumulated potential energy in the first half of the step of the pedipulator. In Fig. 2 shows the dependence of the variation of work "A" on the stiffness of the elastic element ***j*** (N/m) and the forces of weight in the second stage $\beta_{1,2} > 45^o$ of displacement, that is, during the transformation of the potential energy into the kinetic energy of the robot's motion. At the second stage of displacement $45^0 \le \beta_{1,2} \le 90^0$ drive the of pedipulator is turned off to save energy resources of the robot, and it moves only due to kinetic energy. Analysis of these graphs shows that to increase the kinetic energy of the robot movement, it is advisable to increase the rigidity, despite the fact that in this case the counteraction to the drive increases in the first half of the step, that is, the efficiency of the drive decreases. However, this negative manifestation can be compensated for by an increase in the transmission ratio (see item 10, figure 1) of pedipulators.

The second principle, as noted above, involves the integration of displacement drives [17] with the aim of reducing them, and hence of reducing the mass of the robot. It is known that in the Cartesian space we have six degrees of freedom – three translational movements and three rotational, each of which according to the classical solutions corresponds to an autonomous drive. The method of Fig. 3 – technical implementation of this principle eliminates the need for drives for each of the coordinate axes. To do this, the robot is equipped with flexible running mechanisms 2 mounted on the body 1. Each pair of legs of the robot through the transmissions 3 is provided with electric drives 4. The grippers 5 keep the robot on the surface moving, and the rotary actuators 6 change the position of the grippers relative to the displacement surface. The robot platform has a power supply unit 7, a hydraulic or pneumatic valve unit 8 and a gas or liquid pressure generator and a controller 9 for controlling the robot. Due to the fact that each foot of the robot is made in the form of a compressed set of hemispherical rings inside which corrugated pipes are placed under different pressures, the robot has the ability to work in different coordinate systems: rectangular Cartesian, spherical and cylindrical without additional drives on each axis of coordinates.

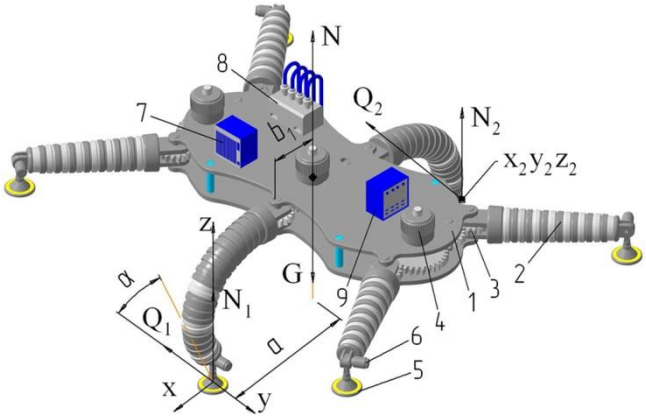


Fig.3. *Model of the robot with flexible pedipulators*

In each leg of the robot there are four corrugated pipes. Two pipelines with pressure p_1 p_2 are placed in a vertical plane and two other pipelines – in a horizontal plane with pressure p_3 and p_4. Due to the action of these pressures, forces appear that, while bending the robot's leg, orient the robot in the technological space:

$$F_1 = p_1\frac{\pi d^2}{4}; F_2 = p_2\frac{\pi d^2}{4}; F_3 = p_3\frac{\pi d^2}{4}; F_4 = p_4\frac{\pi d^2}{4}, \qquad (3)$$

where *d* – the internal diameter of the corrugated tubes. Since the axes of the pipelines are offset from the pedipulator axis by the eccentricity e, there are moments M_1 and M_2 that flex the robot's leg:

$$M_1 = \frac{\pi d^2}{4}(p_1 - p_2)e;\ M_2 = \frac{\pi d^2}{4}(p_3 - p_4)e \qquad (4)$$

where: *e* – eccentricity of placement of corrugated pipelines in the plane of the coordinate system.

To develop a robot, it is necessary to establish a connection between the forces of adhesion of its legs to the displacement surface and the permissible technological load to ensure the

reliability of its industrial operation. Having formulated the system of equilibrium equations on the basis of the Herman–Euler–D`Alambert principle (here we omit the record for brevity), we find the corresponding reaction forces $N_{1,2}$ and the frictional forces $Q_{1,2}$ by the robot foot to the displacement surface and then compare them with the technological load N in depending on the angle α of the robot inclination to the horizon.

The reaction forces of N_2 and the frictional forces Q_{2y} of the robot supports with the displacement surface are determined as follows (the designation of the parameters, see Fig.3):

$$N_2 = Q_2 + a_3 G - b_3 N; \quad Q_{2y} = d_3 G + h_3 N, \tag{5}$$

where for the compactness of the incoming values of variables is denoted:

$$a_3 = d_1 b_2 - b_1 d_2 / \Delta;\ b_3 = b_2 h_1 + b_1 h_2 / \Delta;\ d_1 = y_c \cos\alpha - z_c \sin\alpha;$$
$$b_2 = x_2 \cos(\varphi - \alpha);\ d_3 = d_2 a_1 - d_1 a_2 / \Delta;\ h_3 = h_2 a_1 + a_2 h / \Delta;$$
$$a_1 = y_2 \cos(\varphi - \alpha) + z_2 \sin(\varphi - \alpha);\ a_2 = -x_2 \sin(\varphi - \alpha);$$
$$d_2 = x_c \sin\alpha;\ b_1 = y_2 \sin(\varphi - \alpha) - z_2 \cos(\varphi - \alpha);$$
$$h_1 = y_c \cos\psi + z_c \sin\psi;\ h_2 = x_c \sin\psi;\ \Delta = a_1 b_2 - b_1 a_2;$$

x_2, y_2, z_2 – coordinates of the contact point of the second leg of the robot with the displacement surface; x_c, y_c, z_c are the coordinates of the center of gravity of the robot; α, φ – angles of inclination to the horizon of surfaces on which the robot's legs rest; ψ is the angle of inclination of the central axis of the robot passing through its center of gravity G (see Fig.3). Then, from the same system of equilibrium equations, we find the remaining unknown reactions N_1 and the frictional forces Q_{1y}:

$$N_1 = Q_1 + G a_4 - N h_4; \quad Q_{1y} = G h_5 + N h_6, \tag{6}$$

where also for the compactness of writing variables is defined:

$$a_4 = \cos\alpha - a_3 \cos(\varphi - \alpha) - d_3 \sin(\varphi - \alpha);$$
$$h_4 = \cos\psi - b_3 \cos(\varphi - \alpha) + h_3 \sin(\varphi - \alpha);$$
$$h_5 = \sin\alpha - d_3 \cos(\varphi - \alpha) + a_3 \sin(\varphi - \alpha);$$
$$h_6 = \sin\psi - h_3 \cos(\varphi - \alpha) - b_3 \sin(\varphi - \alpha).$$

For the stability of the robot, the frictional forces of each of its legs must not exceed the boundary values:

$$Q_{1y} < \mu N_1; \quad Q_{2y} < \mu N_2; \quad N_1 > 0;\ N_2 > 0, \tag{7}$$

where μ – the coefficient of friction of the grip of the robot's leg with the surface along which the robot moves. Substituting in expression (7) the expressions above the found reactions of forces (5) and (6), we find limitations for the technological load of the robot taking into account the forces acting on it:

$$N_1 > 0 \Rightarrow N < \frac{Q_1 + G a_4}{h_4};\ N_2 > 0 \Rightarrow N < \frac{Q_2 + G a_3}{b_3};$$
$$N < \frac{\mu Q_2 + G(\mu a_3 - d_3)}{h_3 + \mu b_3};\ N < \frac{\mu Q_1 + G(\mu a_4 - h_5)}{h_6 + \mu h_4}. \tag{8}$$

Among the values of the reaction N of the technological load calculated in accordance with conditions (8), we choose the largest, which simultaneously satisfies all inequalities, which allows to determine the maximum technological load of the robot, for example, for drilling, rivets, dowels, etc. technological operations.

As a result of the simulation, the limiting values of the technological load are obtained (Fig.4): curves 1 and 2, respectively, determine the separation states from the displacement surface of the first and second legs of the robot, and curves 3 and 4 are the beginning of slippage of the said robot legs, respectively.

The robot of arbitrary orientation can be on such surfaces as a floor, a wall or a ceiling. Accordingly, if the robot is on the floor, then in the above dependences it is necessary to substitute the value $\varphi = 0^o$, $\alpha = 0^o$; if on a vertical wall, then $\varphi = 90^o$, $\alpha = 90^o$ and if on the ceiling, then $\varphi = 180^o$, $\alpha = 180^o$ and so on.

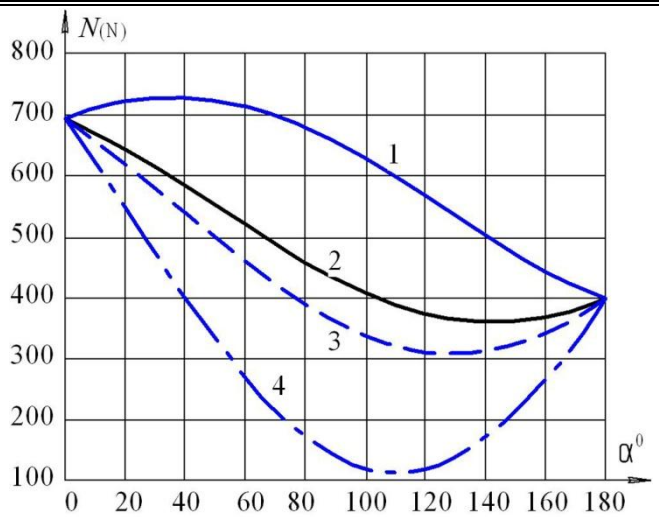


Fig.4. *Graphs of the boundary values of the technological force N of the robot as a function of the angle α of the inclination to the horizon*

And, finally, the third principle – the use of traction generators as a means of counteracting the gravitational force is realized by the robot [18], shown in Fig. 5. Like the previous one, it also has flexible pedipulators 2, grippers 3, gear 4 and electric drives 5 on the body 1. The main difference of this robot is the installation in the center of its masses suspension Cardan 6 with three degrees of freedom and a pneumatic generator of traction 7. The location of the thrust generator on the Cardan suspension allows the thrust generator to maintain the coincidence of the lines of action of opposing forces: the rise of G_1 and the gravitational force G, regardless of the position of the robot in the XYZ space. This principle allows us to differentiate the approach to regulating the lifting force of the robot, depending on its orientation in space.

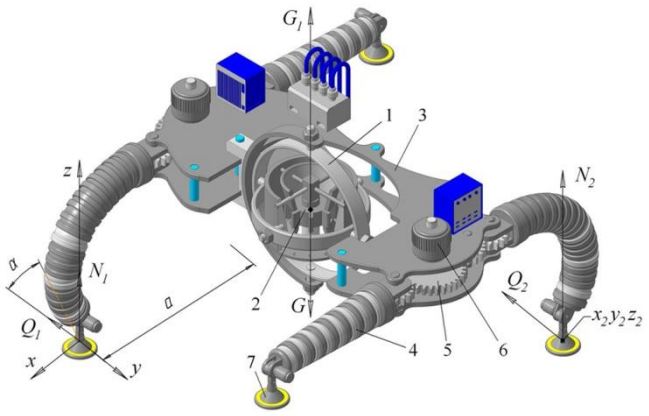


Fig.5. *Mobile robot with pneumatic generator of aerodynamic lift*

Similarly to the previous case, from the system of equilibrium equations of the robot determine the forces of normal reactions N_i of the legs of the robot and the corresponding frictional forces Q_i (see Fig.5):

$$N_2 = b_{12}(G - G_1), \tag{9}$$

where: G – the weight of the robot; G_1 – traction force; α - angle of inclination of the plane of movement of the robot to the horizon $b_{12} = \cos\alpha\, y_c - \sin\alpha\, z_c / 2y_2$; y_c, z_c – coordinates of the center of gravity of the robot; y2 – coordinate of contact with the moving surface of the second part of the robot.

The frictional force Q_{1y} and the normal reaction N_1 are determined as

$$Q_{1y} = (G - G_1)(-\mu b_{12} + \frac{1}{2}\sin\alpha);\ N_1 = (G - G_1)(-b_{12} + \frac{1}{2}\cos\alpha).$$

As can be seen from the graphs of Fig. 6 with positive reactions N_1 and N_2 with the angle of inclination of the displacement surface $\alpha \le 54^0$, the weight of the robot increases the

technological load. This means that the inclusion of the jet engine is more suitable for the values of the angle of inclination of the robot to the horizon at $\alpha \geq 54^0$. Of course, the critical angle of inclination depends on the other centrifugal characteristics of the robot. However, using the generator of aerodynamic forces ensures reliable retention of the robot on surfaces of arbitrary orientation with any structural and technological parameters of the robots. To calculate the critical angle of inclination to the horizon and, accordingly, to regulate the force of the reactive thrust, that is, the aerodynamic force of the pneumatic generator, it is necessary to take into account other characteristics of the robot.

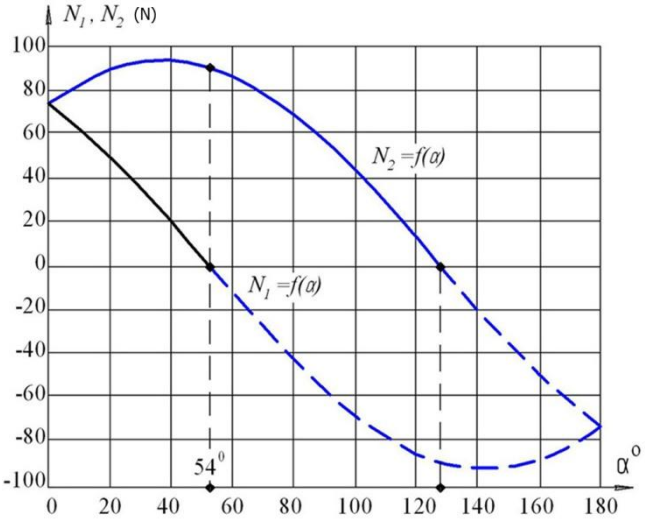


Fig.6. *Graphs of the dependence of the normal reactions N_1, N_2 of the robot on the angle α of its inclination to the horizon*

4. Results and discussion

The creation of means for accumulating the potential energy of the drives, and then transforming them into kinetic energy of the robot's motion, and also the integration of drives for longitudinal and vertical movement, can significantly reduce the total power that is of fundamental importance for mobile robots of arbitrary orientation in space, since reduces the gravitational load.

The use of a pneumatic motor as a means of counteracting the gravitational force makes it possible, when adjusting the traction force, depending on the angle of the robot's inclination to the horizon, to increase the reliability of holding the robot on the surface of an arbitrary orientation, which in turn makes it possible to reduce the power of the clutch actuators of the robot with the surface.

A fundamentally new realization of the legs of mobile robots in the form of a set of hemispherical rings and corrugated pipelines at different gas or liquid pressures makes it possible to achieve an arbitrary orientation of the mobile robot in different working spaces: a rectangular Cartesian, spherical and cylindrical coordinate system. This effect ensures the expansion of technological capabilities of mobile robots of arbitrary orientation in the technological space.

5. Conclusion

The concept of the synthesis of mobile robots is based on three principles of constructing their designs. These principles can be used autonomously and in combination, depending on the technological purpose of the robot and its profitability, which, in turn, is determined by the area of industrial operation. The proposed approach to the synthesis of mobile robots can reduce the weight of structures by reducing the total number of drives. This increases the energy resource for improving the efficiency of both transport and technological operations performed by the robot in various areas of industry. The next stage of the research is the experimental approbation of this concept of the synthesis of mobile robots.

References

1. Kuznetsov Yu.N. Challenges of the fourth industrial revolution "Industry 4.0" in front of scientists of Ukraine. – Vestnik KhNTU, Kherson. 2 (61), 2017, p. 67-75.

2. Raju D.D. Developments in wall climbing robots: a review.– International journal of engineering research and general science. 2 (3), 2014, p. 37 (Raju D.D., Jaju S.B).

3. Gradetskii V.G. Controlled movement of mobile robots over arbitrarily oriented surfaces in space. – Moscow: Nauka, 2001, 360p. (Gradetskii V.G.,Veshnikov V.B., Kalinichenko S.V.).

4. Chernous'ko F.L. Mobile robots: research, development, prospects. http://www.ras.ru/news/shownews.aspx?id=f5c75bcf-2fa5-40e6-b067-4492c5ab22&print=1. Last accessed 20 iyulya 2018. (Chernous'ko F.L. Bolotnik N.N. and Gradetskii V.G.)

5. Polishchuk M.N. Modernization of the vacuum gripper of the mobile walking robot.– Mechanics and Advanced Technologies, vol. 2 (80), 2017, p. 59–64.

6. Kuznjecov Ju.M. Robotic systems complexes of pharmaceutical and biotechnological productions. Kiev, GhNOZIS, 2012, 335 p. (Kuznjecov Ju.M., Shybecjkyj V.Ju.).

7. Pavlenko I.I.. Industrial work: calculation basics and design. KNTU. Kirovoghrad, 2007, 420 p.

8. Sinev A.V. The vehicle for moving along the surfaces arbitrarily oriented in space. State Register of Patents of Russia, Pat. № 2262461, 2005, 6 p. (Gradetskii V.G., Kravchuk L.N., Popovich V.A., Lebedenko I.B., Kochetov O.S.).

9. Baranov V. E. Vehicle for moving on inclined and vertical surfaces. State Register of Patents of Russia Pat. № 2267434, 2006, 8 p.(Baranov V. E., Vagin S.G., Zatsepin V. A., Kokorin A. G.)

10. Chashchukhin V.G. Investigation of the movement parameters of a robot with a sliding seal.–Vestnik Nizhegorodskogo universiteta im. N.I. Lobachevskogo, vol 4 (2), 2011, pp. 347–349.

11. Shamim Hasan. Smartphone Controlled Spy Robot with Video Transmission and Object Collector, International Journal of Engineering and Manufacturing (IJEM), Vol.7, No.6, 2017, p.50-58. (Shamim Hasan, Khalid Hossain Jewel, Niaz Mostakim, Nabil Hossain Bhuiyan, M.K. Rahman, Sheikh Dobir Hossain and Khalid Hossain).

12. Tin Lun Lam. Tree Climbing Robot: Design, Kinematics and Motion Planning. New York: Springer Heidelberg. 2012, p. 37–46. (Tin Lun Lam, Yangsheng Xu).

13. Yehya M. Unipolar Electroadhesion Pad Technology for Adhesion Mechanism of Wall Climbing Robot. – International Journal of Robotics and Mechatronics, vol. 2 (1), 2014, p. 1–10. (Yehya M, Hussain S, Wasim A, Jahanzaib M, Abdalla H A.).

14. Yampolskiy L.S. Method and device for movement of pedipulators of walking robot. State Register of Patents of Ukraine, Pat. 111021, 2016, 11p. (Yampolskiy L.S., Polishchuk M.N., Persikov V. K.).

15. Polishchuk M. Mobile climbing robot with elastic energy accumulators. – Mechanics and Advanced Technologies, vol. 1 (82), 2018, p. 116 – 122 (Polishchuk M., Oliinyk V.).

16. Kuznetsov Yu.M.. Walking mobile robot Kuznetsova – Polishchuka. Ukrainian Institute of Intellectual Property, Ukraine, application for a patent № a2018079762018, p.16 (Kuznetsov Yu.M., Polishchuk M.M.).

17. Polishchuk M. Walking Mobile Robot of Arbitrary Orientation, International Journal of Engineering and Manufacturing (IJEM), vol.8, No.3, 2018, p.1-11 (Polishchuk M., Opashnianskyi M., Suyazov N.).

18. Polishchuk M.N. Antigravity mobile robot Polishchuk. Ukrainian Institute of Intellectual Property, application for a patent № a201805661, 2018, p. 8–10.

IMPACT OF THE SPEED OF SLIDING OF FRICTION LINING ON THE TRIBOLOGICAL PARAMETERS OF FRICTION CLUTCHES OF MOTOR VEHICLES

M.Sc. Sasko Milev [1)*], PhD. Simeon Simeonov [1)*], PhD.Nikola Avramov [2)*], PhD.P.Simonovski [2)*], M.Sc.Gorgi Duskov [3)*], Eng. Elica Simeonova [3)*]

[1)*] Faculty of Mechanical Engineering – Goce Delcev University in Stip, Macedonia
[2)*] Faculty of Mechanical Engineering - Ss. Cyril and Methodius University in Skopje, Macedonia
[3)*] Ruen Inox Automobile, Production of automotive clutches – Kocani, Macedonia

sasko.milev@ugd.edu.mk

Abstract: *Friction clutches are mechanisms placed between the engine and the gearbox and are used to transmit the torque from the engine of the vehicle to the transmission. The clutches should provide start and stopping of the vehicle without vibration and need to have a certain lifetime. The tribological parameters of the linings in these clutches depend on several factors: the quality of the linings, the conditions of the test (exploitation), the temperature between the friction surfaces, the specific pressure between the friction surfaces, the speed of sliding of the friction linings, the number of turns on the clutch, etc. In this paper, will be analyzed the impact of the speed of sliding of friction linings on the tribological parameters of the linings.*

Keywords: FRICTION CLUTCHE, FRICTION LINNING, SPEED OF SLIDING, TRIBOLOGICAL PARAMETERS

1. Introduction

The quality of friction lining in friction clutches is expressed by tribological parameters-coefficient of friction and specific wear. These parameters depend on the sliding that occurs during the engagement of the clutch.

The linings are made from different materials and there are various factors that determine whether a material is quality or not. These factors are: the speed, the temperature and the pressure between the friction surfaces, the number of engagements of the clutch, etc.

The temperature in the lining depends on the load and the number of engagements of the clutch in the unit time. Greater temperature in the liner is created at higher loads and at a larger number of engagement. The temperature is one of the most influential factors. It acts on the structure of the lining. The raised temperature leads to the softening of the lining, decreasing of the coefficient of friction and increasing of the specific wear of the coating. The lining in its composition should have substances that will enable removal of the heat from the lining, that is, the lining should be resistant to high temperature, provide a stable coefficient of friction and wearing within the permissible limits.

The pressure of the lining is achieved by the compressive force of diaphragm wound springs or diaphragm springs. This force creates a friction torque between the friction surfaces of the lining and the pressure plate of the clutch, which transfers the engine power to the transmission. By reducing the specific pressure between the friction surfaces, the friction torque between them decreases, the switch-on time increases, which leads to an increase in the friction and in the temperature. The increasng of the pressure leads to increas in the switch off force, so in this case, when the clutch reloads, the clutch's protective role on one side decreases, and on the other hand, the switch-on time is too short. This means that the pressure affects the temperature of the lining. The specific pressure has a greater impact on the wearing of the lining, and the smaller the friction coefficient. The wearing of the lining is the smallest at a pressure of 20 [N / mm^2]

By increasing the number of engagements of the clutch in the unit time, the temperature increases, thereby decreasing the coefficient of friction, and increasing the lining wearing. / 1/2/5 /

2. Research

The purpose of this research is to determine the impact of the sliding speed on the tribological parameters.

Determination of tribological parameters is performed according to the following expressions:

The specific workload when switching on the clutch is determined by expression [1]:

$$a = \frac{A_r}{F_{vk}} \quad \left[J/cm^2\right] \tag{1}$$

A_r [J]- work of sliding during the engagement of the clutch

F_{vk} [cm^2] - total friction surface

$$F_{vk} = z \cdot F \ \text{[cm}^2\text{]} \tag{2}$$

$$F = \frac{\pi}{4} \cdot \left(D^2 - d^2\right) \ \text{[cm}^2\text{]} \tag{3}$$

z- [-] number of friction surfaces

D - [cm] – outside diameter of the lining

d – [cm] – inner diameter of the lining

After determining of the specific workload, the specific heat load is determined by expression :

$$q = a\frac{x}{60} \ \text{[W/cm}^2\text{]} \tag{4}$$

X [1/min] – clutch engagement frequency

The work of sliding accomplished during the engagement of the clutch is :

$$A_r = \frac{1}{2} J \cdot \omega^2 \ \left[J\right] \tag{5}$$

$\omega\left[1/s\right]$ - angular speed on the bench test

$$\omega = \frac{\pi \cdot n}{30} \quad (6)$$

n - [1/min] – number of rotation

The specific depletion of the lining is determined by the expression :

$$\vartheta = \frac{\Delta b \cdot F}{A_{vk}} \ [\text{cm}^3/10\text{MJ}] \quad (7)$$

A_{sr} [J] - average work per cycle

$$A_{vk} = \sum_{1}^{n} A_{sr} \quad (8)$$

n [-] – number of cycles

Clutch work of the sliding for a single cycle is calculated according to the expression :

$$A = \frac{M_{sr} \cdot \omega \cdot t}{2} \quad [\text{J}] \quad (9)$$

M_{sr} - the mean value of the torque read from the diagram of the machine for a given cycle

ω [1/s] - angular speed of the driven part

t [s] – time of sliding for given cycle

After determining A for each cycle, A_{sr} is determined as the mean value for one cycle, and then A_{vk} is determined as the total work from one test (product of the number of cycles and A_{sr}).

The coefficient of friction is determined by the expression :

$$\mu = \frac{M}{z \cdot r_{sr} \cdot P} \quad (10)$$

M [N m] – torque of the clutch

z – [-] number of friction surfaces

r_{sr}- [m] - average radius of friction lining

P [N] – pressing force of the clutch

$$r_{sr} = \frac{1}{2} \cdot d_{sr} \ [\text{m}] \quad (11)$$

$$d_{sr} = \frac{2}{3} \cdot \left(\frac{D^3 - d^3}{D^2 - d^2} \right) \ [\text{m}] \quad (12)$$

3. Experiment

The examination was carried out on a test bench with the following characteristics :

Electric motor with direct current. and having the following characteristics:

• rated power ..... 204 [KW]

• nominal torque ..... 955 [Nm]

• number of rotations

(with continuous change) ……..... (0-2,000) [1 / min]

- Main swing table with inertial torque …..... 40 [kg m2]

- Shutdown time with setting ..... (0-24) [mm]

- Force of disconnection ……..... 15 [KN]

- Torque that can be tested:

• maximum torque ..... 5.000 [Nm]

• dynamic limit torque ..... 3,500 [Nm]

- Additional inertia:

• own inertial torque ……..... J_s = 2.43 [kg m^2]

• inertial torque of the variable swing weights:

1. J_s = 1.98 [kg m^2]

2. J_s = 3.79 [kg m^2]

3. J_s = 5.8 [kg m^2]

4. J_s = 8.07 [kg m^2].

The following measurements were performed on the existing installation of the test bench:

- Measurement of the torque the clutch is transmitted at the moment of its engagement,

- Measuring the number of rotations of the drive unit,

- Measuring the number of rotations of the driven part,

- Measurement of the ambient temperature of the clutch

These data during the experiment are visually monitored on the given indicators of the measurement sizes.

To control the duration of a cycle, 4 potentiometers are used for individual parts of the cycle:

- t_1 - sliding time when switching on the clutch,

- t_2 - shutdown time,

- t_3 - time of slowing down the driven part,

- t_4 - time of control of the state of relative rest (this time is

at time t_3).

Test mode:

- the inertial torque - 10.22 [kg · m^2]

- switching frequency 0.6 [1 / min]

- speed [m / s] (number of rotations [1 / min]):

7.13 (500), 11.4 (800), 171 (1200), 22.7 (1600)

- specific work [J / cm^2]: 10.5, 27, 60, 107

The test was performed in three samples for 4 speeds and the mean values of the tribological parameters was used:

Table 1: *The mean values of the used tribological parameters*

a[J/cm^2]	10.5	27	60	107
V[m/s] (n[1/min])	7,13 (500)	11,4 (800)	171 (1200)	22,7 (1600)
μ	0,45	0,44	0,42	0,40
ϑ[cm3/10Mj]	0,21	0,41	0,68	0,82

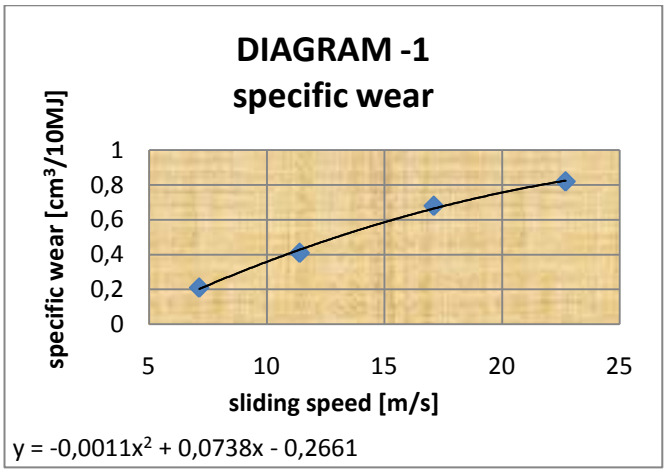


Fig.1. *Change of the specific wear of the clutch depending on speed of sliding*

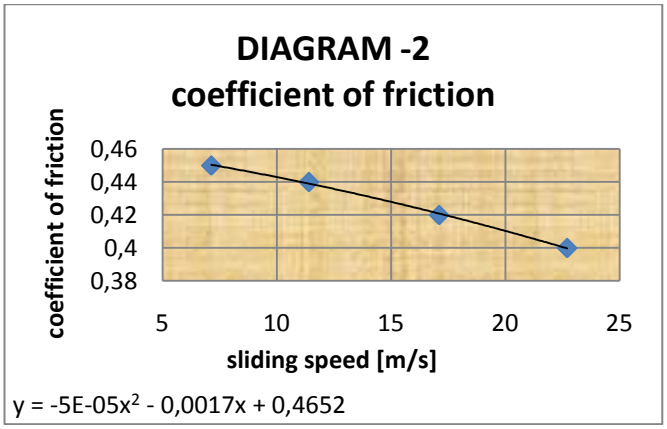


Fig.2. *Change of the coefficient of friction of the clutch depending on speed of sliding*

4. Analysis and conclusion

The speed of sliding on the friction surfaces depends on the number of rotations of the clutch and from the frictional radius of the clutch. The radius for a given clutch is constant, and the speed of sliding depends on the number of rotations of the clutch. Higher speed of sliding creates more heat on the lining, while the wearing torque, and therefore the coefficient of friction decreases. The wear of the lining is increasing. At lower speed, there is a greater friction coefficient, and less wearing.

The dependence of the frictional parameters on the speed of the tested lining is given with the expressions:

For the coefficient of friction: $y = -0{,}001x^2 + 0{,}0078x - 0{,}2661$

For specific wear: $y = -5E^{-05}x^2 - 0.0017x + 0.4652$

These diagrams refer to a certain quality of linings. With another quality, similar curves will be obtained.

The performed tests, from a methodological approach, provide the possibility for further research in the domain of determining the influential components of the structure of the material of friction clutches, on the performance of the clutch, By expanding the tests, the dependence of the coefficient of friction and the specific wear of the friction lining at different temperatures of the friction surfaces, the specific pressure between the friction surfaces, etc. can be determined.

5. REFERENCES

[1] S.Simeonov, "Influence of the components of friction material linings structure on to the performances of friction clutch for heavy motor vehicles" , PhD Thesis, Skopje 1999.

[2] V.Mikarovska, "Laboratory simulations of operating modes of friction clutches for passenger motor vehicles" PhD. Thesis, Skopje, 1995.

[3] Michael Urbakh, Joseph Klafter, Delphine Gourdon & Jacob Israelachvili. The nonlinear nature of friction.Nature Publishing Group. June 2004, 10.1038/nature 02750

[4] Ovidiu Bratcu, Constantin Spânu. Contributions to state concept definition for sliding tribosystems material characterisation. The annals of University "DUNĂREA DE JOS" of Galati fascicle VIII, Tribology. 2003 ISSN 1221-4590

EMBEDDED MICROPROCESSORY SCADA SYSTEM FOR SUPERVISORY, CONTROL AND DATA ACQUISITION IN THE PROCESS OF PURIFICATION OF GASSES IN FERRO-NICKEL FACTORY.

Engineer Iliev Dejan.[1] Ph.D Goce Stefanov[2]
[1]Feni Industry –Kavadarci, s.Vozarci b.b. Republic of Macedonia
[2] Faculty of Electrical Engineering – Stip Republic of Macedonia
E-mail: dtwbb@yahoo.com, goce.stefanov@ugd.edu.mk

Abstract: *In this paper is presented development and implementation of embedded microprocessory SCADA system in factory for production of Ferro-Nickel. In the process of refining of the molten metal are released huge amount of hot gasses that should be purified before letting them to the atmosphere. The project is to change old system of rellay logic and separately located indicators and controllers with centralised SCADA system with PLC and HMI interface, to monitor and control the work of gas Scrubbers and venting system. The paper presents SCADA system functionality and the advantages from the new digital over the old analog equipment.*

Keywords: SCADA, SUPERVISORY, CONTROL, DATA LOGGING, PLC, OPTIMISATION

1. Introduction

With the development of industry and more complex manufacturing processes, management of modern industrial plants is unthinkable without the help of modern monitoring systems or SCADA (Supervisory Control and Data Acquisition) designed for full supervision, better control and greater reliability in the production processes. These systems are present in all branches of the economy, but mostly in the process industry, energy, telecommunications, oil and gas industry, transportation, etc. Surveillance or monitoring of the plants, as the basic function of SCADA systems, uses communication protocols and a graphical user bond to present data for the state of the system to the end users or operators and provide a clearer image of the process.

Nickel-refining plant is the place of Ferro-Nickel factories where the final processing of the metal or refining is performed until the required parameters of the customers are reached. The metal in the plant arrives in a liquid state with a temperature around 1600 degrees Celsius. Upon receiving, the liquid metal is poured into huge vessels called Converters. In them, the metal is additionally heated by oxygen and air, adding limestone for reducing the unwanted elements such as sulfur, iron, etc. During this process, a lot of gases are produced which are further treated in the gas system and released into the atmosphere after their purification. The gas exiting the Converters passes through several aggregates for cooling and cleaning. First pass through the Hood where they are cooled down, then through the Quencher or primary Scrubber, which also cools them and removes the larger particles. From Quencher, they continue along through Scrubber, which also removes the tiny particles and finally the gas continues through a fan that sucks the gases from the Converter itself through the purification units to the exhaust chimney and the atmosphere.

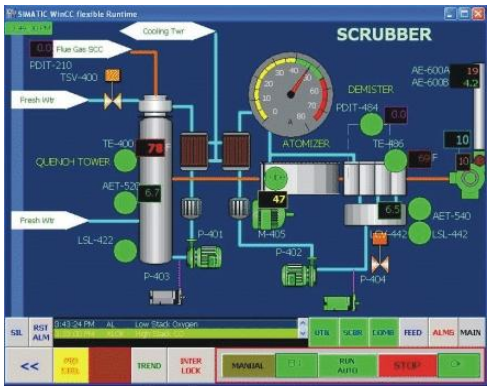


Fig. 1 *Example of SCADA for gas cleaning process.*

For all this to function impeccably it is necessary to constantly observe and monitor the properties of gas and water in the system. For this purpose, there are measuring instruments of different type: flow transmitters, pressure, differential pressure, level, position, temperature, PID controllers etc. Due to the durability of the equipment, the lack of spare parts and the need for more reliable and safe operation of the process, it was necessary to develop a project for replacing the existing equipment with new sophisticated equipment that would have a full visualization of the process.

The purpose of this paper is to present the design of a centralized SCADA system in which all process values with graphic display and the aggregates themselves with their physical position in the plant will be displayed on few screens for safer and more efficient work of the plant. The implementation of this project significantly improves the operation of the plant. Through this system, operators from one place can observe the entire process. In addition to real-time values, the program saves important data and draws up trends for past process conditions, thus avoiding defects even before they occur. An example of that is the fan vibration chart, when vibrations increase workers can take precaucons like balancing so as can be avoided serious damages to the bearings. With the early warning itself, stalls are avoided, making huge savings for the company.

2. Hardware configuration

The project uses a standard PC for the SCADA program and PLC Siemens from the family S7-300 model 314C-2DP with analogue cards SM331 AI8x13bit.



Figure 2*: PLC Siemens with analogue cards*

The PLC itself, besides the processing unit, has both built-in input/output analogue and digital cards as well as a memory SD card where the program is stored. The I/O are physically divided into two cards. The first has 8 digital inputs, 5 analog inputs and 2 analog outputs, and the second 16 digital inputs and 16 digital outputs. Channels for analog inputs and outputs can be used as current or voltage

depending of the configuration in the software and the appropriate wiring connection.

Since we have multiple measurement points, to cover every of them, the PLC allows us to extend it with additional analogue cards. In this project, 5 cards per PLC are additionally connected, in total 10 analogue cards SM331 AI8 * 13bit. Analog cards as well as PLCs use a 24VDC power supply. They have 8 channels that can be used as current or voltage inputs, and on some of the inputs can be connected both directly thermocouples or RTD temperature probes.

The power supply of the PLC and I/O cards is from the same manufacturer Siemens model PS307 with the following technical characteristics:

Input voltage:	220VAC 50Hz
Input current:	1.3A
Output voltage:	24VDC
Output current:	5A

Table 1: Technical specifications of the power supply

During the elaboration of the project for visualization and control of the gas purification process, some of the existing measuring instruments, transmitters, actuators, controllers were used, and where needed new were installed and calibrated.

For measurement of pressure, differential pressure, water flow and level were used Endress&Hausser PMD75 and PMD 70 transmitters. These are multifunctional proven transmitters that can be quickly parameterized and calibrated to measure the required medium and the required value. As an output, they provide an analog signal 4-20mA and digital impulses through transistor outputs.



***Figure 3**: Pressure, flow, temperature transmiters used in the project*

Temperature measurement is done with PT100 RTD probes of platinum, which give 0.38 Ω per degree of Celsius. In measuring places where there are higher temperatures, the measurements are performed using thermocouples type J. They are connected to PRETOP 5333 transmitters, which turn the ohm signal into a current 4-20mA and send it to the current input on the PLC.

For regulating the flow of the cooling water and gas through the system are used actuators and valves. The water flow is regulated with pneumatic valves which are controlled by the SCADA system and Siemens controllers. Operator sets needed flow so the controllers via 4-20mA signal and 3-15psi air pressure puts the valve in the needed position for the given flow. Air flow and the differential pressure is regulated with louver-dampers equipped with Andco actuators. They are also controlled from the SCADA or controllers with 4-20mA signal. SCADA program check feedback signal from potentiometers if the set position is reached.

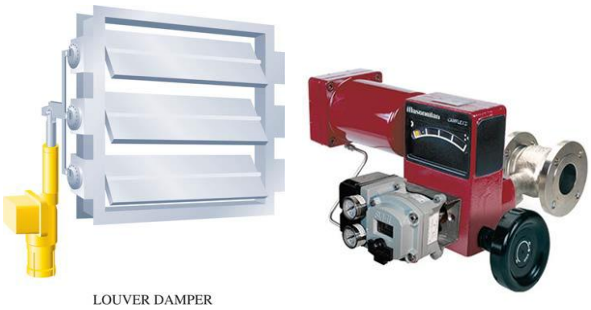


***Figure 4**: Actuator and valve controlling water and air flow*

For setting and calibrating the equipment were used Fluke 179 multimeter and 717 Pressure calibrator. Calibrating of the temperature transmitters was made with Chauvin Arnaux calibrators.

3. Software configuration

For the development and implementation of the software in this project were used Siemens software packages. SCADA was programmed with WinCC Flexible and PLC programming was in Step 7 Simatic Manager 5.5.

SIMATIC Manager is software from the company Siemens that allows to provide detailed network configuration (with basic network and subnets), monitoring of the variables, their "forced activation" and more. We can program in one of the offered languages: STL-assembler which is low-level language, higher-level language SCL similar to Pascal, LADDER programming or graphically oriented and similar to relay patterns. FBD is also a graphic language that is very suitable for streaming the signal path and the S7-GRAPH language being the basis to draw a process flow chart, suitable for technological engineers. Simatic Manager is the part of the program where is done the all the math work. The raw signal from the I/O cards is scaled, and converted in format understandable for the final user. Programming starts with opening new project and setting of the hardware. It is very important to set all the equipment and the communication type between them. In this project we use Profibus communication that uses special communication cards, cable and connectors. Program is divided in several block with one main OB1 from are called all other blocks and functions. In the block we make all the connections between input raw values, scaling and calculations and the output values. All this is done with using of databases and symbols. Use of symbols make this program more flexible and with little changing in the programming it would be useable in lots of other processes and applications.

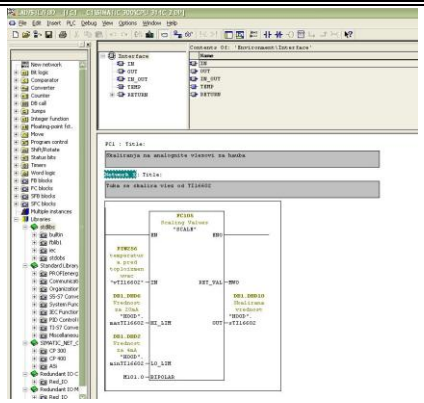


***Figure 5**:Part of a Function Block in Simatic Manager*

Scada software SIMATIC WinCC flexible is powerful HMI software for controling, monitoring and data collection in automated systems that use personal computers. In addition, it enables the defining and displaying the alarm conditions in the system, displaying trends, i.e. displaying changes in the system variables in time, forming alarm reports, trends and operators activities, and their archiving or permanent data storage. The process is displayed graphically on the screen, through a whole set of graphic elements to which they are associated with process tags or labels. Process or external tags allow communication between the components of the automated process, for example, HMI devices and PLCs (in our case, the computer and S7-300 PLC), or provide communication and direct connection between the operator and the process. The external tag is an image of a particular memory location in the PLC. The operator can read and adjust the values of process values through the HMI device, using process tags via a memory location in the PLC. There are also internal tags that are stored in the memory of the HMI device and serve to perform internal (local) calculations. These labels have no connection to the PLCs.

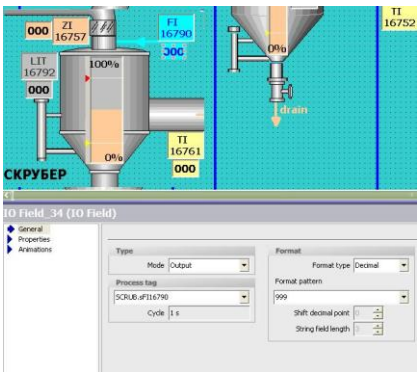


***Figure 6**:Configuring I/O field in Simatic WinCC Flexible*

4. Results of SCADA configuration

As a result of the software and hardware configuration, making measurement, calibration and parameterization of the instruments, in this paper is made SCADA project showing the process variables divided in three screens: Main screen, Admin, Scrubber and Motor & Ventilator.

The main screen displays the process values from all measurement points in the plant in real time. For that purpose we use digital indicator fields and visualization with a bar graphs. They are arranged in the display screen just as they are distributed across the aggregates through the plant, thus providing the operator with a clear picture of the state of the process for cooling and purifying the gases, the condition of the aggregates themselves, critical conditions, etc. Each alarm state is displayed on the screen in yellow and red color, so it's easy to see in which part of the process is the problem. For each kind of measurement, such as pressure, flow, temperature, etc., there are different colors of indicators that are of great importance for the delineation of the displayed values. Also with selecting the I/O field we can set desired value that we need for the process.

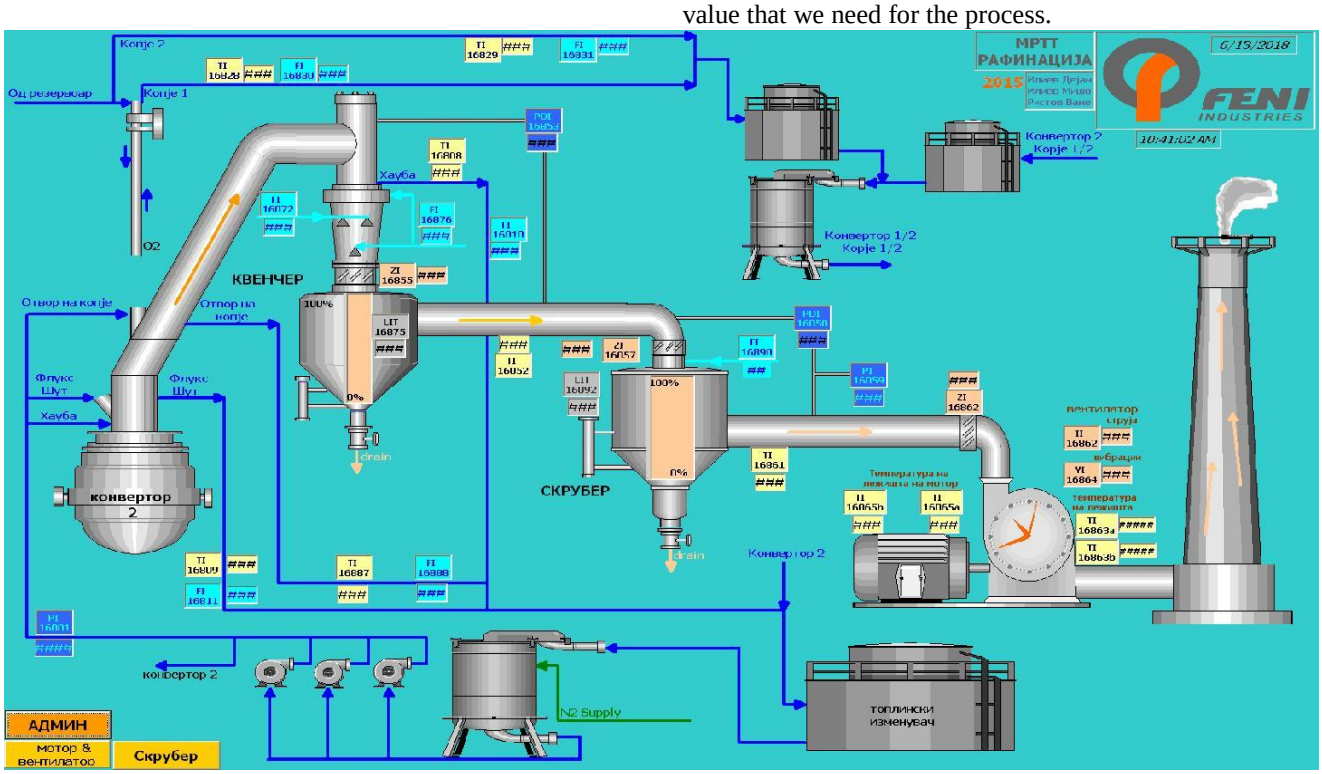


***Figure 7**: SCADA main screen with process values*

On the screen Motor & & Ventilator are displayed values of the measuring points of these aggregates. On the screen also are added trends or graphs about past system conditions. It monitors the currents of the engines that also serve us to regulate the flow of air through the system, the engine and vent bearing temperatures as well as the engine vibration. This is of great importance because with the help of trends we can track changes in values in the past, in case of defects, we can find out what caused the defect and thus avoid similar situations in the future. The SCADA system is a great tool for diagnosing problems and their future avoidance.



***Figure 8**: Motor & Ventilator screen showing values and trends*

The Admin Screen or Admin serves to set up the system by the technical staff. There are settings of the last scaling of the values in a form understandable to the operator. For each measurement point, the threshold of scaling range is assigned for operator to obtain the value in digital understandable form. The thresholds for the alarm and critical state of the system are also given so that new alarm values can be added for each point or, if necessary, and even more measuring points.

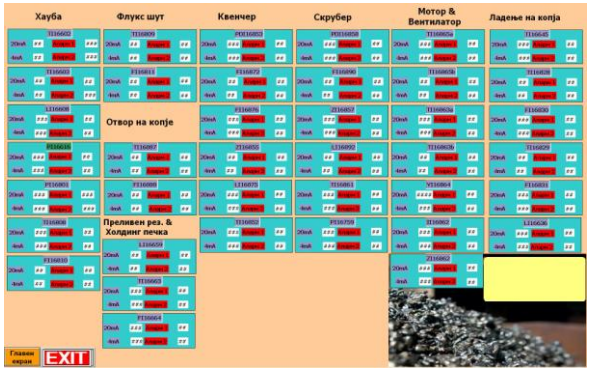


***Figure 9**: Admin screen for setting the system thresholds*

5. Conclusion

In this paper is presented embedded microprocessor SCADA system for Supervisory, Control and Data Acquisition in a process of purification of Gasses in Ferro-Nickel factory. There is a short view of the hardware and software setting in the system. The system is build to replace and old system with lots of separate indicators, controllers, alarm cards and paper recorders. From an economic aspect, there is an initial investment, but the total amount of the system is far cheaper and more cost-effective than the cost of only a few process indicators. The work done by 80 indicators, the same number of alarm cards and annunciators, and paper recorders or data loggers is now only performed by two processor units, 10 input analogue cards and two personal computers, which saves at least half the value of the old system. Hardware equipment is from the company Siemens leading in the world of automation and the software solution is made also in Simatic Manager Step 7 and WinCC Flexible 2008 products of Siemens. Any future upgrade or modification in the system will be programmable with a small additional wiring and little or no cost at all. Programming is made on a separate computer and in the end only need to copy on the process computer, with minimal or no stopping of the process.

6. Literature

[1] D. Bailey, E. Wright, “Practical SCADA for industry” Linacre House, Jordan Hill, Oxford OX2 8DP 200 Wheeler Road, Burlington, MA 01803

[2] C. T. Jones, “STEP 7 in 7 Steps - A Practical Guide to Implementing S7-300/S7-400 Programmable Logic Controllers” 1st Edition, Patrick-Turner Publishing, United States, 2006.

[3] SIMATIC HMI WinCC flexible 2008 Compact / Standard / Advanced User's Manual, 07/2008 A5E01024750-02

THE CONCEPT OF KNOWLEDGE MANAGEMENT IN THE REGION AS A BASIS OF ESTIMATION OF CONDITIONS OF INNOVATIVE ACTIVITY

Prof. dr. Zaborovskaia O.
State Institute of Economics, Finance, Law and Technology, Russia
E-mail: ozabor@mail.ru
Babskova O.
PhD Student of Peter the Great St. Petersburg Polytechnic University

Abstract: *Innovative activity in a region is considered in terms of the knowledge management concept. An approach is proposed for assessing the conditions for innovative activity on the basis of three groups of indicators: indicators, characterizing the financial conditions for innovative activity; indicators, characterizing human resources; indicators, characterizing the knowledge generation sources in a region and their accessibility. The obtained integral estimation allows us to classify regions and, on this basis, differentiate innovation policy.*

Keywords: HUMAN RESOURCES, KNOWLEDGE MANAGEMENT, INNOVATIVE ACTIVITY

1. Introduction

Information and knowledge play an important role in modern socioeconomic systems. Knowledge economy is formed when knowledge becomes a commercial commodity. Knowledge acts as a specific commodity, which is sold and bought similarly to traditional consumer products. However, a knowledge market has some specifics.

A knowledge-based economy must have the following common features:

1) intensive development of knowledge, which is reflected in a form of constantly increasing importance of the science intensive sector, growing volumes of production and sale of modern high technologies, accelerating computerization processes in the economy and the entire life of society;
2) growing capitalization of the market share of companies involved in advanced research and development;
3) one of the priorities of the state policy is capitalization of costs in man, who is one of the most important resources;
4) high rates of fixed capital renewal in life-supporting sectors of material production and servicing infrastructure;
5) provision of a decent living standard for every citizen in the country: housing, job, information and transport support, etc.

The socioeconomic development of Russia is characterized by a high level of interregional differentiation and it must be considered in the pursuit of innovation policy. Evaluating the conditions of innovative activity allows us to estimate the capabilities of regions to generate and use innovations to increase competitive advantages. This estimation must consider the factors of knowledge formation in a region.

2. The concept of knowledge management in a region as a basis for estimating the conditions of innovative activity

The concept of knowledge management is based on interpretations of the essence of knowledge, its role in the economy, classification [1, 3, 4, 5].

Knowledge is spread chaotically, and brain drain from regions occurs. Consequently, mechanisms are necessary which would regulate the flow of those who are involved in intellectual labor and have unique knowledge. In the 1950s in the USA the concept of knowledge management appeared so that this problem could be tackled. First it was applied to private firms and organizations, but since the mid 1990s this concept has been adapted for a regional level.

Today knowledge management is understood as systematic processes thanks to which the main elements of intellectual capital are created, sustained, distributed and applied. Knowledge plays an important role in advancing innovations, creativity and idea exchange [2, 6, 7, 8].

Knowledge management includes the following basic processes:

- creation: the result of this action is new knowledge;
- search: search for and formalization of inexplicit knowledge, which makes it possible to create a common knowledge base for collective use;
- systematization (organization): categorization and classification of knowledge for its further well-targeted extraction;
- access: actions which make knowledge spread and exchange;
- utilization: application of knowledge in every day activity, particularly, in decision-making [9].

The concept of knowledge management can be considered not only at the level of organizations, but also at the level of regions. Development and pursuit of innovation policy of a region, functioning of the regional innovation systems must be considered given the processes of knowledge generation, development and utilization.

The forever growing volume of knowledge under the conditions of constant advancement of technology and modernization of today's economy determines knowledge management as a major resource of the country. The intellectual potential of a region can often affect its competitiveness, while the capability to bring innovative ideas to the stage of commercialization under the conditions of innovative development of society becomes a major factor not only for successful functioning, but also for survival in the global arena. At the same time, globalization processes accompanying innovative activity contribute to an effective exchange of knowledge and experience and speed up commercialization of innovation.

The innovation potential of a region allows us to determine the development prospects of the regional economy and estimate its capabilities for innovative activity. Improving the well-being of regions becomes a top priority objective of their economic development. Economic growth with the economy transiting to an innovative way of development is directly connected with successful fulfillment of innovation potential. Innovation potential depends to a large degree on the quality of human capital.

For effective fulfillment of a region's innovation potential, capabilities for both extensive and intensive development have to be united. The problem of staff replacement in the scientific research sector must be solved, but it is also important to think of the quality of intellectual resources. Some knowledge, abilities and

skills cannot be replaced with their holder being gone. Consequently, ways should be found to keep this knowledge and make it accessible to those people who need it. I.e. conditions should be created that would allow us to identify and realize human potential as well as to acquire knowledge management skills. Thus, the role of knowledge management takes the leading position in increasing both a region's innovation potential and the innovation potential of the entire country.

Let us point out the factors of knowledge management which affect the formation of favorable conditions for innovative activity in a region:

- the total volume of costs associated with forming and improving knowledge infrastructure, the structure of these costs;

- the volume and quality of human capital whose holders take part in innovative activity;

- availability and accessibility of knowledge generation sources.

The concept of knowledge management is grounded at a regional level on the following statements: the cost of producing innovation and creating modern knowledge infrastructure in a region takes up regional costs and determines financial conditions for innovative development of a region; knowledge, abilities and skills of man represent a specific form of capital (human capital); formation of human capital, whose quality meets the demands of innovative development, calls for financial and organizational resources and well as time resources; the knowledge sources of a region are represented by databases and access to these databases, thanks to which the process of knowledge generation takes place. Regional innovation policy should be considered in the context of the developing concept of knowledge management at a regional level taking into account the processes of human capital formation.

Let us look at the factors of knowledge management in more detail. Research and development costs as a whole determine the general capabilities for implementing innovative activity. According to the Industrial Research Institute – IRI (USA), in 2015 the share of Russia and CIS countries in the total volume of R&D funding was 3.0% (the share of the USA was 25.8%, that of China was 20.1%, in 2017 these indicators were 2.8%, 25.5% and 20.8% respectively [10]. The projected value for Russia for the year 2018 is 2.6% [11]. At the same time , according to the data of "Battelle", "R&D Magazine", "World Factbook", the International Monetary Fund and the World Bank, Russia took the 8th position in 2016 (50.9 billion USD) in terms of the absolute amount of costs [12, 13]. Researchers D.B. Izyumov and E.L. Kondratyuk point out that "the state funding of R&D in 2016 doubled over the last 5 years. However, this indicator is still incomparable with the expenses of China and the USA" [17].

As for the sources of R&D funding, Russia is different from the majority of developed countries. Most R&D activity in the country is funded by the state. About 60% of all funds spent on science arrive from the state budget and this indicator has had a fairly stable position over many years. Of course, there is growth in the participation of business in funding innovations, but it is insignificant.

Low expenditure on scientific activity and worsening of the conditions for the fulfillment of scientific research potential resulted in a fall in the status of a scientific worker in society and, consequently, manpower drain from this sphere. Since 2007 the ratio of the internal R&D costs to GDP has been increasing. The size of manpower in the category "Researchers" has decreased insignificantly over the last decade - by 3% only (even though there has been growth of manpower in this category since 2014). A positive trend is also the fact that the share of scientists aged 30-40 is going up. As a result, the threat of loss of the continuity of generations is still there, but a positive trend has been set too. Aging of scientific manpower in this sector is still a problem, but the vector of positive development has been set since the size of manpower with PhD degrees is growing. The problem of the lack of the young in science has been there for more than 20 years. In 2013 the specific weight of graduates hired by R8D organizations in the total number of graduates from higher educational institutions was 0.6% [14, 15]. This indicator halved in comparison to the data of 1995.

With relatively low expenditure on R&D in the Russian Federation, human resources involved in scientific research have quite a considerable weight. In the analysis of the total employment of population, the share of scientific workers in the country corresponds to the average value of this indicator among the countries being studied [14, 15]. Almost two thirds of researchers are employed in the public sector.

An essential problem in creating new knowledge in the private sector is a limited interaction with R&D conducted in the public sector. The majority of scientific workers in the public sector of science have virtually no interest in commercializing the results of their activity. This is proved by a relatively low number of both patent applications and issued patents. However, Russia belongs to the ten countries involved most intensely in innovative activity in terms of the number of patent applications and the number of patent applications per 1000 workers employed in the R&D sector in 2015 [14,15]. The invention activity coefficient (the number of patents issued per 10 thousand people of the country's population) was 1.18 in 1995, 1.68 in 2014, and 2.04 in 2015. Various technology innovations, developments in the field of transportation, chemistry and metallurgy are the most common to patent [16].

Innovative activity performance in the Russian Federation is not high enough. But it is not because of the lack of highly-qualified manpower, but because there are no favorable conditions for scientific activity in the country: Russia is a major exporter of scientific workers aged 30-35 [14]. In order to fulfill innovation potential in the country, it is necessary to improve the labor conditions of scientific workers and provide opportunities for career growth, which will be quite an important factor for forming favorable conditions for innovative activity of a region.

The conditions for innovative activity are noticeably different in Russian regions. At the same time, these conditions must be evaluated in order to manage innovative activity and identify priorities for funding.

3. Solution of the examined problem: evaluating the conditions for innovative activity in a region

When methods are chosen for evaluating the conditions for innovative activity in a region, non-uniformity of socioeconomic development of the regions in the Russian Federation should be considered. Ways to improve innovation climate that will work for one region might have no effect in other subjects of the Russian Federation.

The existing systems for evaluating the innovative development of regions are based on an "input/output" model. I.e. resources available at the input and results obtained at the output are looked at. It implies that results are evaluated rather than original (background) conditions. At the same time background conditions have to be evaluated so that effective innovation policy can be developed. In order to evaluate the conditions for forming and improving regional innovation policy, it is suggested using only "input" elements, which define the conditions for innovative activity.

Evaluating regional conditions for innovative development is the first stage in developing regional innovation policy. A productive approach to carrying out such evaluation is to evaluate integratively the factors of knowledge management: financial conditions for knowledge management; characteristics of human capital in terms of participation in innovative activity; availability

and accessibility of knowledge sources (knowledge generation points).

It is suggested that the following set of indicators should be used:

a) financial conditions for knowledge management:

- gross regional product, mil. RUR,
- internal R&D cost, mil. RUR,
- remuneration of workers involved in R&D, RUR,
- average salary of workers in organizations in a region, RUR,
- information-communication technology costs in a region, mil. RUR;

b) capabilities for human knowledge development:

- population size, thousand people,
- average annual number of the employed, thousand people,
- manpower involved in R&D in a region,
- researchers with academic degrees (PhDs and Doctors of Sciences),
- number of students in higher educational institutions;

c) knowledge sources in a region:

- number of enterprises and organizations,
- R&D organizations in a region,
- organizations involved in training PhD students and doctoral students,
- organizations having broadband access to the Internet.

We will use the concept of an "ideal system" for integral estimation. It implies choosing reference values of indicators and comparison of the achieved values of indicators in a region with the reference values. Thus, having no opportunity to determine a reference region by all indicators that are analyzed, a region should be chosen where a specific indicator has the best value ("ideal" at a certain time for a specific indicator). A set of indicators "ideal" for a certain moment characterize an "ideal" region.

Indicators must be limited for integral estimation so that estimates can be obtained in unit fraction. For example, indicators which characterize financial conditions for innovative activity for an entire region and are related to R&D costs and costs associated with information-communication technology are limited in relation to gross regional product.

After limited indicators are obtained, their values are compared to the "ideal" ones and deviations are identified. Integral estimation is calculated on the basis of the geometric mean of the obtained deviation coefficients.

4. Results and discussion

This set of indicators is presented in the official statistics, but the comparability of indicators by regions must be taken into account. In terms of the entire system (the national innovation system of the Russian Federation), common points of development can be set for all regions. These points must be significant for all regions given the regional differences in formation of regional innovation policy and conditions for its pursuit. These points should also provide for compliance with the principles of federalism. Deviations of the studied objects from the set points give a basis for analysis and determination of measures to eliminate these deviations.

It is important that the balanced state of the conditions for innovative activity should be taken into account.

On the basis of the integral estimates of the conditions for innovative activity obtained by regions a rate scale can be set and regions can be classified depending on the value of the integral estimate. Moreover, regions can be ranked depending on the estimation.

5. Conclusion

Advancing innovative activity is an important factor for competitiveness growth of regions. Regional innovation policy must consider the conditions actually existing in a region. The concept of knowledge management can be effectively used at the level of a region as a methodological basis for estimating the conditions for innovative activity.

In terms of this concept, the estimation of the conditions for undertaking innovative activity involves:

- estimation of the financial conditions for innovative activity;
- estimation of human capital, whose holders are involved in innovative activity;
- estimation of the availability and accessibility of the knowledge generation sources in a region.

Each of the knowledge management factors includes an integral indicator of the consistent elements, which reflect some aspects of innovative activity, like funding, scientific manpower or knowledge generation sources. Depending on the obtained estimates of the conditions for innovative activity it appears possible to make a reasonable choice of the priority direction for a certain region. Further on, provided there is constant monitoring, it is possible to identify the effectiveness trends of the pursued innovation policy and wisely alter its course.

6. References

1. Rudenko, I. V., Vinzhegin, O. M. Evolution and basic concepts of knowledge management in modern conditions // The Bulletin of Omsk State University. Series: Ekonomics. 2009. No. 3. URL: https://cyberleninka.ru/article/n/evolyutsiya-i-osnovnye-kontseptsii-upravleniya-znaniyami-v-sovremennyh-usloviyah (retrieval date: 06.07.2018).
2. Izychev, Aleksandr Mikhailovich. The specifics of the knowledge management mechanism in the conditions of knowledge economy // Socioeconomic phenomena and processes. 2012. No.2. URL: https://cyberleninka.ru/article/n/osobennosti-mehanizma-upravleniya-znaniyami-v-usloviyah-ekonomiki-znaniy (retrieval date: 06.07.2018).
3. Mokyr J. The Gifts of Athena: Historical Origins of the Economy. – Princeton University Press, 2002.
4. Skyrme D.J., Amidon D.M. Creating the Knowledge-Based Business. – Wimbledon: Business Intelligence Ltd, 1997.
5. Stewart T.A. Intellectual capital: the New Wealth of organization. – N.Y.: Currency Doubleday, 1997.
6. Michael E. D. Koenig. What is KM? Knowledge Management Explained. Jan 15, 2018. http://www.kmworld.com/Articles/Editorial/What-Is/What-is-KM-Knowledge-Management-Explained-122649.aspx
7. Nonaka I., H. Takeuchi The Knowledge – Creating Company. – New York: Oxford University Press. 1995.
8. Henry N. Knowledge management: A New Concern For Public Administration // Public Administration Review. – 1974. - No.34.
9. Innovative development: economics, intellectual resources, knowledge management / Edited by B.Z. Milner. - Moscow: Research Center INFRA-M, 2013.
10. 2017 Global R & D Funding Forecast. Available at: http://digital.rdmag.com/researchanddevelopment/2017_global_r_d_funding_forecast?pg=2#pg2 .
11. 2018 Global R & D Funding Forecast. https://digital.rdmag.com/researchanddevelopment/2018_global_r_d_funding_forecast?pg=2#pg2
12. IMF Annual Report – 2016. Available at: http://www.imf.org/external/russian/pubs/ft/ar/2016/pdf/ar16_eng.pdf.
13. Annual report of the World Bank for 2014, 2015 and 2016. Available at: https://openknowledge.worldbank.org/handle/10986/24985
14. Science indicators: 2017. The statistical bulletin of the Higher School of Economics // https://www.hse.ru/primarydata/in2017
15. Science indicators:2018. The statistical bulletin of the Higher School of Economics // https://www.hse.ru/data/2018/02/12/1162058327/Science_and_Technology_Indicators_2018.pdf
16. Figures about science or how statistics helps understand the scientific potential of a country. The article of ITMO.NEWS publisher. 14.02.2017 // http://news.ifmo.ru/ru/education/official/news/6434/
17. Izyumov, D.B., Kondratyuk, E.L. Analysis of Global Expenditure on Research and Development in 2014–2016. Innovation and expertise. Issue 1(19). 2017. P.113-122. http://inno-exp.ru/archive/19/innov_2017-1_113-122.pdf

USING PATTERNS IN ARCHITECTURE OF SOFTWARE ENGINEERING

M.Sc. Ivanova Milka
Faculty of Mechanical Engineering – Technical University of Sofia, Bulgaria
milkachr@tu-sofia.bg

Abstract: *Architecture patterns help define the basic characteristics and behavior of an application. Some architecture patterns lend themselves toward highly scalable applications, whereas other architecture patterns naturally lend themselves toward applications that are highly agile. Knowing the characteristics, strengths, and weaknesses of each architecture pattern is necessary in order to choose the one that meets your specific business needs and goals.As a software architect, you must always justify your architecture decisions, particularly when it comes to choosing a particular architecture pattern or approach. The goal of this report is to give you enough information to make and justify that decision.*

Keywords*: SOFTWARE ENGINEERING, PATTERN, SOFTWARE ENGINEERING ARCHITECTURES, ARCHITECTURAL PATTERNS,*

There are five types software engineering architecture where patterns are used

Layered Architecture

The most common architecture pattern is the layered architecture pattern, otherwise known as the n-tier architecture pattern. This pattern is the de facto standard for most EE applications and therefore is widely known by most architects, designers, and developers. The layered architecture pattern closely matches the traditional IT communication and organizational structures found in most companies, making it a natural choice for most business application development efforts.

Event-Driven Architecture

The event-driven architecture pattern is a popular distributed asynchronous architecture pattern used to produce highly scalable applications. It is also highly adaptable and can be used for small applications and as well as large, complex ones. The event-driven architecture is made up of highly decoupled, single-purpose event processing components that asynchronously receive and process events. The event-driven architecture pattern consists of two main topologies, the mediator and the broker. The mediator topology is commonly used when you need to orchestrate multiple steps within an event through a central mediator, whereas the broker topology is used when you want to chain events together without the use of a central mediator. Because the architecture characteristics and implementation strategies differ between these two topologies, it is important to understand each one to know which is best suited for your particular situation.

Microkernel Architecture

The microkernel architecture pattern (sometimes referred to as the plug-in architecture pattern) is a natural pattern for implementing product-based applications. A product-based application is one that is packaged and made available for download in versions as a typical third-party product. However, many companies also develop and release their internal business applications like software products, complete with versions, release notes, and pluggable features. These are also a natural fit for this pattern. The microkernel architecture pattern allows you to add additional application features as plug-ins to the core application, providing extensibility as well as feature separation and isolation.

Microservices Architecture Pattern

The microservices architecture pattern is quickly gaining ground in the industry as a viable alternative to monolithic applications and service-oriented architectures. Because this architecture pattern is still evolving, there's a lot of confusion in the industry about what this pattern is all about and how it is implemented. This section of the report will provide you with the key concepts and foundational knowledge necessary to understand the benefits (and trade-offs) of this important architecture pattern and whether it is the right pattern for your application.

Space based architecture

Most web-based business applications follow the same general request flow: a request from a browser hits the web server, then an application server, then finally the database server. While this pattern works great for a small set of users, bottlenecks start appearing as the user load increases, first at the web-server layer, then at the application-server layer, and finally at the database-server layer. The usual response to bottlenecks based on an increase in user load is to scale out the web servers. This is relatively easy and inexpensive, and sometimes works to address the bottleneck issues. However, in most cases of high user load, scaling out the web-server layer just moves the bottleneck down to the application server. Scaling application servers can be more complex and expensive than web servers and usually just moves the bottleneck down to the database server, which is even more difficult and expensive to scale. Even if you can scale the database, what you eventually end up with is a triangle-shaped topology, with the widest part of the triangle being the web servers and the smallest part being the database

In any high-volume application with an extremely large concurrent user load, the database will usually be the final limiting factor in how many transactions you can process concurrently. While various caching technologies and database scaling products help to address these issues, the fact remains that scaling out a normal application for extreme loads is a very difficult proposition.

The space-based architecture pattern is specifically designed to address and solve scalability and concurrency issues. It is also a useful architecture pattern for applications that have variable and unpredictable concurrent user volumes. Solving the extreme and variable scalability issue architecturally is often a better approach than trying to scale out a database or retrofit caching technologies into a non-scalable architecture.

Pattern Description

The space-based pattern minimizes the factors that limit application scaling. This pattern gets its name from the concept of tuple space, the idea of distributed shared memory. High scalability is achieved by removing the

central database constraint and using replicated in-memory data grids instead. Application data is kept inmemory and replicated among all the active processing units. Processing units can be dynamically started up and shut down as user load increases and decreases, thereby addressing variable scalability. Because there is no central database, the database bottleneck is removed, providing near-infinite scalability within the application.

Most applications that fit into this pattern are standard websites that receive a request from a browser and perform some sort of action. A bidding auction site is a good example of this. The site continually receives bids from internet users through a browser request. The application would receive a bid for a particular item, record that bid with a timestamp, and update the latest bid information for the item, and send the information back to the browser.

There are two primary components within this architecture pattern: a processing unit and virtualized middleware. Figure 1 illustrates the basic space-based architecture pattern and its primary architecture components.

The processing-unit component contains the application components. This includes web-based components as well as backend business logic. The contents of the processing unit varies based on the type of application— smaller web-based applications would likely be deployed into a single processing unit, whereas larger applications may split the application functionality into multiple processing units based on the functional areas of the application. The processing unit typically contains the application modules, along with an in-memory data grid and an optional asynchronous persistent store for failover. It also contains a replication engine that is used by the virtualized middleware to replicate data changes made by one processing unit to other active processing units.

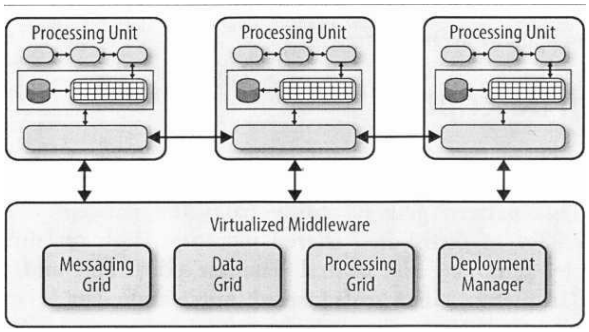


Figure 1. *Space-based architecture pattern*

The virtualized-middleware component handles housekeeping and communications. It contains components that control various aspects of data synchronization and request handling. Included in the virtualized middleware are the messaging grid, data grid, processing grid, and deployment manager. These components, which are described in detail in the next section, can be custom written or purchased as third-party products.

Pattern Dynamics

The magic of the space-based architecture pattern lies in the virtualized middleware components and the in-memory data grid contained within each processing unit. Figure 2 shows the typical processing unit architecture containing the application modules, inmemory data grid, optional asynchronous persistence store for failover, and the data-replication engine.

The virtualized middleware is essentially the controller for the architecture and manages requests, sessions, data replication, distributed request processing, and process-unit deployment. There are four main architecture components in the virtualized middleware: the messaging grid, the data grid, the processing grid, and the deployment manager.

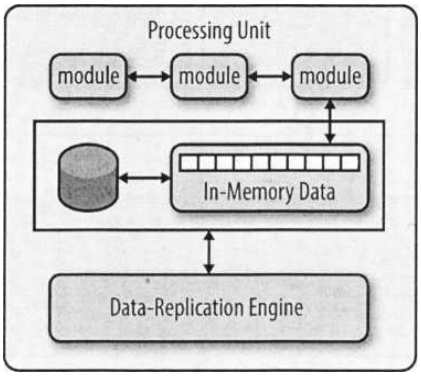


Figure 2. *Processing-unit component*

Messaging Grid

The messaging grid, shown in Figure 3, manages input request and session information. When a request comes into the virtualized- middleware component, the messaging-grid component determines which active processing components are available to receive the request and forwards the request to one of those processing units. The complexity of the messaging grid can range from a simple round-robin algorithm to a more complex next-available algorithm that keeps track of which request is being processed by which processing unit.

Data Grid

The data-grid component is perhaps the most important and crucial component in this pattern. The data grid interacts with the data- replication engine in each processing unit to manage the data replication between processing units when data updates occur. Since the messaging grid can forward a request to any of the processing units available, it is essential that each processing unit contains exactly the same data in its in-memory data grid.

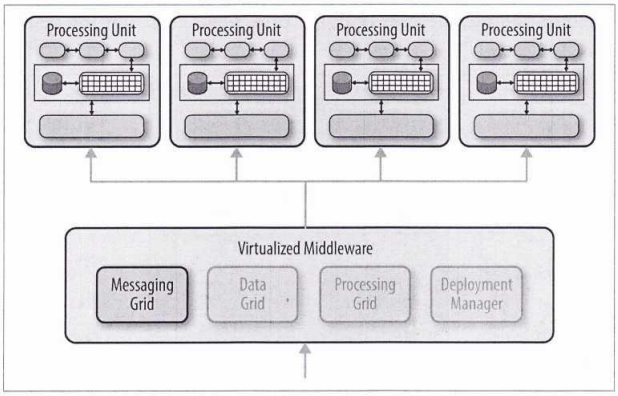


Figure 3 *Processing-grid component*

Although Figure 4 shows, a synchronous data replication between processing units, in reality this is done in parallel

asynchronously and very quickly, sometimes completing the data synchronization in a matter of microseconds (one millionth of a second).

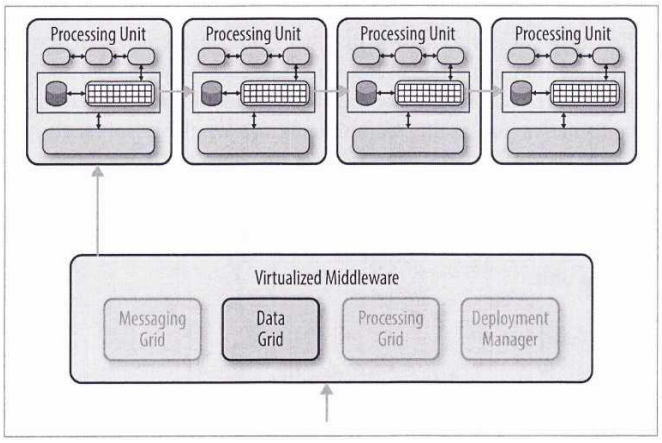


Figure 4. *Processing-unit component*

Processing Grid

The processing grid, illustrated in Figure 5, is an optional component within the virtualized middleware that manages distributed request processing when there are multiple processing units, each handling a portion of the application. If a request comes in that requires coordination between processing unit types (e.g., an order processing unit and a customer processing unit), it is the processing grid that mediates and orchestrates the request between those two processing units.

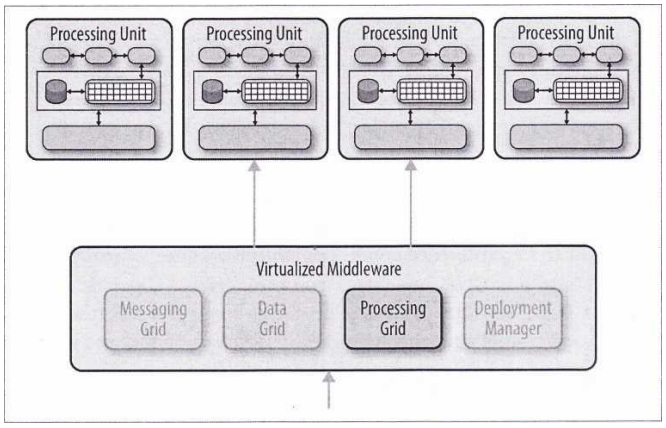


Figure 5. *Processing-grid component*

Deployment Manager

The deployment-manager component manages the dynamic startup and shutdown of processing units based on load conditions. This component continually monitors response times and user loads, and starts up new processing units when load increases, and shuts down processing units when the load decreases. It is a critical component to achieving variable scalability needs within an application.

Considerations

The space-based architecture pattern is a complex and expensive pattern to implement. It is a good architecture choice for smaller web-based applications with variable load (e.g., social media sites, bidding and auction sites). However, it is not well suited for traditional large-scale relational database applications with large amounts of operational data.

Although the space-based architecture pattern does not require a centralized data store, one is commonly included to perform the initial in-memory data grid load and asynchronously persist data updates made by the processing units. It is also a common practice to create separate partitions that isolate volatile and widely used transactional data from non-active data, in order to reduce the memory footprint of the in-memory data grid within each processing unit.

It is important to note that while the alternative name of this pattern is the cloud-based architecture, the processing units (as well as the virtualized middleware) do not have to reside on cloud-based hosted services or PaaS (platform as a service). It can just as easily reside on local servers, which is one of the reasons I prefer the name "space-based architecture."

From a product implementation perspective, you can implement many of the architecture components in this pattern through third- party products. Because the implementation of this pattern varies greatly in terms of cost and capabilities (particularly data replication times), as an architect, you should first establish what your specific goals and needs are before making any product selections.

Pattern Analysis

The following table contains a rating and analysis of the common architecture characteristics for the space-based architecture pattern. The rating for each characteristic is based on the natural tendency for that characteristic as a capability based on a typical implementation of the pattern, as well as what the pattern is generally known for. For a side-by-side comparison of how this pattern relates to other patterns in this report, please refer to Appendix A at the end of this report.

Overall agility

Rating: High

Analysis: Overall agility is the ability to respond quickly to a constantly changing environment. Because processing units (deployed instances of the application) can be brought up and down quickly, applications respond well to changes related to an increase or decrease in user load (environment changes). Architectures created using this pattern generally respond well to coding changes due to the small application size and dynamic nature of the pattern.

Ease of deployment

Rating: High

Analysis: Although space-based architectures are generally not decoupled and distributed, they are dynamic, and sophisticated cloud-based tools allow for applications to easily be "pushed" out to servers, simplifying deployment.

Testability

Rating: Low

Analysis: Achieving very high user loads in a test environment is both expensive and time consuming,

making it difficult to test the scalability aspects of the application.

Performance

Rating: High

Analysis: High performance is achieved through the in-memory data access and caching mechanisms build into this pattern.

Scalability

Rating: High

Analysis: High scalability come from the fact that there is little or no dependency on a centralized database, therefore essentially removing this limiting bottleneck from the scalability equation.

Ease of development

Rating: Low

Analysis: Sophisticated caching and in-memory data grid products make this pattern relatively complex to develop, mostly because of the lack of familiarity with the tools and products used to create this type of architecture. Furthermore, special care must be taken while developing these types of architectures to make sure nothing in the source code impacts performance and scalability.

Summary

Table A-l summarizes the pattern-analysis scoring for each of the architecture patterns described in this report. This summary will help you determine which pattern might be best for your situation. For example, if your primary architectural concern is scalability, you can look across this chart and see that the event-driven pattern, microservices pattern, and space-based pattern are probably good architecture pattern choices. Similarly, if you choose the layered architecture pattern for your application, you can refer to the chart to see that deployment, performance, and scalability might be risk areas in your architecture

	Layered	Event-driven	Microkernel	Microservices	Space-based
Overall Agility	↓	↑	↑	↑	↑
Deployment	↓	↑	↑	↑	↑
Testability	↑	↓	↑	↑	↓
Performance	↓	↑	↑	↓	↑
Scalability	↓	↑	↓	↑	↑
Development	↑	↓	↓	↑	↓

Table 1

While this chart will help guide you in choosing the right pattern, there is much more to consider when choosing an architecture pattern. You must analyze all aspects of your environment, including infrastructure support, developer skill set, project budget, project deadlines, and application size (to name a few). Choosing the right architecture pattern is critical, because once an architecture is in place, it is very hard (and expensive) to change.

Bibliography:

1. O'Reilly, Software Architecture Patterns, Mark Richards'2016

CALCULATION OF PARAMETERS OF TENSELY DEFORMED STATE OF DISK PIEZOELEMENTS WITH SURFACES PARTIALLY COVERED BY ELECTRODES

Dr. Bazilo C. PhD.
Faculty of Electronic Technologies and Robotics – Cherkasy State Technological University, Ukraine
b_constantine@ukr.net

Abstract: *A mathematical formulation of the boundary problems of mathematical physics is made, sequential solution which allows describing the stress-strain state and the transfer characteristics of the piezoelectric elements with surfaces partial covering by electrodes. The set of formulated boundary problems makes mathematical content of energy-power method of analysis of the physical condition of the piezoelectric elements in the regime of forced oscillations under the influence of an external source of electrical energy. The proposed sequence of computational procedures can be used in the study of forced oscillations of microelectromechanical structures.*

Keywords: PIEZOELECTRIC ELEMENT, PARTIALLY COVERING BY ELECTRODES, MICROELECTROMECHANICAL STRUCTURES, ELECTRICAL IMPEDANCE, STRESS-STRAIN STATE.

1. Introduction

The relevance of the use of various functional elements of piezoelectronics in power and informational systems is due, above all, to their high reliability. The final goal of mathematical modeling of the vibrating piezoelectric elements physical condition is a qualitative and quantitative description of characteristics and parameters of existing electrical and elastic fields [1-2].

In 1986 [3] for the first time in the pages of scientific journals appeared abbreviation MEMS, which replaced the long spoken phrase microelectromechanical structures. Currently leading companies – manufacturers of electronic components serially produced a rather extensive list of elements, in which various MEMS are included. This, above all, the various accelerometers, which are produced by millions of copies, resonators and implemented on the basis of their electrical signals filters, transformers and other microminiature electromechanical systems.

MEMS manufacturing technology are currently called as microsystem technology. MEMS or what is the same, piezoelectric elements produced by means of microsystem technology have much in common with conventional piezoelectric elements, i.e. not of microscopic size, which are made of piezoelectric ceramics. For the realization of various features in MEMS used polycrystal ferroelectrics, which are polarized by a constant electric field in a predetermined direction. Conventional piezoelectric elements are made of piezoelectric ceramics, which initially is a polycrystalline ferroelectric, which on the last process step of the piezoceramic product manufacturing is polarized by constant electric field of given orientation. A distinctive feature between the MEMS and conventional piezoelectric elements is a method of working surfaces covering by electrodes. Conventional piezoelectric elements are usually of continuous electrodes surface. In some special cases, the electrodes are divided (cut) into areas which have no galvanic connection between them. In MEIS usually is used partial working surfaces covering by electrodes, when only part of the polarized ferroelectric surface is covered with a metal film. This method of covering by electrodes makes it possible to excite in volume of MEMS several types of elastic vibrations. Manipulating the geometric parameters of surfaces covering by electrodes, you can manage energy oscillatory processes in MEMS, i.e. create conditions where one type of oscillatory motions will dominate over the rest in amplitude of the elastic displacement vector of material particles.

Partial surfaces covering by electrodes has the effect that the electric field in the volume of the ferroelectric become dependent on the values of the coordinates of the observation point for the parameters of the electric field. This phenomenon is absent in the conventional piezoelectric elements. On the condition of constancy of the alternating electric field intensity in the volume of the piezoelectric element, created by external generator of electrical signals are based methods of calculation the stress-strain state of the piezoelectric plates and shells [4]. In the case of a partial surfaces covering by electrodes of the piezoelectric element these methods do not work.

The latter encourages the search for new approaches to the procedure of calculating the parameters of the stress-strain state and the transfer characteristics of the piezoelectric elements with partial surfaces covering by electrodes. Below we will present the general scheme of the computational procedures execution, which, in principle, allows you to estimate the parameters of the stress-strain state and the transfer characteristics of the piezoelectric elements with partial surfaces covering by electrodes. This scheme can be used as a theoretical basis for the mathematical modeling of MEMS.

2. Sequence of computational procedures in the calculation of the piezoelectric elements

Consider a piezoelectric element for certainty in the form of a plate bounded by arbitrarily curved contour K (Fig. 1).

The plate is located in the Cartesian coordinate system (x_1, x_2, x_3) so that the origin of the system is on the middle surface of the plate. To simplify the subsequent discussion, we assume that the plate is made of polarized in thickness, i.e. in the axis direction Ox_3, piezoelectric ceramics. We also assume that the polarization is made by a constant electric field, the axial component of the intensity vector which had a constant value at any point in the volume of the plate. This allows to assert that material constants of the piezoelectric plate (the dielectric constant tensor components, piezoelectric modules and elasticity modules) does not depend on the coordinates of the point inside the volume of the plate and are given by matrices of the following form:

a) matrix of the dielectric constants χ_{ij}^{ε}, that are experimentally determined in the mode of constancy (equality to zero) of elastic deformations (upper symbol ε):

$$\left|\chi_{ij}^{\varepsilon}\right| = \begin{vmatrix} \chi_{11}^{\varepsilon} & 0 & 0 \\ & \chi_{22}^{\varepsilon} & 0 \\ & & \chi_{33}^{\varepsilon} \end{vmatrix}, \qquad (1)$$

where $\chi_{11}^{\varepsilon} = \chi_{22}^{\varepsilon} \neq \chi_{33}^{\varepsilon}$;

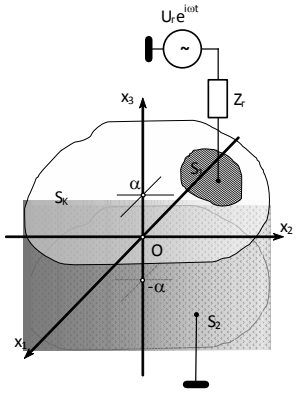


Fig. 1. *Piezoelectric element with partial surfaces covering by electrodes* $x_3 = \pm\alpha$

b) matrix of the piezoelectric modules $e_{k\beta}$ ($k=1,2,3$; $\beta=1,2,3,4,5,6$ – Voigt index):

$$\left|e_{k\beta}\right| = \begin{vmatrix} 0 & 0 & 0 & 0 & e_{15} & 0 \\ 0 & 0 & 0 & e_{24} & 0 & 0 \\ e_{31} & e_{32} & e_{33} & 0 & 0 & 0 \end{vmatrix}, \quad (2)$$

where $e_{31}=e_{32}\neq e_{33}$; $e_{15}=e_{24}=\left(e_{33}-e_{31}\right)/2$;

c) matrix of the elasticity modules $c^E_{\beta\lambda}$, that are experimentally determined in the mode of constancy (equality to zero) of electric field intensity (upper symbol E), ((β, λ) = 1, … , 6 – Voigt index):

$$\left|c^E_{\beta\lambda}\right| = \begin{vmatrix} c^E_{11} & c^E_{12} & c^E_{13} & 0 & 0 & 0 \\ & c^E_{22} & c^E_{23} & 0 & 0 & 0 \\ & & c^E_{33} & 0 & 0 & 0 \\ & & & c^E_{44} & 0 & 0 \\ & & & & c^E_{55} & 0 \\ & & & & & c^E_{66} \end{vmatrix}, \quad (3)$$

where $c^E_{11}=c^E_{22}\neq c^E_{33}$; $c^E_{12}=c^E_{13}=c^E_{23}$; $c^E_{44}=c^E_{55}$; $c^E_{66}=\left(c^E_{11}-c^E_{12}\right)/2$.

Suppose that on the upper ($x_3=\alpha$) and lower ($x_3=-\alpha$) surfaces of the piezoelectric plate are arbitrarily located areas S_1 and S_2 accordingly (Fig. 1), which are coated with a thin layer of metal, i.e. covered by electrodes. Thus, in general $S_1\neq S_2\neq S_K$, where S_K – surface of the plate bounded by the contour K. The electrical potential $U_0e^{i\omega t}$ is supplied to the surface S_1 from the electrical signals generator (U_0 – amplitude of the electrical potential on the surface S_1 covered by electrodes; naturally, $U_0\neq U_g$, where U_g – amplitude value of the electric potential at the output of the generator; $i=\sqrt{-1}$; ω – angular frequency; t – time). Symbol Z_g in Fig. 1 denotes an electric output impedance of the electrical signals generator.

Denote the amplitude value of intensity vector of the alternating electric field by symbol $\vec{E}^*(x_k)$. Will determine the electric polarization, which is created by an alternating electric field in the volume of the piezoelectric plate, by the time-varying electric induction vector according to the law $e^{i\omega t}$, amplitude value of which is denoted by $\vec{D}^*(x_k)$. At the same time there is the linear conformity between the components of the electric induction vector and the electric field intensity vector of the following form

$$D^*_k(x_k)=\chi^{\varepsilon}_{kj}E^*_j(x_k). \quad (4)$$

In (4), and in all subsequent recordings of this type is assumed the summation over twice repeated index. In the formula (4) such index is symbol j which sequentially assumes values 1, 2, 3.

Characteristics of an alternating electric field in the volume of the piezoelectric element are determined by Maxwell's equations, which for the amplitude values of the electric and magnetic components of the electromagnetic field can be written in the following form

$$rot\,\vec{H}^*(x_k)=\vec{J}^*(x_k)+i\omega\vec{D}^*(x_k), \quad (5)$$

$$rot\,\vec{E}^*(x_k)=-i\omega\vec{B}^*(x_k), \quad (6)$$

where $\vec{B}^*(x_k)=\mu_0\vec{H}^*(x_k)$; $\mu_0=4\pi\cdot10^{-7}$ H/m – magnetic permeability of vacuum; $\vec{B}^*(x_k)$ and $\vec{H}^*(x_k)$ – amplitudes of harmonically time-varying vectors of induction and magnetic field intensity; $\vec{J}^*(x_k)$ – amplitude of the conduction current surface density vector. Since the piezoelectric ceramics is a pretty good dielectric we can write $\vec{J}^*(x_k)=0$. This means that the properties of the ideal dielectric are attributed to real piezoelectric ceramics.

Calculating the divergence of the left and right parts of the Maxwell equations (5), we obtain, in the case of an ideal dielectric, the following result

$$div\,\vec{D}^*(x_k)=0. \quad (7)$$

In [4] it is proved that in the frequency range from zero to tens of megahertz equation (6) for ideal dielectrics can be written in the following form

$$rot\,\vec{E}^*(x_k)\cong 0. \quad (8)$$

Condition (8) indicates a potential character of the alternating electric field in the piezoelectric element volume. For this reason, is possible the description of this field with the help of the scalar potential $\Phi^*(x_k)e^{i\omega t}$. At the same time amplitude value $\vec{E}^*(x_k)$ of intensity vector of the alternating electric field created by an external source, i.e. generator of electrical signals, is defined in the standard [5] way

$$\vec{E}^*(x_k)=-grad\,\Phi^*(x_k). \quad (9)$$

Substituting the definition (9) into (4), and the obtained result into condition (7) of the absence of electricity free carriers, we obtain the Laplace differential equation whose solution determines the amplitudes of the electric potential $\Phi^*(x_k)$:

$$\frac{\partial^2\Phi^*(x_k)}{\partial x_1^2}+\frac{\partial^2\Phi^*(x_k)}{\partial x_2^2}+\xi^2\frac{\partial^2\Phi^*(x_k)}{\partial x_3^2}=0, \quad (10)$$

where $\xi^2=\chi^{\varepsilon}_{33}/\chi^{\varepsilon}_{11}$ – squared coefficient of anisotropy of the piezoelectric ceramics dielectric constant.

The general solution of the differential equation (10) must satisfy the following conditions at the boundaries of the region of existence:

$$\Phi^*(x_k)\big|_{x_3=\alpha}=U_0\;\forall(x_1,x_2)\in S_1; \quad (11)$$

$$\left.\frac{\partial\Phi^*(x_k)}{\partial x_3}\right|_{x_3=\alpha}=0\;\forall(x_1,x_2)\in S_K-S_1, \quad (12)$$

$$\frac{\partial\Phi^*(x_k)}{\partial n}=0\;\forall(x_k)\in K, \quad (13)$$

$$\left.\frac{\partial\Phi^*(x_k)}{\partial x_3}\right|_{x_3=-\alpha}=0\;\forall(x_1,x_2)\in S_K-S_2, \quad (14)$$

$$\Phi^*(x_k)\big|_{x_3=-\alpha}=0\forall(x_1,x_2)\in S_2, \quad (15)$$

where symbol $\partial/\partial n$ denotes the derivative in the direction of the outward unit normal to the lateral surface of the plate, which relies on the contour K.

Conditions (11) and (15) are self-evident. Conditions (12) – (14) are approximate [4] and are performed the more accurate when the dielectric constant of the piezoelectric the more differs dielectric constant of vacuum $\chi_0=8{,}85\cdot10^{-12}$ F/m. For piezoelectric ceramics PZT-type dielectric constant is $\chi^{\varepsilon}_{ij}\geq10^3\chi_0$ and thus the boundary conditions (12) – (14) can be considered practically exact. If the dielectric constant of polarized ferroelectric in MEMS less than $10\chi_0$, that, incidentally, has not yet happened, then the conditions (12) – (14) must be reformulated, taking into account the existence of the stray fields.

Solution of the boundary problem (10) – (15) is the first computational procedure when performing calculations of parameters of the stress-strain state of the piezoelectric elements that are compatible with microsystem technologies. At this stage, actually determined energy levels of the electric field at any arbitrarily predetermined point in the volume of the piezoelectric

element. It must be emphasized that the potential $\Phi^*(x_k)$ is calculated assuming that it is completely determined by the geometric parameters of the piezoelectric element, and does not depend on the parameters of the elastic and electric fields, that are generated in the volume of the vibrating piezoelectric element.

After determining the potential $\Phi^*(x_k)$ the equation of physical condition of oscillating piezoelectric element, calculation scheme is shown in Fig. 1, can be written in the following form

$$\sigma_{ij} = c^E_{ijk\ell}\frac{\partial u_\ell}{\partial x_k} - e_{kij}\left(\frac{\partial \Phi}{\partial x_k} + \frac{\partial \Phi^*}{\partial x_k}\right), \quad (16)$$

$$D_m = e_{mij}\frac{\partial u_i}{\partial x_j} + \chi^\varepsilon_{mj}\left(\frac{\partial \Phi}{\partial x_j} + \frac{\partial \Phi^*}{\partial x_j}\right), \quad (17)$$

where σ_{ij} – amplitude value of the tensor component of the resulting mechanical stresses; u_ℓ – amplitude of the time-varying ℓ-th component of the displacement vector of a piezoelectric material particles according to harmonic law $e^{i\omega t}$; $\Phi \equiv \Phi(x_k)$ – scalar potential of the internal electric field [6], which arises as a result of the displacement of a piezoelectric ions from equilibrium positions from the crystal lattice sites; $\Phi^* \equiv \Phi^*(x_k)$ – known scalar potential of the alternating electric field created by an external source (generator). By its physical content the equation of physical condition (16) is a generalized Hooke's law for an elastic medium with piezoelectric effects, and equation (17) is the law of the electric polarization of the dielectric with piezoelectric properties.

Newton's second law in differential form or what is the same – the motion equation of a material particle of the elastically deformable solid, in the general case can be written as follows:

$$\frac{\partial \sigma_{ji}(x_k, t)}{\partial x_j} = \rho_0 \frac{\partial^2 u_i(x_k, t)}{\partial t^2}, \quad (18)$$

where ρ_0 - density of deformable solid. Substituting the equation (16) into the definition (18), and taking into account that all of the physical fields in the volume of a deformable piezoelectric element change in time according to harmonic law $e^{i\omega t}$ we obtain the following equation

$$c^E_{ijk\ell}\frac{\partial^2 u_\ell}{\partial x_k \partial x_j} - e_{kij}\frac{\partial^2 \Phi}{\partial x_k \partial x_j} + \rho_0 \omega^2 u_i = f_i^K(x_k), \quad (19)$$

where $f_i^K(x_k) = e_{kij}\frac{\partial^2 \Phi^*}{\partial x_k \partial x_j}$ – amplitude value of the i-th component of volume density of the Coulomb forces that are generated by an external source (generator) of the electric field. Naturally, the second term on the left-hand side of equation (19) also makes sense as the i-th component of the volume density vector amplitude value of the Coulomb forces, which arise in the volume of the deformable piezoelectric by internal electric field and prevent its deformation by electric fields of external sources. For small values of piezoelectric modules, i.e. when $e_{kij} \le 1$ C/m^2 the second summand in the equation, in principle, can be ignored. But for piezoelectric ceramics of PZT type, that have $e_{kij} \le 20$ C/m^2 the Coulomb forces of internal electric field cannot be ignored. These forces, i.e. the second summand in equation (19), act in accordance with the forces of elasticity (the first summand) and increase the effective rigidity of the piezoelectric. In some directions the rigidity of piezoelectric ceramics can be increased more than 50%.

Condition (7) of the electricity free carriers absence in piezodielectric is true, obviously, for any representation of the electric induction vector. Since $div\vec{D}(x_k) = 0$, then after substitution the equation (17) into this condition, we obtain the following result

$$\frac{\partial^2 \Phi}{\partial x_1^2} + \frac{\partial^2 \Phi}{\partial x_2^2} + \xi^2\frac{\partial^2 \Phi}{\partial x_3^2} + \frac{1}{\chi_1^\varepsilon}e_{mij}\frac{\partial^2 u_i}{\partial x_m \partial x_j} = 0. \quad (20)$$

Equations (19) and (20) are, in general, are a system of four differential equations of second order partial derivatives. Uniqueness of the solution of this equations system is provided by the boundary conditions. If the piezoelectric element fluctuates in a vacuum, i.e. has no mechanical contact with other material objects, then on his lateral surfaces due to the execution of the third law of Newton the normal and tangential stresses that acting on the elementary areas of these surfaces should turn to zero. With regard to the calculation scheme, which is shown in Fig. 1, the foregoing can be written as follows:

$$c_{3jk\ell}\frac{\partial u_\ell}{\partial x_k} - e_{k3j}\left(\frac{\partial \Phi}{\partial x_k} + \frac{\partial \Phi^*}{\partial x_k}\right)\Bigg|_{x_3 = \pm\alpha} = 0 \,\forall (x_1, x_2) \in S_K, \quad (21)$$

$$n_i\left[c_{ijk\ell}\frac{\partial u_\ell}{\partial x_k} - e_{kij}\left(\frac{\partial \Phi}{\partial x_k} + \frac{\partial \Phi^*}{\partial x_k}\right)\right] = 0 \,\forall\, x_k \in K, \quad (22)$$

where n_i – vector components of the outward unit normal to the lateral cylindrical surface of the piezoelectric element, whose base is curved contour K (Fig. 1).

The scalar potential $\Phi(x_k)$ of the internal electric field must satisfy the following boundary conditions

$$\Phi(x_k)\big|_{x_3 = \alpha} = 0 \,\forall (x_1, x_2) \in S_1, \quad (23)$$

$$\frac{\partial \Phi(x_k)}{\partial x_3}\Bigg|_{x_3 = \alpha} = 0 \,\forall (x_1, x_2) \in S_K - S_1, \quad (24)$$

$$\frac{\partial \Phi(x_k)}{\partial x_1}\Bigg|_{x_3 = \alpha} = \frac{\partial \Phi(x_k)}{\partial x_2}\Bigg|_{x_3 = \alpha} = 0 \,\forall (x_1, x_2) \in S_1, \quad (25)$$

$$n_i\frac{\partial \Phi(x_k)}{\partial x_i} = 0 \,\forall\, x_k \in K, \quad (26)$$

$$\Phi(x_k)\big|_{x_3 = -\alpha} = 0 \,\forall (x_1, x_2) \in S_2, \quad (27)$$

$$\frac{\partial \Phi(x_k)}{\partial x_3}\Bigg|_{x_3 = -\alpha} = 0 \,\forall (x_1, x_2) \in S_K - S_2, \quad (28)$$

$$\frac{\partial \Phi(x_k)}{\partial x_1}\Bigg|_{x_3 = \alpha} = \frac{\partial \Phi(x_k)}{\partial x_2}\Bigg|_{x_3 = \alpha} = 0 \,\forall (x_1, x_2) \in S_1. \quad (29)$$

Formulated by (19) – (29) the boundary problem is the most complete and general mathematical formulation of the electroelasticity boundary problem of the finite size piezoelectric elements steady harmonic vibrations.

It can be argued that the exact solution of the boundary problem cannot be implemented. However, it is possible to create an algorithm for the approximate solution of the problem (19) – (29). Computational procedure, which will be discussed, can be called the method of sequential approximations. In this case, the unknown components of the displacement vector $u_\ell(x_k)$ and scalar potential $\Phi(x_k)$ are represented by convergent series as follows

$$u_\ell(x_k) = u_\ell^{(0)}(x_k) + \sum_{\nu=1}^{\infty}\Delta u_\ell^{(\nu)}(x_k),$$

$$\Phi(x_k) = \Phi^{(0)}(x_k) + \sum_{\nu=1}^{\infty}\Delta\Phi^{(\nu)}(x_k), \quad (30)$$

where $u_\ell(x_k)$, $\Phi(x_k)$ – exact solutions of equations (19), (20) system; $u_\ell^{(0)}(x_k)$ and $\Phi^{(0)}(x_k)$ – zero approximation to exact solutions; $\Delta u_\ell^{(\nu)}(x_k)$ and $\Delta\Phi^{(\nu)}(x_k)$ – ν-th order corrections to zero approximations of the exact $u_\ell(x_k)$ and $\Phi(x_k)$.

Zero approximation $u_\ell^{(0)}(x_k)$ to the exact value of the ℓ-th component amplitude of piezoelectric element material particles displacement vector is found by solving the following stationary boundary problem

$$c_{ijk\ell}^E \frac{\partial^2 u_\ell^{(0)}}{\partial x_k \partial x_j} + \rho_0 \omega^2 u_\ell^{(0)} = f_i^K, \quad (31)$$

$$\left[c_{3jk\ell}^E \frac{\partial u_\ell^{(0)}}{\partial x_k} - \sigma_{3j}^K \right]_{x_3 = \pm\alpha} = 0 \forall (x_1, x_2) \in S_K, \quad (32)$$

$$n_i \left[c_{ijk\ell}^E \frac{\partial u_\ell^{(0)}}{\partial x_k} - \sigma_{ij}^K \right] = 0 \forall x_k \in K, \quad (33)$$

where $\sigma_{3j}^K = e_{k3j}\left(\partial \Phi^* / \partial x_k\right)$, $\sigma_{ij}^K = e_{kij}\left(\partial \Phi^* / \partial x_k\right)$ – Coulomb forces surface densities of external source electric field or, which is the same, the Coulomb tensions.

Thus, the zero approximation to the exact values of the displacement vector components of the piezoelectric material particles is formed by solution of the boundary problem (31) – (33). According to the physical content, this boundary problem of the elasticity dynamic theory is the problem of the excitation of piezoelectric element harmonic oscillations by the system of the volumetric (f_i^K) and surface (σ_{ij}^K) loads. It should be emphasized that at full piezoelectric elements surfaces covering by electrodes and even in the case of separated electrodes the Coulomb forces volume density is zero, and the excitation of elastic waves in such piezoelectric elements is operated by surface loads σ_{ij}^K.

After solving the boundary problem (31) – (33) the zero approximation to the exact value of the internal electric field scalar potential is determined. Equation (20) can be written in the following form

$$\frac{\partial^2 \Phi^{(0)}}{\partial x_1^2} + \frac{\partial^2 \Phi^{(0)}}{\partial x_2^2} + \xi^2 \frac{\partial^2 \Phi^{(0)}}{\partial x_3^2} = -\frac{\rho_{pe}^{(0)}}{\chi_1^\varepsilon}. \quad (34)$$

where $\rho_{pe}^{(0)} = e_{mij} \frac{\partial^2 u_i^{(0)}}{\partial x_m \partial x_j}$ - zero approximation to the exact value of volume density of the polarization electric charge in the volume of the deformable piezoelectric. The general solution of the Poisson equation (34), i.e. the function $\Phi^{(0)}(x_k)$ must satisfy the boundary conditions (23) – (29).

After the determination of the zero approximation $\Phi^{(0)}(x_k)$ the correction $\Delta u_\ell^{(1)}$ is calculated. For this purpose, into the equation (19) values $\vec{u}(x_k) \approx \vec{u}^{(0)}(x_k) + \Delta \vec{u}^{(0)}(x_k)$ and $\Phi(x_k) \approx \Phi^{(0)}(x_k)$ are inserted. Equation (19) takes the form

$$c_{ijk\ell}^E \frac{\partial^2 \Delta u_\ell^{(1)}}{\partial x_k \partial x_j} + \rho_0 \omega^2 \Delta u_\ell^{(1)} = f_i^{(0)}, \quad (35)$$

where $\Delta u_\ell^{(1)}$ and $\Delta u_i^{(1)}$ – first-order corrections to the zero approximations $u_\ell^{(0)}$ and $u_i^{(0)}$ of the components exact values $u_\ell(x_k)$ and $u_i(x_k)$ of the piezoelectric material particles displacement vector; $f_i^{(0)} = e_{kij} \frac{\partial^2 \Phi^{(0)}}{\partial x_k \partial x_j}$ – zero approximation to the i-th component exact value of the Coulomb forces volume density vector, which are formed by the internal electric field in the volume of the deformable piezoelectric.

Uniqueness of the system (35) solution is ensured by the boundary conditions that can be written as follows:

$$\left[c_{3jk\ell}^E \frac{\partial \Delta u_\ell^{(1)}}{\partial x_k} - \sigma_{3j}^{(0)} \right]_{x_3 = \pm\alpha} = 0 \forall (x_1, x_2) \in S_K, \quad (36)$$

$$n_i \left[c_{ijk\ell}^E \frac{\partial \Delta u_\ell^{(1)}}{\partial x_k} - \sigma_{ij}^{(0)} \right] = 0 \forall x_k \in K, \quad (37)$$

where $\sigma_{3j}^{(0)} = e_{k3j}\left(\partial \Phi^{(0)} / \partial x_k\right)$, $\sigma_{ij}^{(0)} = e_{kij}\left(\partial \Phi^{(0)} / \partial x_k\right)$ – zero approximations to the exact value of the Coulomb forces surface densities, which are formed by the internal electric field in the volume of the vibrating piezoelectric element.

It should be emphasized that the boundary problem (35) – (37) can be solved by the same manner in which the boundary problem (31) – (33) has been solved. This means that after the construction of an analytical expression for $\vec{u}^{(0)}(x_k)$, i.e. for the zero approximation to the exact value of the piezoelectric element material particles displacement vector, is not need to re-construct general solutions for first-order correction $\Delta \vec{u}^{(1)}(x_k)$ and for all subsequent orders corrections $\Delta \vec{u}^{(\nu)}(x_k)$. To obtain the numerical values of corrections $\Delta \vec{u}^{(\nu)}(x_k)$ is necessary only to substitute into general solutions of the boundary problem (31) – (33) the corresponding values of the Coulomb forces volume and surface densities, which are formed by internal electric field in the volume of the piezoelectric vibrating element.

After receiving the first approximation $\vec{u}^{(1)}(x_k) = \vec{u}^{(0)}(x_k) + \Delta \vec{u}^{(1)}(x_k)$ to the exact value of the material particles displacement vector, you can implement the assessment of correction $\Delta \Phi^{(1)}(x_k)$ to the exact value $\Phi(x_k)$ of the internal electric field scalar potential. Substituting $\vec{u}^{(1)}(x_k) = \vec{u}^{(0)}(x_k) + \Delta \vec{u}^{(1)}(x_k)$ into equation (34) and setting at the same time that $\Phi(x_k) \approx \Phi^{(0)}(x_k) + \Delta \Phi^{(1)}(x_k)$ we get the Poisson equation to determine the correction $\Delta \Phi^{(1)}(x_k)$:

$$\frac{\partial^2 \Delta \Phi^{(1)}}{\partial x_1^2} + \frac{\partial^2 \Delta \Phi^{(1)}}{\partial x_2^2} + \xi^2 \frac{\partial^2 \Delta \Phi^{(1)}}{\partial x_3^2} = -\frac{\Delta \rho_{pe}^{(1)}}{\chi_1^\varepsilon}, \quad (38)$$

where $\Delta \rho_{pe}^{(1)} = e_{mij} \frac{\partial^2 \Delta u_i^{(1)}}{\partial x_m \partial x_j}$ – first-order correction to the exact value zero approximation of the polarization charge volume density in the volume of the deformable piezoelectric. Uniqueness of the equation (38) solution is ensured by the boundary conditions (23) – (29).

Again, as in the determination of correction $\Delta \vec{u}^{(1)}(x_k)$, can be made obvious conclusion. To receive correction $\Delta \Phi^{(1)}(x_k)$ as, obviously, all subsequent corrections $\Delta \Phi^{(\nu)}(x_k)$, is no need for a new solution of (38) and subsequently satisfaction of the boundary conditions (23) – (29). To determine the correction $\Delta \Phi^{(1)}(x_k)$ is necessary and sufficient to substitute the value $\Delta \rho_{pe}^{(1)}$ into general solution of equation (34) instead of the volume density $\rho_{pe}^{(0)}$. It is obvious that the correction of ν-th order, i.e. the value $\Delta \Phi^{(\nu)}(x_k)$ is determined by the general solution of equation (34), in the right-hand part of which is written the correction $\Delta \rho_{pe}^{(\nu)}(x_k)$.

Approximate calculation of the components of the displacement vector and scalar potential of the internal electric field forms the

content the second computational procedure for the processes mathematical modeling, which are developed in the volume of the piezoelectric element with partial surfaces covering by electrodes.

The results that are obtained after the first and second computing procedures, i.e. formulas for calculating the electric field potential $\Phi^*(x_k)$ created in the volume of the piezoelectric element by electrical signals generator, for the scalar potential $\Phi(x_k)$ of the internal electric field and the displacement vector $\vec{u}(x_k)$ of material particles, linearly depend on electric potential U_0 that exists on the surface S_1 covered by electrodes. From the above it follows that these relations can be calculated in the following form

$$\Phi^*(x_k) = U_0\tilde{\Phi}^*(x_k,\Pi),\ \Phi(x_k) = U_0\tilde{\Phi}(x_k,\omega,\Pi), \qquad (39)$$

$$u_\ell(x_k) = U_0\frac{e_{33}}{c_{33}^E}\tilde{u}_\ell(x_k,\omega,\Pi), \qquad (40)$$

where $\tilde{\Phi}^*(x_k,\Pi)$, $\tilde{\Phi}(x_k,\omega,\Pi)$ и $\tilde{u}_\ell(x_k,\omega,\Pi)$ – dimensionless functions of the observation point coordinates and set of physical, mechanical and geometrical (symbol Π in the argument list) parameters of the piezoelectric element; construction of the right part of (40) is due to the values dimension included in it.

Since the potential $U_0 \neq U_g$, i.e. the potential U_0 is actually the uncertain quantity, so the third and final computational procedures aim to determine the potential amplitude value on the piezoelectric element surface covered by electrodes.

Obviously, the influence of the piezoelectric element to the amplitude of the electric current in the conductor, which connects it to the electric signals generator, can be described using the electrical impedance $Z_{el}(\omega)$ of the piezoelectric element. Electrical impedance $Z_{el}(\omega)$ must satisfy the basic terms and definitions of theoretical electrical engineering and, therefore, Ohm's law for the section of electrical circuit, i.e.

$$Z_{el}(\omega) = \frac{U_0}{I}, \qquad (41)$$

where I – amplitude of the electric current in the conductors which are connected to the piezoelectric element surface sections covered by electrodes (Fig. 1). Current or amplitude value of I is directly proportional to the velocity variation in time of the electric charge Q on the piezoelectric element surface covered by electrodes. For harmonic changing in time according to $e^{i\omega t}$ the amplitude I is determined as follows

$$I = -i\omega Q_1 = -i\omega Q_2, \qquad (42)$$

where Q_1 and Q_2 – amplitude values of the electric charges on the surfaces S_1 and S_2 (Fig. 1).

The amplitude value of the electric charge Q_1 is determined as follows:

$$Q_1 = \iint_{S_1} D_3(x_1,x_2,\alpha)\,dS_1 =$$

$$= \iint_{S_1}\left[e_{3ij}\frac{\partial u_i}{\partial x_j} + \chi_{3j}^{\varepsilon}\left(\frac{\partial\Phi}{\partial x_j} + \frac{\partial\Phi^*}{\partial x_j}\right)\right]\Bigg|_{x_3=\alpha} dS_1 =$$

$$= U_0 C^{\varepsilon}(\omega,\Pi), \qquad (43)$$

where $C^{\varepsilon}(\omega,\Pi)$ – dynamic electric capacitance of the piezoceramic element.

Thus, $I = -i\omega U_0 C^{\varepsilon}(\omega,\Pi)$ and the electrical impedance of the piezoelectric element is

$$Z_{el}(\omega) = -\frac{1}{i\omega C^{\varepsilon}(\omega,\Pi)}. \qquad (44)$$

From the connection diagram of the electrical signals generator (Fig. 1) it follows that

$$U_0 = \frac{U_g Z_{el}(\omega)}{Z_g + Z_{el}(\omega)} = \frac{U_g}{1 - i\omega Z_g C^{\varepsilon}(\omega,\Pi)}, \qquad (45)$$

where $C^{\varepsilon}(\omega,\Pi)$ is defined by a double integral in (43).

Calculation of the electric potential U_0 is the content of the third computational procedure in mathematical modeling of piezoelectric elements with partial surfaces covering by electrodes.

After completing the third and last computational procedure we can write an expression for calculating the displacement of the piezoelectric element material particles in the next, final, form

$$u_\ell(x_k) = \frac{e_{33}U_{\tilde{a}}}{c_{33}^E\left[1 - i\omega Z_{\tilde{a}} C^{\varepsilon}(\omega,\Pi)\right]}\tilde{u}_\ell(x_k,\omega,\Pi). \qquad (46)$$

3. Discussions and Conclusions

Equation (46) is a mathematical model of the dynamic stress-strain state of the piezoelectric element with partial surfaces covering by electrodes and is a key relation for quantitative estimates of the transfer characteristics of the piezoelectric element in all variants of its functional use. Frequency dependent function $C^{\varepsilon}(\omega,\Pi)$ is the theoretical basis for the equivalent circuits construction in the sense in which they were proposed in 1925 – 1928 by Walter G. Cady to radio engineers, who were involved in the calculation and design of high-frequency electrical signal generators with the quartz resonator in the generation frequency stabilization circuit.

The main results of this work can be formulated as follows:

1. For the first time the sequence of computational procedures is proposed, which allows when calculating transfer characteristics to use the full range of physical, mechanical and geometrical parameters of the piezoelectric element and the final value of the output electric impedance of the electrical signals generator.

2. For the first time the method is proposed, which allows you to perform real situation adequate assessment of the connectivity effect of elastic and electric fields in the case of their arbitrary distribution in the volume of vibrating piezoelectric element.

3. The formulated complete set of boundary problems of technical electrodynamics and elasticity dynamic theory is the mathematical content of the energy-power method [7] of piezoelectric elements physical state analysis in the regime of forced oscillations under the influence of the electrical energy external source.

4. The proposed sequence of computational procedures can be recommended as a theoretical basis for characteristics calculating of the piezoelectric elements with partial surfaces covering by electrodes and microelectromechanical structures (MEMS).

4. References

[1] Bogdan A.V., Petrishchev O.N., Yakimenko Yu.I., Yanovskaya Yu.Yu. (2009). Investigation of the characteristics of the piezoelectric transformer on the basis of the radial oscillations in a thin piezoceramic disks. Electronics & Communications, P. 1, pp. 269–274.

[2] Bogdan A.V., Petrishchev O.N., Yakimenko Yu.I., Yanovskaya Yu.Yu. (2009). Mathematical modeling of vibrations of thin piezoceramic disks to create functional piezoelectronics elements. Electronics & Communications, P. 2, pp. 35–42.

[3] Varadan V., Vinoy K., Jose K. RF MEMS and their applications. Moscow: Technosphera, 2004, 528 p.

[4] Grinchenko V.T., Ulitko A.F., Shulga N.A. Mechanics of related fields in elements of constructions. Kyiv: Nauk. dumka, 1989, 280 p.

[5] Tamm I.E. Fundamentals of the electricity theory. Moscow: Nauka, 1976, 616 p.

[6] Petrishchev O.N. Harmonic oscillations of piezoceramic elements. Kyiv: Avers, 2012, 300 p.

[7] Sharapov V. Piezoceramic sensors. Heidelberg, Dordrecht, London, New York: Springer Verlag, 2011, 498 p.

KNOWLEDGE, CREATIVITY AND INNOVATION IN KNOWLEDGE SOCIETY FORMATION

ЗНАНИЯ, КРЕАТИВНОСТЬ И ИННОВАЦИИ В ФОРМИРОВАНИИ ОБЩЕСТВА ЗНАНИЙ

Zhavoronkova G., Doctor of Economic Sciences, Professor,
National Aviation University,
Zavalko K. Doctor of Pedagogical Sciences, Professor,
National Dragomanov Pedagogical University,
Zhavoronkov V., PhD (Economics), Associate Professor,
National Aviation University, Kyiv, Ukraine.
zhavor@ukr.net

Annotation *The concept of a society of knowledge is considered in the article. It is proved that the knowledge economy, the core of which is the creative economy, provides the formation of a knowledge society. Today, the cultural industry, or creative economy, is considered as a new type of industry. The essence and peculiarities of the creative potential of a specialist are determined. The forecast indicators of Ukraine's creative potential development are presented. It is revealed that modern problems of economic development are connected with the intellectualization of labor, giving the highest priority to the processes of producing new knowledge. To achieve predictive indicators of intellectual and creative activity in Ukraine, it is necessary to fulfill certain tasks.*
KEYWORDS*: KNOWLEDGE SOCIETY, KNOWLEDGE ECONOMY, CREATIVE CORE OF KNOWLEDGE ECONOMY, CREATIVE POTENTIAL, INNOVATIVE WORK.*

1. Introduction

Today, the knowledge intensity of manufactured products is complicated, and the market for intellectual goods and services is growing. The growth of technologies in the broad sense comes at the same time as the growth of the role of knowledge-intensive technologies in the economic space; the system of education itself is transformed by the emergence of new educational technologies that change the nature of the object being studied. The need for continuous education throughout the working life faces workers in a context of constant renewal of knowledge, innovation transformations and tough competition. The above features are characteristics of the knowledge society. This concept postulates the development of ideas and approaches of T. Husen [1], who was the first to propose a model of a "learning society," and where "lifelong learning" is the necessity for every person throughout his or her life!

The trend towards the formation of a knowledge society and creative economy, carrying creative, complex and integrative nature, is clearly traced today in the leading countries of the world. Scientists put in the notion of creativity such characteristics that are inherent in the national economy as a whole, and not only in its separate areas, which are associated with purely creative activities. The creative economy is able to integrate culture, innovation, information and entrepreneurship into the overall technology of development and, on this basis, ensure the competitiveness of social systems [2]. Focusing on the long-term perspective is a key aspect in the implementation of creative development technologies. Moreover, the main emphasis should be on stimulating cultural and creative activity, establishing interaction between actors and means of their activity in the process of realizing creative potential.

2. The creative potential of the knowledge economy

Creative activity and the person's ability to creativity in socially useful activities become crucial in the knowledge economy. The purpose of this activity is the reproduction of intellectual capital. Accordingly, the agent of ownership also changes. "Homo creator", an agent with another system of values, needs and motives, is replacing rational "homo economicus". From the standpoint of the methodology, it is important to use the socio-personal approach in which the individual's mental capacities, creativity, initiative, the system of preferences and internal orientations, system thinking, analytical abilities, information susceptibility, etc. should serve as the object of analysis.

Today, commerce and creativity are so united and so inseparably linked with each other in the economy, which is almost impossible to distinguish between them. After all, cultural production leads to fusion, blurring of borders and mixing of genres - at the level of works, and at the level of professional activity. As a result, the borders between commerce and creativity, advertising and art, etc. are erased. So, a writer or scriptwriter can work as a copywriter in an advertising agency, filmmakers can create promotional and popular videos, and composers can write music screensavers or music for computer games. [3].

Large corporations are engaged in the financing of the production and distribution of a huge amount of commercial goods of culture, bringing incredible income. These companies occupy strategically beneficial countries and regions, provide an impact and have such an infrastructure that allows them to accumulate capital in accordance with their own payment systems and copyright. In other words, these companies have a definitive effect on the way of contracting with authors, contracting with contractors, as well as on economic recognition and reward for creativity.

In addition, large corporations have a significant influence on the formation of consumer preferences, their habits, professional assessment of marketers, and ultimately they are "talent hunters." Today, the cultural industry (creative economy) is recognized as a new type of industry. J. O'Connor writes that people who work in the cultural industry make a more significant contribution to the social changes in our era, which he called "an epoch of post-deficiency," when "cultural hierarchies are much fragmented and numerous" [4]. Cultural works are becoming commercial in the economy through a process that involves many people in marketing, advertising and public relations.

The planned indicators of Ukraine's creative development are determined on the basis of indicators for the leading countries by the end of 2010 (Table 1).

The analysis of the considered categories shows that the innovative potential of the individual is impossible without creative potential. In our context, creative potential is characterized as a combination of opportunities for purposeful transforming activity, the realization of the essential forces of the individual, depending on the activity of the agent, its target settings and external conditions. One can determine the essence and peculiarities of the creative potential of a specialist as a dynamic personality structure,

which includes a set of creative instincts that manifest and develop themselves in innovative professional activities.

Table 1 *Forecast indicators of Ukraine's creative potential development*

Показник	2010		2020 (forecast)
	Leader countries	Ukraine	Ukraine
Number of creative class,% of the employed population	35-47	20,5	35
Share of the population covered by higher education	28-38	25,3	35
Costs for research and technological development,% of GDP	2-3	0,83	2,3
Number of patents per 1 million population	0,7-1,3	0,36	1
Number of researchers,% of the employed population	250-600	84,3	350
Place in the world ranking in terms of creative development	1-30	49	25-30

3. Creative core of intellectual activity

In the economic theory of the information society, the category of "intellectual activity" is called to play a key role, similar to that which was played by the category "commodity - labor" for the creation of economic science by Marx, since creative work in the form of intellectual activity is the main source of value creation and a special factor in production in the information society, as well as the final stage in the development of human evolution in economic life.

Today, potential partners and investors are focusing not on tangible assets, but on the availability and value of intangible assets. Investments in the intangible assets in Ukraine remain negligible and equal to 3.3% of deposits in tangible assets. In 2016, there was a significant decline in investment in NMA, due to the volatile political and economic situation in the country (Figure 1).

In the EU, the volume of intangible assets is 50-80% of the book value of enterprises and organizations, and in Ukraine, they do not exceed 1.5% of the cost of fixed assets, while according to expert estimates, the real value of such assets is not less than 20 billion. UAH [5].

Creativity of intellectual activity of a person means the generation and production of such knowledge and skills, the use of which will not lead to negative social and socio-economic consequences in the life of the individual and society. Thus, in the knowledge economy, intelligence is focused on building knowledge and mental faculties of the agent, operating in the conditions of human morality, justice and a high level of general and economic culture.

The creative potential of the company lies in the willingness of staff to accept creative ideas and use innovative technologies, and creative process is a set of sequential steps that lead to success in its implementation, namely: understanding ideas, preparation for sale, comprehension, insight, confirm the idea by other people. Therefore, the creative sphere of activity of a modern enterprise is one of the most difficult to predict and obtain the result. To achieve the goal it is important to provide a creative atmosphere in the team to accumulate creative ideas, stimulate the development of the process of self-fulfillment of employees.

On the basis of the analysis of intellectual activity, the following components of the innovation activity of human brain function are distinguished [6]:

- *intellectual activity* - aimed at the analysis and systematization of existing knowledge, the formation of connections and the hierarchy of knowledge;
- *creative activity* - aimed at generating new ideas;
- *combinatorial activity* - aimed at the synthesis of various knowledge;
- *synergistic activity* - characterized by the speed of picking up an idea and the emergence of a chain creative reaction.

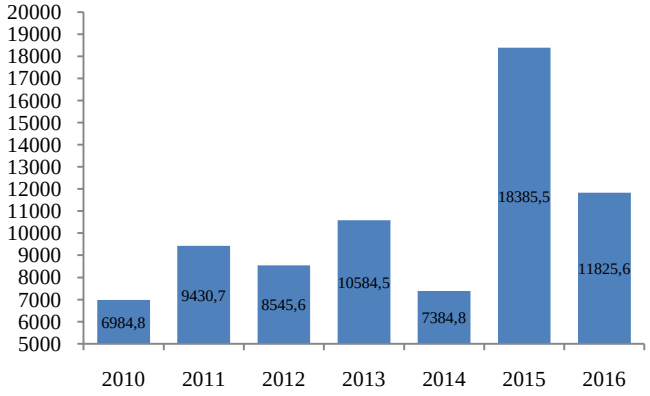


Figure 1. *Investments in intangible assets of enterprises Ukraine, mln. UAH.*

The notion of "innovative potential" is directly related to the notion of "creative potential", which in the general-philosophical aspect is interpreted as a set of possibilities of purposeful transformation activity, and at the level of individual manifestation of creativity is defined as "creative potential of the individual".

Creative potential is a dynamic personality structure, which includes a set of creative instincts that are manifested and developed in intellectual activity, as well as a complex of psychic neoplasms of the person, acquired during its age ripening. It is based on imagination, associative relationships, and the richness of intuitive processes, emotional diversity and empathic feelings that are realized in the process of creative activity. According to psychologists [7], creative potential is a psycho-energetic tension that arises between the aspirations, possibilities and the real life of a person. It is realized in a reflexive and creative effort aimed at reaching previously unattainable, on the realization of what was not accomplished to this moment, on aspirations beyond yourselves. With the help of creative effort, a person can gain in his life what was not given by nature or in the process of upbringing and education. It defines the uniqueness and life strategy of the individual.

4. Intellectual and creative activity of the person in innovative work

Modern problems of economic development are connected with the intellectualization of labor, giving the highest priority to the processes of producing new knowledge that can provide socio-economic progress to any society.

Innovative work as the most important component of the knowledge economy embraces a cycle from the development of a scientific and technical idea to its commercialization. The result of innovation work is a new product that materializes the ideas of the authors of innovations, that is, innovators. In the conditions of competition among enterprises, organizations, individual entrepreneurs for economic survival, innovative work is oriented towards the market. In general, the essence of innovation work can be illustrated through a model (Figure 2).

An important intellectual resource of the company is its personnel, the optimal use of which dictates the need to develop new approaches to its formation, assessment and motivation. The human resources management system should include a block of management of intellectual labor resources that will adequately reflect the professional and personal characteristics of employees engaged in creative activity [8]. The meaningful specifics of this block of corporate management are determined, above all, by the degree of intellectualization of production processes, the role of intellectual resources in the overall effect. The block should include: selection of intellectual personnel, search of talents,

estimation of their contribution to the effectiveness of the organization, methods of motivation for intellectual activity.

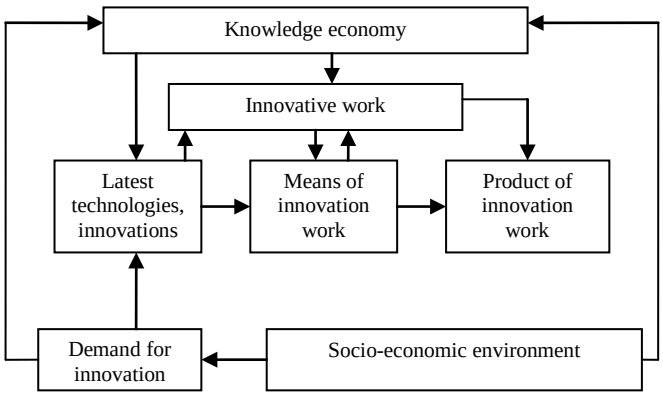


Figure 2. *Model of innovation work in the system of knowledge economy*

The intellectual resources of the organization are highly educated workers engaged in creative activity and are absolutely adequate to the business processes of the organization, the result of which is an intellectual product in the form of a technological or managerial decision [9]. The source of these resources for the firm is not the labor market, but investment in their preparation and development. Thus, the selection of intelligent personnel - is, firstly, the result of organizing their internal brand movement; and secondly, an important strategic direction of management of the organization as a whole. The content of intellectually-creative activity of human in the professional activities of various social groups is represented in Table 2.

Table 2 *Intellectual and creative activity of social groups*

Social group	На робочому місці застосовують	The share of intellectual and creative work				
		0-20%	20-40%	40-60%	60-80%	80-100%
Workers, peasants	Knowledge + Skills	■				
Service industry workers	Knowledge + Skills	■	■			
Creative social group, including creative core	Knowledge + Skills + Talent	■	■	■		
	Knowledge + Skills + Talent + Active action			■	■	■

Creativity is a prerequisite for the formation of a professional, but at the same time, this personality quality must have a certain orientation associated with professional activity. Innovative potential manifests itself in mastering of new effective professional technologies, in innovative solution of production tasks. Thus, the analysis of the activity and the personal qualities of the personnel who have achieved significant professional results, just ascertains his or her innovative activity [10].

5. The development of a creative personality in the knowledge economy

Florida R. knowledge economy refers to the creative economy, which is the core of the creative class. It is based on the principle of three "T": technology, talent and tolerance [11]. He believes that only the availability of all three components can help generate innovation and stimulate economic growth. An indication of the fact that it is creative people and, in particular, the creative core, one of the factors contributing to the competitiveness of national economies, is the positioning of the present century as an era of struggle for talents.

Characteristics that allow recognizing the economy as creative include [12]:

- the positioning of the creative person as the main engine of progress and the most valuable resource of development;
- the existence of a system of capitalization of creative and cultural potentials;
- growth of social activity;
- strategic planning of balanced development taking into account economic, environmental, social and cultural determinants;
- the formation of competitive advantages due to the unique natural, creative and cultural resources, optimal use of them;
- activization of creative industries as priority sectors of the economy;
- development of cultural products market.

The creative economy is a special sector of the knowledge economy that is associated with intellectual activity of people, because today the external environment requires new business laws, because the structure and motivation of consumers has changed. There was a need for products with high intellectual content. Therefore, entrepreneurs need to be aware of new trends in customer behavior and needs. Understanding the peculiarities of the creative economy makes it possible to turn the creative ideas of both business owners and their employees into profitable activities. These features include [13]: the high role of new technologies and inventions in various fields of human activity; high degree of uncertainty; a large amount of existing knowledge and the urgent need to generate new knowledge.

The evolution of the formation of the knowledge economy demonstrates how, over time, changes in the perception of those human qualities that are used in production processes. The main motive of the worker's activity is self-realization, the desire to acquire knowledge, the search for new possibilities of creativity. In the information society there is a transformation of the nature of labor, which traditionally was aimed at the creation of material values. Its place is occupied by intellectual activity of a person, which is based on the totality of scientific knowledge, spiritual and cultural values and is not subject to regulation, which is usually characteristic of labor in the traditional sense [14].

Today we are talking about the phenomenology of intellectual talent of a person, which includes three gradual stages with phenomena: 1) "competence", 2) "talent" and 3) "wisdom", which is the result of long-term subordination to certain laws of the process, the essence of which is the organization and enrichment of the individual mental experience [15]. The development of a creative person combines the specifics of intellectual activity and mentality, and the interdependence of experience and knowledge occurs through their dualism under the influence of the continuous action of external factors (Figure 3).

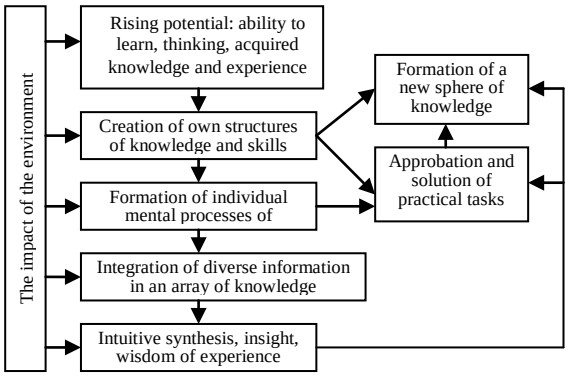


Figure 3. *The scheme of individual intellectual resources development*

Consequently, from a scientific point of view, in the context of innovation activity, there is a close relationship between creativity and personality innovation. Thus, creativity is a prerequisite for any creative activity that is motivated by the individual's aspirations for self-expression and self-affirmation, including as a prerequisite for innovation. Innovation, directly related to the ability of an agent at the cognitive and behavioral levels to ensure the emergence, perception, as well as the possible revision and implementation of new and original ideas, that is, the creation of innovation.

6. Conclusion

Activation of the concept of knowledge society manifested in solving economic problems and social management based on knowledge. It began to be considered in a fundamentally new socio-political and technological context as a factor for modernization or as a scientific model for modernizing society based on the knowledge economy and its core – creative economy.

Appropriate institutional support, systematic studies of the preconditions and trends in the development of cultural and creative potential, and on this basis, strategic programming of development, taking into account cultural and creative determinants, is needed for the formation of a creative economy.

In modern conditions, knowledge, skills, work skills, initiative and other personality characteristics of employees should become an increasingly important strategic resource compared to financial and industrial capital. It is human potential that creates an innovative potential, which, depending on the subject, is the ability of a person, enterprise, industry or population to create and apply innovation.

Innovation-intellectual potential is a key factor in the formation of a knowledge-based economy. The quality and pace of development of the whole society will depend on the activity of the process of reproduction of intelligence and knowledge. In addition, the study of literary sources and their own studies make it possible to highlight the factors that most influence the formation of the knowledge economy, that is: human potential, innovative activity and development of intellectual potential, which becomes a capital after its application. The given factors will be devoted to further scientific and practical research.

In order to achieve predictive indicators of intellectual and creative activity in Ukraine, the following tasks must be performed:

- an increase in the size of the creative social group, in particular the creative core as the main source of socio-economic development at different levels of the system hierarchy;
- stimulate the development of creative industries to accelerate economic growth;
- construction of spatial-sectoral infrastructure with the creation of creative cities and creative territories for the concentration of creative professionals.

7. References

1. Husén T. Talent. Equality and Meritocracy / Husén T. – The Hague: Nijhoff, 1974.
2. Вахович І.М. Розвиток креативних індустрій: регіональний вимір : монографія / Вахович І.М., Чуль О.М. – Луцьк : Вежа-друк, 2014. – 288 с.
3. Негус К. Креативность. Коммуникация и культурные ценности / Негус К., Пикеринг М., Пер. с англ. – Х.: Изд-во Гуманитарный центр, 2011. – 300 с.
4. O`Connor, J. Popular Culture, Reflexivity and Urban Chang / O`Connor, J. – Helsinki: University of Art Design, 1999.
5. Біла книга. Інтелектуальна власність в інноваційній економіці України / Г.О. Андрощук, О.В. Дем'яненко, І.Б. Жиляєв, Л.В. Сахарова та ін. – К.: Парламентське вид-во, 2008. – 448 с.
6. Лукичева Л.И. Управление интеллектуальным капиталом: Учебн. пособие / Л.И. Лукичева. – М.: Омега-Л, 2007. – 552 с.
7. Степанов С. Ю. Рефлексивная практика творческого развития человека и организаций / Степанов С. Ю. – М.: Наука, 2000. – 174 с.
8. Collins C.J. Knowledge exchange and combination: the role of human resource practices in the performance of high-technology firms / Collins C.J., Smith K.G. // Academy of Management Journal. – 2006. – Vol. 49 – P. 544-560.
9. Zhavoronkova, G.; Shkoda, T. Intellectual capital and human capital interrelation. // Performance management: From strategy to delivery: PMA 2012 Conference. 11-13 July 2012, Fitzwilliam College, University of Cambridge, UK. – Conference proceedings.
10. Enkel E. Creative imitation: exploring the case of cross-industry innovation / Enkel E., Gassman O. // R&D Management. – 2010. – Vol. 40. – №3. – P. 256-270.
11. Florida R. The Rise of the Creative Class: And How It's Transforming Work, Leisure, Community, and Everyday Life / Florida R. – N-Y.: Basic Books, 2003. – 464 p.
12. Структурно-інституціональні трансформації та економічна безпека держави: монографія / За заг. ред. д.е.н., проф., чл.-кор. НАНУ О.С. Власюка, д.е.н., проф. А.І. Мокія. – Львів: Апріорі, 2013. – 836 с.
13. Гура В.Л. Особливості креативної економіки / Гура В.Л. // Парадигмальні зрушення в економічній теорії XXI ст. : матер. II Міжнар. наук.-практ. конф. – К., 2015. – С. 242-244.
14. Zhavoronkova G., Skoda T. Human capital management problems in Ukraine in crisis period // KRYSYS FINANSOWY: przebieg i skutki społeczno-gospodarcze w Europie Srodkowej i Wschodniej / Pod redakcja Ŝlawomira Partyckiego. – T. 2. – Lublin: Wydawnictwo KUL, 2012. – P. 733-740.
15. Холодная М.А. Психология интеллекта. Парадоксы исследования / Холодная М.А. – 2-е. изд., перераб. и доп. – СПб.: Питер, 2002. – 272 с.

SUPERPARAMAGNETIC PROPERTIES IN LANTHANUM STRONTIUM MANGANITES DOPED WITH ZINC

Prof. Eremina R. Dr.[1, 2], Yatsyk I. PhD.[1, 2], Seidov Z. PhD.[3], Badelin A. PhD.[4] Prof. Krug von Nidda H.-A. Dr.[5]
Zavoisky Physical-Technical Institute, FRC Kazan Scientific Center of RAS, Kazan, Russia [1]
Kazan (Volga Region) Federal University, Kazan, Russia[2]
Institute of Physics, Azerbaijan National Academy of Sciences, Baku, Azerbaijan[3]
Astrakhan State University, Astrakhan, Russia[4]
Experimental Physics V, Center for Electronic Correlations and Magnetism, University of Augsburg, Augsburg, Germany[5]

I.Yatzyk@gmail.com

Abstract: *Lanthanum strontium manganites, doped with zinc have been studied by magnetic resonance. In the paramagnetic phase, regions with a ferromagnetic order with superparamagnetism properties are observed. Using the theory of Raikher and Stepanov for superparamagnetic particles, the analysis of the temperature dependence of the magnetic resonance linewidth and resonance field was performed. This analysis allowed to estimate the size of ferromagnetically correlated regions and the magnitude of the magnetic anisotropy.*

Keywords: MANGANITES, MAGNETIC RESONANCE, GRIFFITHS PHASE

1. Introduction

Hole doped manganites having the general formula $A_{1-x}B_xMnO_3$, where A is one or several trivalent cations from the group of lanthanides and B is a divalent alkaline-earth metal such as Ca, Ba, or Sr, have a quite rich phase diagram resulting from the interplay between the spin, orbital, charge, and lattice degrees of freedom. In addition to the problems related to the orbital, charge, and magnetic ordering, these materials attract considerable current interest owing to such phenomena as the colossal magnetoresistance and phase separation [1, 2].

More than 40 years ago, it was predicted the formation of ferromagnetic drops [3]. The idea of the existence of ferromagnetic correlated regions in the paramagnetic phase of manganites was developed by Kugel et al. [4]. They explain the transport and magnetic properties of manganites of various types. According to their estimates, the size of ferromagnetically correlated regions (FM droplets) is about 30 Å.

Khokhlov et al [5] study of magnetic and transport properties of $Nd_{0.52}Sr_{0.48}MnO_3$ films of different thicknesses, it was found that the films are phase-separated and are composed of magnetic clusters (droplets) in an electrically insulating paramagnetic (at $T > T_N$), or antiferromagnetic (at $T < T_N$) matrix. In the same paper it has been suggested that the ferromagnetic clusters in a magnetic field of 1 T and above can decay into smaller areas, consisting of magnetic polarons of small radius of the order of 1-2 nm.

Electron spin resonance (ESR) turned out to be very sensitive to the formation of ferromagnetic regions in the paramagnetic phase, as has been reported e.g. for $La_{1-x}Sr_xMnO_3$ in the regime $0.075 \le x \le 0.175$, where weak, strongly anisotropic ferromagnetic resonance (FMR) lines appear besides the paramagnetic resonance line at $g \approx 2$ already below 270 K far above the magnetic ordering temperature [1]. The nature of these ferromagnetic resonances can be explained in terms of a Griffiths phase arising due to the presence of correlated quenched disorder in the orthorhombic cooperative Jahn-Teller phase.

In the paper [6], the authors studied the $La_{1-x}Sr_xMn_{0.925}Zn_{0.075}O_3$ (x = 0.075, 0.095, and 0.115) ceramic by magnetic resonance and magnetization. For all three samples, the magnetic moment of the ferromagnetically correlated region turns out to be about $\mu = (175\pm10)\mu_B$, the decay parameter is $\alpha=0.025\pm0.005$, and the resonance field is $H_0=3400\pm10$ Oe. The average linear size of the ferromagnetically correlated regions is of the order of 1–2 nm. However, the concentration of holes was controlled by only one impurity. Therefore, it is not clear that effects are associated with magnetic properties or changes in the crystal lattice. Controlling the concentration of holes with the help of two impurities, you can try to answer the question posed. The aim of this study is to determine the magnetic moment, the resonance field and the decay parameter for the ceramic $La_{1-x}Sr_xMn_{1-y}Zn_yO_3$ (where c=x+y is constant). The substitution of divalent Zn^{2+} ions for manganese leads to the growth of the Mn^{4+} content and hence to the simultaneous lowering of the Mn^{3+} content. Zn^{2+} ions having the $3d^{10}$ electron configuration break the transport and exchange coupling between manganese ions [7]. The zinc doping enhances the tendency to charge localization and thus reduces the mobility of charge carriers. This favors the formation of the regions with ferromagnetically correlated spins within the paramagnetic phase.

2. Theoretical background

To evaluate our ESR data, we refer to the theory of Raikher and Stepanov published in a series of papers, e.g. Refs. 8 and 9, in which theoretical expressions are obtained for the temperature dependence of the magnetic resonance linewidth of an ensemble of superparamagnetic particles with uniaxial anisotropy. The linewidth $\Delta H(T)$ of the superparamagnetic ensemble basically consists of two contributions

$$\Delta H = \Delta H_S + \Delta H_U \tag{1}$$

i.e. the homogeneous broadening ΔH_S due to superparamagnetic fluctuations and the inhomogeneous contribution ΔH_U resulting from the statistical distribution of resonance fields caused by the uniaxial anisotropy given by

$$\Delta H_S = \frac{2\alpha H_0}{\sqrt{3}} \frac{\xi_0 - L_1}{\xi_0 L_1}, \text{ with } \xi_0 = \frac{\mu_{eff} H}{k_B T} \tag{2}$$

$$\Delta H_U = 3\sigma H_0 \frac{\xi_0 - 3L_1}{\xi_0^2 L_1}, \text{ with } \sigma = \frac{W_{A,eff}}{k_B T} \tag{3}$$

respectively. The average resonance field reads

$$H_{res} = H_0 \left(1 - 2\sigma \frac{(\xi_0 - 3L_1)^2}{\xi_0^3 L_1} \right) \tag{4}$$

Here H_0 denotes the external magnetic field, α is a damping parameter, and $L_1 = \coth \xi_0 - 1/\xi_0$ abbreviates the Langevin function. The effective magnetic moment μ_{eff} and anisotropy energy $W_{A,eff}$ of the superparamagnetic particles can be empirically written as [10]

$$\mu_{eff} = \mu \frac{1}{\left(1 - T^*/T\right)} \tag{5}$$

$$W_{A,eff} \equiv \mu_{eff} H_A = W_A \frac{1}{\left(1 - T^*/T\right)} \tag{6}$$

with the magnetic moment μ, the magnetic ordering temperature T^*, and the anisotropy field H_A.

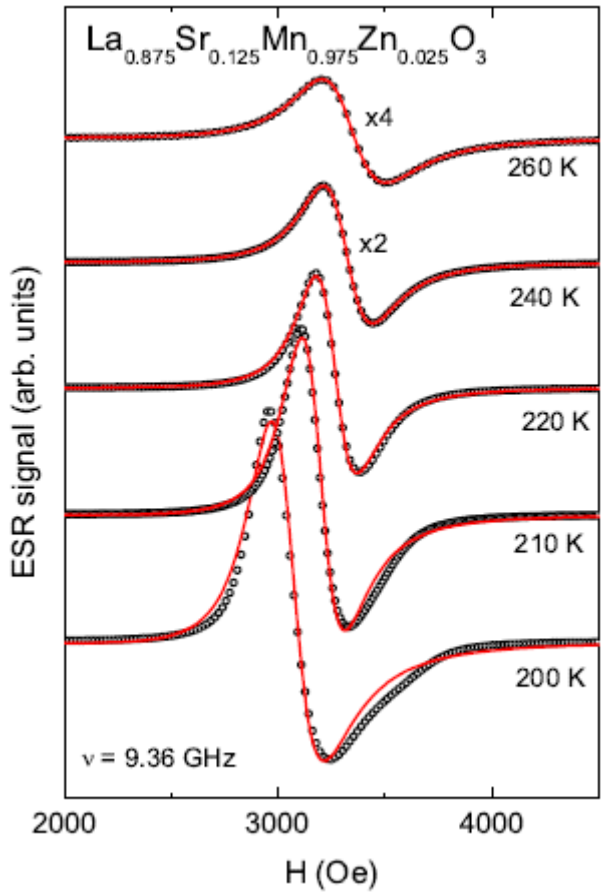


Fig. 1. *Magnetic resonance spectra of $La_{0.875}Sr_{0.125}Mn_{0.975}Zn_{0.025}O_3$ taken at several temperatures above magnetic order. The solid lines represent the field derivative of Lorentzian profiles including dispersion and counter resonance following Ref. 11, which is necessary in the case that the linewidth is of the same order of magnitude like the resonance field*

3. Experimental details

Polycrystalline samples of $La_{1-x}Sr_xMn_{1-y}Zn_yO_3$ were synthesized by traditional ceramic processing. The starting components (dried La_2O_3, $SrCO_3$, $BaCO_3$, MnO_2, ZnO powders) were mixed in stoichiometric proportions and ground in a ball mill with addition of ethanol. The obtained powder was pressed into pellets, which then were preliminarily annealed at 1273 K for 4 hours. This operation was followed by trituration in a mortar, fine grinding in a ball mill for 10 hours, introducing a binder (an aqueous solution of polyvinyl alcohol), drying and granulation. From the obtained powder, rings of standard size (7 x 4 x 2 mm) were pressed. After burning out the binder, the final sintering step was performed at 1473 K for 10 hours and in the end the samples were cooled down together with the furnace.

The magnetic resonance measurements were performed on a Bruker ER 200 SRC (EMX/plus) spectrometer at X-band frequency. The temperature was controlled in the temperature range from 100 K to 340 K using a Bruker nitrogen-evaporation cryostat. ESR probes the microwave absorption due to magnetic dipolar transitions between the Zeeman levels split by an external magnetic field H. Lock-In amplification with field modulation experimentally yields the field derivative of the absorption signal. In case of conducting samples a contribution of dispersion is admixed to the absorption due to the skin effect resulting in an asymmetry of the absorption lines. For the microwave field with a frequency of ν≈9 GHz the skin depth is comparable to the size of the samples (~ 1 mm) in the experimental temperature range. Therefore, to eliminate the influence of the skin effect on the shape of the ESR, the ceramic samples were powdered and mixed with NaCl.

4. Results and discussion

Typical ESR spectra as observed in all manganites under consideration are shown in Figure 1 exemplarily for $La_{0.875}Sr_{0.125}Mn_{0.975}Zn_{0.025}O_3$. In the paramagnetic regime the spectrum of magnetic resonance consists of a single exchange-narrowed line, which is well described in terms of a Lorentz shape with a small contribution of dispersion [11]. Deviations from the ideal Lorentzian appear only on approaching magnetic order.

$La_{0.875}Sr_{0.125}Mn_{0.975}Zn_{0.025}O_3$ as obtained from the Lorentz fit. As observed for all samples under consideration, the resonance field is approximately constant at high temperatures corresponding to an effective g-value of g≈1.98. Only within a temperature range ΔT≈50 K above the onset of magnetic order, the resonance field significantly shifts to lower fields with decreasing temperatures. As shown earlier, the observed paramagnetic resonance signal with an effective g value slightly below g = 2, is due to all manganese ions, Mn^{3+} and Mn^{4+}, in the compound [12].

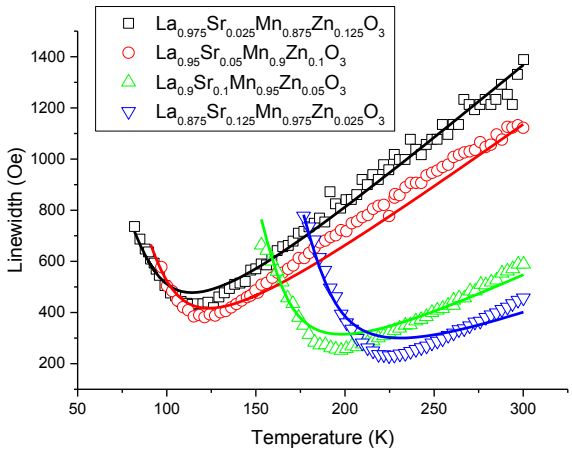


Fig. 2. *Temperature dependence of the linewidth in $La_{1-x}Sr_xMn_{1-y}Zn_yO_3$.*

The linewidth exhibits a minimum close to the temperature, where the resonance field starts to diverge from its high-temperature value. To higher temperatures we observe a monotonous, approximately linear increase, while to lower temperatures the linewidth strongly diverges. This behavior is well described by Eq. 1 developed for the superparamagnetic ensemble: At low temperatures the linewidth is large due to the distribution of directions of the anisotropy fields of the particles (inhomogeneous broadening); as the temperature increases the thermally induced tendency to make the magnet isotropic at first causes the linewidth to decrease, but then the superparamagnetic fluctuations induce another increase to higher temperatures.

Table 1. *Characteristics of the ferromagnetic correlated regions in the $La_{1-x}Sr_xMn_{1-y}Zn_yO_3$*

x	0.025	0.05	0.1	0.125
y	0.125	0.1	0.05	0.025
μ, μ_B	280	250	208	249
K_V, 10^4 J/m^3	1.9	1.8	1.6	1.97
α	0.048	0.037	0.02	0.019
H_0,Oe	3402	3400	3355	3373
H_A,Oe	206	215	234	236
T^*,K	77	85	153	177

Temperature dependence of the magnetic resonance linewidth in $La_{1-x}Sr_xMn_{1-y}Zn_yO_3$, are shown in Figures 2. As we can see, the

behavior of the temperature dependence of the positions and linewidths of the electronic magnetic resonance in $La_{1-x}Sr_xMn_{1-y}Zn_yO_3$, is similar that for superparamagnetic particles [8, 9]. For low temperatures linewidth is large due to the scatter in directions of the anisotropy fields of the particles (inhomogeneous broadening); as the temperature increases the thermally induced tendency to make the magnet isotropic causes linewidth to decrease, but in the fluctuation region it once again begins to increase (Fig. 2).

We have described the temperature dependence of the magnetic resonance field, the linewidth of the magnetic resonance in $La_{1-x}Sr_xMn_{1-y}Zn_yO_3$, using the formula 1- 4. Obtained from the approximation of the temperature dependence of the linewidth and resonance field parameters: the magnetic moments, the anisotropy energy of the ferromagnetically correlated regions W_A, magnetic moment μ as well as the damping coefficient α, resonance field H_0, anisotropy field $H_A = W_A/\mu$ [13], the ordering temperature T^*, and the blocking temperature $T_b = \frac{K_v V}{25 k_B}$ [14], are shown in Table I.

As can be seen, the average value of the magnetic moment in the ferromagnetically correlated regions of the ceramic $La_{1-x}Sr_xMn_{1-y}Zn_yO_3$ is about $\mu = (250 \pm 30)\ \mu_B$. Taking into account that the magnetic moment of the Mn^{3+} ion in perovskites is about 3.5 μ_B, ferromagnetically correlated regions contains about 70 of the manganese ions. If we consider that the grating period is about 7 Å [15], whereas the size of ferromagnetically correlated regions is about 1-2 nm.

4. Summary

The study of magnetic properties of ferromagnetic correlated regions in ceramic $La_{1-x}Sr_xMn_{1-y}Zn_yO_3$ was carried out by the electron magnetic resonance. Temperature dependence of electron magnetic resonance spectra over the entire range of measured temperatures have features which characterize the magnetic resonance of superparamagnetic particles. As a result of approximation of the temperature dependence of electron magnetic resonance spectra there were obtained the value of the magnetization, the anisotropy energy of ferromagnetically correlated regions and the ordering temperature. The average size of ferromagnetically correlated regions in the ceramic manganites $La_{1-x}Sr_xMn_{1-y}Zn_yO_3$ may reach the values about of 1-2 nm.

5. Acknowledgments

This work was partially supported by the Russian Federal Program, grant no 18-52-06011.

6. References

[1] J. Deisenhofer, D. Braak, H.-A. Krug von Nidda, J. Hemberger, R. M. Eremina, V. A. Ivanshin, A. M. Balbashov, G. Jug, A. Loidl, T. Kimura, and Y. Tokura, Phys. Rev. Lett. 95, 257202 (2005)

[2] A.M. Kadomtseva, Yu. F. Popov, G. P. Vorobiev, K. I. Kamilov, A. A. Mukhin, V. Yu. Ivanov, and A. M. Balbashov, Phys. Solid State 48, 2134 (2006).

[3] E. L. Nagaev, JETP Lett. 16, 394 (1972). M. A. Krivoglaz, Usp. Fiz. Nauk 106, 360 (1972).

[4] K. I. Kugel, A. L. Rakhmanov, A. O. Sboychakov, M. Yu. Kagan, I. V. Brodsky, and A. V. Klaptsov, J. Exp. Theor. Phys. 98, 572 (2004).

[5] V.A. Khokhlov, A.Yu. Prohorov, Yu. V. Medvedev, Yu. Nikolayenko, A. Muhin, V.P. Paschenko, G.G. Levchenko, V.G. Prohorov, N.I. Solin, V.L. Svetchnikov, J.S. Park, J.B. Kim, G.Y.P. Lee, Technical Physics 81, 95 (2011).

[6] R. M. Eremina, K. R. Sharipov, L. V. Mingalieva, and A. G. Badelin JETP Letters, 2013, Vol. 98, No. 12, pp. 848–852

[7] E. V. Sotirova-Haralambeva, X. L. Wang, K. H. Liu, T. Silver, K. Konstantinov, and J. Horvat, Sci. Technol. Adv. Mater. 4, 149 (2003).

[8] Yu. L. Raikher and V. I. Stepanov, Phys. Rev. B. 50, 6250 (1994).

[9] Yu. L. Raikher and V. I. Stepanov, Sov. Phys. JETP 75, 764 (1992).

[10] Margeat O., Tran M., Spasava M., Farle M. , Phys. Rev. B 75, 134410 (2007).

[11] Janhavi P. Joshi and S. V. Bhat, J. Mag. Res. 168, 284 (2004).

[12] V. A. Ivanshin, J. Deisenhofer, H.-A. Krug von Nidda, A. Loidl, A. A. Mukhin, A. M. Balbashov, and M. V. Eremin, Phys. Rev. B 61, 6213 (2000).

[13] A. G. Gurevich, Magnetic Resonance in Ferrites and Antiferromagnets, Moscow: Nauka, (1973).

[14] S. P. Gubin, Yu. A. Koksharov, G. B. Khomutov, G. Yu. Yurkov, Russian Chemical Reviews 74, 489 (2005).

[15] Q. Huang, A. Santoro, J. W. Lynn, R. W. Erwin, J. A. Borchers, J. L. Peng, and R. L. Greene, Phys.Rev. B 55, 14987 (1997).

CALCULATION OF TEMPERATURE DEPENDENCES OF THERMAL EFFECTS AT COOLING OF METAL ALLOYS

РАСЧЕТ ТЕМПЕРАТУРНЫХ ЗАВИСИМОСТЕЙ ТЕПЛОВЫХ ЭФФЕКТОВ ПРИ ОХЛАЖДЕНИИ МЕТАЛЛИЧЕСКИХ СПЛАВОВ

Ass. Prof., Dr. Eng. Khristenko V.[1], Omelko L.[2], Ass. Prof., Dr. Eng. Donii O.[1]

National Technical University of Ukraine "Kyiv Polytechnic Institute named after Igor Sikorsky" - Kyiv, Ukraine[1]
Physical Technological Institute of Mrtals and Alloys, National Academy of Science of Ukraine[2]

Email: dosha@iff.kpi.ua

Abstract: A method is proposed for determining the temperature dependences of thermal effects (the amount of heat released when the temperature changes) based on data on the temperature-concentration dependences of the free energies of the phases of metallic systems. These dependences are necessary for modeling of the processes of crystallization of alloys. They make it possible to obtain temperature dependences of the dimensions of the thermal effects without introducing the results of measurements of direct calorimetry. The peculiarity of calculating of the temperature dependences of thermal effects upon cooling of binary metal systems from the liquid state to room temperature (including crystallization) is shown using the example of the alloy of the system Pb-Sn.
***KEYWORDS**: ENTHALHY, HEAT CAPACITY, CRYSTALLIZATION, PHASE DIAGRAM*

1. Introduction

Mathematical modeling of crystallization and formation of the structure of metal castings [1], including of castings with freezing [2], is of considerable practical interest. The degree of reliability of such models is largely determined by the accuracy of the temperature dependences of the thermal effects associated with the cooling of the metal. The problem of the availability of such dependencies is particularly acute when it comes to crystallization of alloys, as transformations in multi-component systems occur mostly in the temperature range where the system is in a heterophase state. And for most alloys, only data of the heat capacity averaged over the temperature and composition are generally available.

2. Solution of the problem under consideration

At the same time, data on the temperature-concentration dependences of the free Gibbs energies of the phases forming the system under consideration for many metallic systems are given in the literature. For example, for the case of a two-component system, the molar free energy and enthalpy of the phase are determined as [3]:

$$G(x,T)=G_A(T)\cdot(1-x_B)+G_B(T)\cdot x_B+ \\ +G_{mix}(x,T)+RT\cdot(x_A\ln x_A+x_B\ln x_B), \quad (1)$$

$$H(x,T)=H_A(T)\cdot x_A+H_B(T)\cdot x_B+H_{mix}(x,T), \quad (2)$$

where $G_A(T)$, $G_B(T)$ –are the molar free energy of pure components A and B in the phase at a temperature T; $x_A = (1 – x_B)$, x_B - contents of components A and B in the phase (molar fractions); $G_{mix}(x,T)$ is the excess molar free energy of mixing in the phase of composition x at temperature T; $H_A(T)$, $H_B(T)$ – are molar enthalpies of pure components A and B in the phase at a temperature T; $H_{mix}(x,T)$ is the molar enthalpy of mixing in the phase of the composition x at temperature T.

The temperature-concentration dependences of the excessive mixing energies in phases ($G_{mix}(x,T)$) are widely given in literary sources (they are used to calculate state diagrams). In addition, if the phase structure coincides with the structure of the pure component in the aggregate state under consideration, then its molar enthalpy in the phase ($H_A(T)$ or $H_B(T)$) can be determined from the data on the temperature dependence of the heat capacity ($H=\int C_p dT$). A certain complexity is the determination of the heat capacity of the components in phases whose structures differ from the structure of the component in pure form (for example, in the Al-Si system, silicon, which in its pure form does not have a FCC lattice, is included in the FCC structure of the solid state solution based on aluminum). However, for most metal systems the data are widely represented in the literature (they are also used to calculate the state diagrams) on the lattices' stability parameters (on the temperature dependences of the differences of the molar free energies of pure components in the standard state (as a rule-in liquid one) and in the state with the structure under consideration (with a certain type of crystal lattice)). Therefore, the problem is reduced to the determination of enthalpy of mixing and enthalpies of pure components in phases with the help of known dependences of excess free energy of mixing and of stability parameters of components' lattices. The solution of this problem is complicated by the fact that in expressions for free energies, the entropic and enthalpy terms, as a rule, are not separated.

At the same time, the magnitudes of enthalpy, entropy and isobaric-isothermal potential are interconnected through the heat capacity C_p:

$$\left.\begin{aligned} H&=\int C_p dT,\\ S&=\int\frac{C_p}{T}dT,\\ G&=H-TS=\int C_p dT-T\int\frac{C_p}{T}dT. \end{aligned}\right\} \quad (3)$$

If the temperature-concentration dependence of the excess molar heat capacity of mixing ($C_p^{mix}(x,T)$) in the phase is expressed as a polynomial

$$C_p^{mix}(x,T)=m_3^{mix}(x)+m_4^{mix}(x)T+ \\ +\frac{m_5^{mix}(x)}{T^2}+m_6^{mix}(x)T^2+m_7^{mix}(x)T^3+\ldots, \quad (4)$$

then, in accordance with (3), expressions for molar enthalpies and excess free energy of mixing will take the form [4, 5]:

$$H_{mix}(x,T)=m_1^{mix}(x)+m_3^{mix}(x)T+\frac{m_4^{mix}(x)T^2}{2}- \\ -\frac{m_5^{mix}(x)}{T}+\frac{m_6^{mix}(x)T^3}{3}+\frac{m_7^{mix}(x)T^4}{4}+\ldots, \quad (5)$$

$$G_{mix}(x,T)=m_1^{mix}(x)-m_2^{mix}(x)T+m_3^{mix}(x)T(1-\ln T)- \\ -\frac{m_4^{mix}(x)T^2}{2}-\frac{m_5^{mix}(x)}{2T}-\frac{m_6^{mix}(x)T^3}{6}-\frac{m_7^{mix}(x)T^4}{12}+\ldots, \quad (6)$$

where $m_1(x)$ and $m_2(x)$ are the integration constants.
The dependence of the specific heat of mixing on the composition can be taken into account by introducing of each of the coefficients in (4) in the form of polynomials:

$$m_k^{mix}(x) = m_{k,1}^{mix}(x) + m_{k,2}^{mix}(x)x + m_{k,3}^{mix}(x)x^2 + \ldots \quad (7)$$

In the same way, by introducing of changes of the components' heat capacity in the transition from the standard state to the state under consideration in the form of polynomials,

$$\Delta C_p^i(T) = m_3^i + m_4^i T + \frac{m_5^i}{T^2} + m_6^i T^2 + m_7^i T^3 + \ldots, \quad (8)$$

it is possible to obtain expressions for the temperature dependences of changes of molar enthalpies and free energies of pure components during phase transitions:

$$\Delta H^i(T) = m_1^i + m_3^i T + \frac{m_4^i T^2}{2} - \frac{m_5^i}{T} + \frac{m_6^i T^3}{3} + \frac{m_7^i T^4}{4} + \ldots \quad (9)$$

$$G^i(T) = m_1^i - m_2^i T + m_3^i T(1 - \ln T) - \frac{m_4^i T^2}{2} - \frac{m_5^i}{2T} - \frac{m_6^i T^3}{6} - \frac{m_7^i T^4}{12} + \ldots \quad (10)$$

3. Results and discussion

The idea of the proposed method is based on the thesis that, in the presence of analytical expressions for the temperature-concentration dependence of the excess molar free energy of mixing in the phase and the temperature dependences of the stability parameters of the components' lattices, their values can be determined for an arbitrarily large number of values of temperatures and compositions from the phase's region of the existence. And the values of coefficients m^{mix} and m^i which are interesting for us can be determined by solving the system of equations obtained by equating expressions (6) and (10) with the calculated values of the free energy of the phase and of the stability parameters of the components' lattices. As a result, we obtain the temperature-concentration dependences of the entalpy and the heat capacity of the mixing, as well as the temperature dependences of the changes of the components' enthalpies and heat capacities at phase transitions.
The enthalpy of a heterogeneous system is defined as the sum of enthalpies of individual phases. Therefore, the change of the enthalpy in the transition of a multiphase system from one state to another one is defined as the difference of sums of the phases' enthalpies in these states. In calculating changes of the heterogeneous system's enthalpy caused by changes of temperature, changes of the compositions and quantities of phases remaining in equilibrium (in accordance with the state diagram) must also be taken into account.
The peculiarities of the application of the proposed methodology were investigated on the example of modeling of cooling of the alloy of the system Pb-Sn, containing 36.35 wt. % Sn (a = 0.499 of mole fractions of Sn). Temperature dependencies of thermal effects were calculated at cooling in the range of a temperature from 290^{0}C (563 K) to 30^{0}C (303 K). The whole period of temperature's variation was split into intervals ΔT = 1 K. Changes of enthalpy were determined for each of these intervals. The step of temperature's change ΔT = 1K provides the required accuracy of the calculation. In addition, the thermal effect accompanying cooling by 1K can formally be considered as the average heat capacity in the specified range of temperature. This allows us to apply algorithms of the simulation of crystallization of pure metals [2] to calculate the crystallization of multicomponent alloys. Thermal effects were determined on the basis of 1 mol of alloy. The temperature dependences of the heat capacity of pure components in the liquid state are taken from [6]. The enthalpies of mixing in phases (Table 1) were determined according to the abovementioned method, based on the data on the excess free mixing energies [7]. In accordance with the thermodynamic phases adopted in [7], the values of the enthalpy of mixing in all phases of the Pb-Sn system depend only on the composition and do not depend on the temperature (the heat capacity of the mixing is zero).

Table 1. *Dependences of Enthalpies of Mixing in the Phases of Pb-Sn System*

Phase	Enthalpy of mixing $H_{mix}(x,T)$, J/Mole
Melt (L)	$x(1-x)\cdot(4800 + 200\cdot x)$
FCC solid solution based on plumbum (Pb)	$x(1-x)\cdot(6700 - 0.365\cdot x)$
BCC tin solid solution (Sn) OCT solid solution based on tin (Sn)	$x(1-x)\cdot(-203068)$

According to the state diagram of the system Pb-Sn [7], at temperatures above 234^0 C (507 K), the considered alloy is in a single-phase liquid state (Figure 1). Therefore, the thermal effects (changes of enthalpy) when cooling of 1 mol of alloy by $\Delta T_j = T_{j+1} - T_j$ in the indicated region of temperature are defined as:

$$Q_i = (1-x)\cdot\Delta H_i^{Pb} + x\cdot\Delta H_i^{Sn} + \Delta H_i^{mix}(x_i, T_i), \quad (11)$$

where $\Delta H_j^{Pb} = \int_{T_j}^{T_{j+1}} C_p^{Pb}(T)dT$, $\Delta H_j^{Sn} = \int_{T_j}^{T_{j+1}} C_p^{Sn}(T)dT$ – changes of the molar enthalpies of pure tin and plumbum in the liquid phase when it is cooled by ΔT_j, $C_p^{Pb}(T)$ and $C_p^{Sn}(T)$ - the temperature dependences of the molar heat capacity of liquid plumbum and tin;

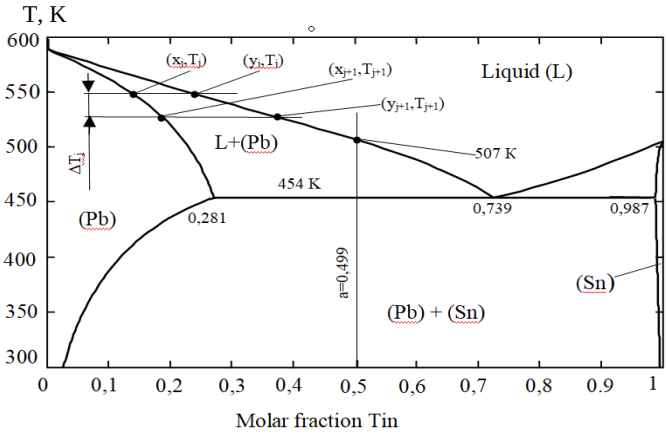


Fig. 1. *Temperature dependences of specific heat effects when cooling the alloy Pb + 0.499 mol. of the fractions of Sn (a) and the scheme for determining the specific thermal effect during crystallization of the eutectic component of the alloy by the differential curve (b).*

(1 - x), x - the content of plumbum and tin in the liquid phase (molar fractions); $\Delta H_i^{mix}(x,T)$ - change of the molar enthalpy of mixing in the phase when the temperature changes from T_j to T_{j+1}.
In the interval from the temperature of liquidus (507 K) to the eutectic temperature (454 K), and also at temperatures less than 454 K, the alloy stays in a two-phase state (Figure 1) (liquid phase + solid solution based on plumbum (Pb) - in the first case, and two solid solutions (Pb) + (Sn) - in the second case). To determine the changes of enthalpy in the process of cooling of the alloy in the two-phase regions of the system's existence, changes of the quantities and phases' constitutions when the temperature was changed by ΔT_j were taken into account:

Table 2. *Temperature Dependences of Changes of Enthalpies (ΔH) and Heat Capacities (ΔC_P) of Components of Pb-Sn Systems* at Phase Transitions

Component	Thermodynamic function	Type of phase transition I → II		
		Liquid phase → (Pb)	Liquid phase → (Sn)	(Pb) → (Sn)
Sn	$\Delta H^{I\to II}(T)$, J/moles	$-5622+0{,}055\cdot T+0{,}012\cdot T^2/2+ +1288342/T$	$-9168-3{,}952\cdot T+0{,}0174\cdot T^2/2+ +967769/T$	5510
	$\Delta C_P^{I\to II}(T)$, J/(moles·K)	$0{,}055+0{,}012\cdot T-1288342/T^2$	$-3{,}952+0{,}0174\cdot T+967769/T^2$	$-7{,}795\cdot 10^{-13}+1{,}47\cdot 10^{-13}\cdot T$
Pb	$\Delta H^{I\to II}(T)$, J/moles	-4700	$209555-1{,}408\cdot T+0{,}00196\cdot T^2/2- -107767/T$	213580
	$\Delta C_p^{I\to II}(T)$ J/(moles·K)	0	$-1{,}408\cdot T+0{,}00196\cdot T^2/2+ +107767/T$	0

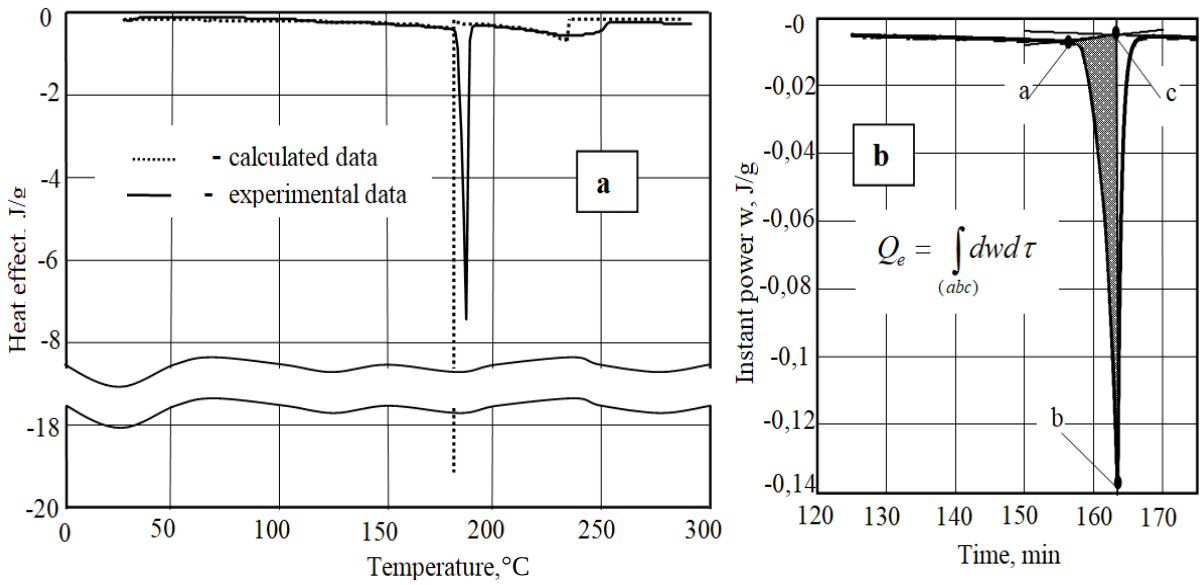


Table 2. *Temperature Dependences of Changes of Enthalpies (ΔH) and Heat Capacities (ΔC_P) Components of Pb-Sn Systems at Phase Transitions*

$$\Delta H_j = [H^I(x_{j+1},T_{j+1})p_{j+1} + H^{II}(y_{j+1},T_{j+1})q_{j+1}] - \\ -[H^I(x_j,T_j)p_j + H^{II}(y_j,T_j)q_j], \qquad (12)$$

where $H^I(x_{j+1},T_{J+1})$, $H^{II}(y_{j+1},T_{j+1})$ are the molar enthalpies of phases I and II at temperatures T_{j+1} containing respectively x_{j+1} and y_{j+1} of molar fractions of tin (according to the diagram of the system's state); $H^I(x_j,T_j)$, $H^{II}(y_j,T_j)$ are the molar enthalpies of phases I and II at temperature T_j containing x_j and y_j of molar fractions of tin (according to the diagram of the system's state); p_{j+1}, p_j are the quantities of phase I, respectively, at temperatures T_{j+1} and T_j; q_{j+1}, q_j are the quantities of phase II at temperatures T_{j+1} and T_j, respectively. The molar enthalpies of the phases were determined according to the proposed method. Changes of enthalpies and heat capacities of pure components at phase transitions (Table 2) were calculated from data on lattices' stability parameters [7]. The quantities and constitutions of phases remaining in equilibrium were calculated on the state diagram in accordance with the lever's rule.

At a temperature of 454 K, the alloy undergoes an eutectic transformation, which occurs at a constant temperature. Therefore, the change of enthalpy was calculated as the difference between the enthalpy of the liquid phase of the eutectic composition and of the sum of the enthalpies of two solid solutions, taking into account their quantities and compositions at eutectic temperature.

To verify the consistency of the proposed method with the help of differential scanning calorimetry, the temperature dependences of the thermal effects accompanying the cooling of the alloy of system Pb-Sn containing 0.499 mol of tin were empirically established (rate of temperature's change was 1K/min). It is established that the experimental and calculated data are in satisfactory compliance (Figure 2a; for the convenience of comparison, the calculated data are given to 1 g of alloy, calorimetric data are in this form). For example, according to the calculations, the specific heat released during the crystallization of the alloy of the given composition is 40.93 J/g, while according to the experimental data, its value is 41.49 J/g (the difference does not exceed 1.5%). For the amount of heat released during the crystallization of the eutectic component of 1 g of alloy, these quantities are 19.29 J and 19.09 J, respectively (the difference does not exceed 1%). It should be noted that, due to the coherence of the dimensions, the temperature field is not homogeneous in terms of the volume of the sample under study. Therefore, the data on thermal effects on the experimental curves appear to be "stretched" along the abscissa axis (Figure 2a) and in order to exclude the influence of the inhomogeneity of the temperature field, the thermal effects at phase transitions were determined by the areas of figures bounded by peaks on the experimental differential curves and characteristic lines (Figure 2 b) [8].

4. Conclusions

1. A procedure for calculating of the temperature dependences of thermal effects accompanying the cooling and heating of multi-component alloys is developed. Their presence makes it possible to develop adequate mathematical models describing the crystallization of alloys of metallic systems.
2. The results of experimental verification indicate that the proposed method provides sufficient accuracy of calculation. The discrepancy between calculated values and experimentally obtained ones does not exceed 1.5%.

5. References

1. Donii O.M. Computer modeling of structure formation during crystallization of metals and alloys / Donii O. M., Kulinich A.A., Yanov O. M., Ryabinina O. O. // Physics and chemistry of solids. - 2003. - Volume 4. - №3. - P. 585 - 588. (Ukrainian).
2. Kirievsky B.A., Omelko L.G. Modeling of the melt freezing process on the outer surface of a cylindrical crystallizer // Casting processes. - 2014. - No. 5. - P. 10 - 15. (Russian)
3.Darken L.S., Gurri R.V. Physical chemistry of metals. - Moscow: Metallurgizdat, 1960. - 581 p. (Russian)
4. Lukas H. L., Weiss J., E.–Th. Hanig. Strategies for calculation of phase diagrams // CALPHAD. – 1982. – v. 6, № 3. – Pp. 229 – 251.
5. Okamoto H. Reevaluation of Thermodynamic Models For Phase Diagram Evaluation // Journal of Phase Equilibria – 1991. – 12, № 6 – P. 623 – 664.
6. Samsonov G.V. Properties of elements. Part 1. - Moscow: Metallurgy, 1976. - 600s. (Russian)
7. Karakaya I., Thompson W.T. The Pb – Sn (Lead – Tin) System // Bulletin of alloy phase diagrams – 1988. – v. 9, № 6. – P. 144 − 152.
8. Berg L. G. Introduction to thermography. - Moscow: Nauka, 1969. - 395 p. (Russian)

RULE-BASED MAMDANI-TYPE FUZZY MODELING OF PERFORMANCE OF HYDROXY (HHO) DRY CELL WITH 12x12 PLATE COMBINATION

Assist. Prof. Dr..Ali Serhat E.[1], Assist. Prof. Dr. Yusuf Y.[1], Mech. Engineer..Burak Buğra Ç.[1], Mech. Engineer ..Taylan P.[1], Assoc.. Prof. Dr..Kevser D.[1]

1Selcuk University, Department of Mechanical Engineering, Konya/TURKEY
Email:ersoyoglu@gmail.com, kdincer@selcuk.edu.tr,

Abstract— *The fossil fuels and the natural gas reserves that have undertaken the role of the locomotive of the industrial period are limited. It is also the biggest factor in environmental problems. All these reasons lead to the need for alternative fuels or resources. Hydrogen is the candidate to be one of these alternatives; is an unlimited clean and efficient fuel. Hydrogen may assume the role of carrier in the process of storage of other alternative energy sources. Today, interest in hydrogen energy is increasing. One of the reasons for this is that hydrogen can be produced from renewable energy sources such as water, biomass, wind and sun as well as hydrogen from primary energy sources. There is no polluting gas emissions when hydrogen is used as fuel. The HHO dry cell is a device that converts water into HHO (oxyhydrogen) gas. In this study, performance of HHO dry cell with 12x12 plate combination was experimentally investigated and modeled with a Rule-Based Mamdani-Type Fuzzy (RBMTF) modeling technique. Input parameters are; plate number, time, current; output parameter is mass flow rate. The coefficient of multiple determination (R^2=98.5) for the mass flow rate. RBMTF results indicated that RBMTF can be successfully used in HHO dry cell with 12x12 plate combination.*

KEYWORDS*:* FUZZY LOGIC MODELLING, HHO DRY CELL, HYDROGEN,

1. Introduction

Hydrogen is the simplest element. An atom of hydrogen consists of only one proton and one electron. It's also the most plentiful element in the universe. Despite its simplicity and abundance, hydrogen doesn't occur naturally as a gas on the Earth - it's always combined with other elements. Water, for example, is a combination of hydrogen and oxygen (H_2O). Hydrogen is also found in many organic compounds, notably the hydrocarbons that make up many of our fuels, such as gasoline, natural gas, methanol, and propane. Hydrogen can be separated from hydrocarbons through the application of heat - a process known as reforming. Currently, most hydrogen is made this way from natural gas. An electrical current can also be used to separate water into its components of oxygen and hydrogen. This process is known as electrolysis. Some algae and bacteria, using sunlight as their energy source, even give off hydrogen under certain conditions [1].

In 1918 Charles Frazer, a North American inventor, patented the first water electrolysis machine act as a hydrogen booster for internal combustion engines. Yull Brown, a Bulgarian born Australian inventor patented and attempted to popularize Browns Gas as a cutting gas and fuel additive during the 1970's and 80's. HHO is an enriched mixture of hydrogen and oxygen bonded together molecularly and magnetically. HHO gas is produced in a common-ducted electrolyser & then sent to the intake manifold to introduce into combustion chamber of the engine. HHO gases will combust in the combustion chamber when brought to its auto-ignition or self-ignition temperature [2-4].

Zadeh in 1965 introduced fuzzy concept to develop a mathematical framework for imprecisely presented data. It is a generalized form of interval analysis, where parameters are defined with lower and upper values. In a traditional set theory, an element is defined as a member of a set. If the element is in the set, the membership grade is unity, otherwise it is zero. A fuzzy set is an extension of the traditional set theory in which the element has certain degree of membership l (0–1) in the set. Fuzzy set establishes relationship between uncertain data and the membership function l, which ranges from 0 to 1 [5, 6].

Fuzzy logic is a superset of Boolean-conventional logic that has been expanded to handle the concept of partial truth and truth values between "completely true" and "completely false." Fuzzy theory should be seen as a methodology to generalize any specific theory from crisp to continuous. Fuzzy modeling opens the possibility for straightforward translation of statements in natural language verbal formulation of the observed problem into a fuzzy system. Its functioning is based on mathematical tools [7].

In this study, performance of HHO dry cell was investigated experimentally and modeled by fuzzy logic method. The performance parameter is the mass flow rate. The highest value of the mass flow rate was 0.261 x 10^{-3} kg /h.

2. Materials and Methods

Hydrocarbon fuel is one of the sources of energy used for electrical power generation, heating and transportation in the world. But they have negative side effects like polluting emissions, large scale oil spill, etc. Due to its widespread dependence and difficulties in getting other alternatives the use of hydrocarbon fuel could not be eliminated. To mitigate the above problems and to reduce the use of hydrocarbon fuel, hydrogen gas can be supplemented. Hydrogen gas to air intake of a combustion process will improve flame speed, lean burn ability and flame quenching distance. But scarcity and production cost makes it more difficult to implement. Hydrogen rich gas produced from electrolysis of water called the Brown's Gas or HHO could solve the potential difficulties [4, 8].

Fuzzy inference system consists of a fuzzification interface, a rule base, a database, a decision-making unit, and finally a defuzzification interface. The function of each block is as follows. A rule base containing a number of fuzzy IF–THEN rules, a database which defines the membership functions of the fuzzy sets used in the fuzzy rules, a decision-making unit which performs the inference operations on the rules, a fuzzification interface which transforms the crisp inputs into degrees of match with linguistic values and a defuzzification interface which transforms the fuzzy results of the inference into a crisp output. Mamdani's method is the most commonly used in fuzzy inference system, due to its simple structure of 'min-max' operations [9].

In this study, performance of HHO dry cell with 12x12 plate combination was experimentally investigated (Fig.1) and modeled with a RBMTF modeling technique. The experimental setup used in this study is illustrated in Fig.1.

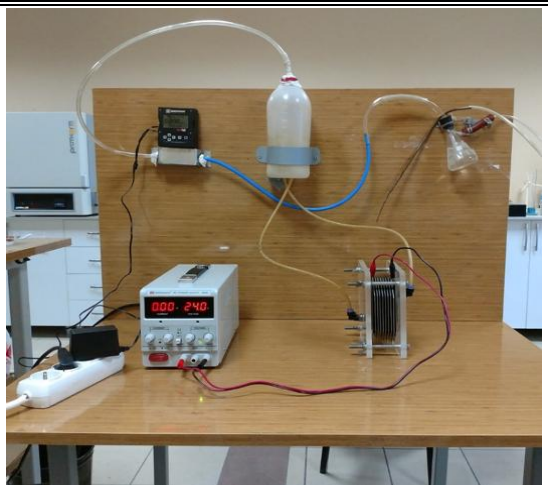


Fig.1. *Experimental system*

In the same way, the used experimental procedure can be presented as follows:

- First the plates are assembled.
- The water outlet of the water tank is connected to the water inlet of the HHO cell.
- The gas inlet pipe of the water tank is fixed to the gas outlet part of the HHO cell.
- Place water in the water tank in such a way that each combination of water level is the same.
- To supply electricity to the HHO cell, the DC power supply is connected to the electric plates of the HHO cell.
- The end of the temperature measuring instrument is attached to the HHO cell plates
- The DC power supply is started and the voltage is fixed at 24 volts.
- Every minute, the current in the DC power supply, the temperature in the temperature meter, and the mass flow rate of the HHO gas read from the mass flow rate are recorded.
- The DC power supply is turned off when the specified time for each experiment is over.
- The gas mixture in the HHO cell is drained.

General structure of RBMTF model developed (three input, one-output) is given in Fig. 2. Input parameters are; plate number (PN), time (t), current (C); output parameter is mass flow rate (MFR).

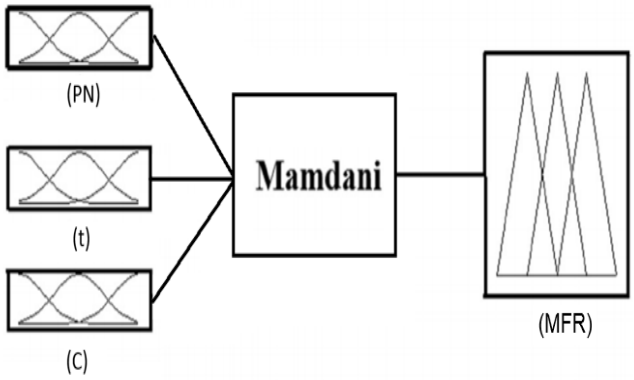


Fig.2. *Designed RMBTF structure*

A fuzzy model expresses a complex system in the form of fuzzy implications. Mamdani model can be built by using these implications (linguistic relationships) and observed data. The Mamdani-based fuzzy models use excessive number of rules for system modeling. Let X be input (regression) matrix and g an output vector defined as Eqs. (1) and (2).

$$X = [x_1, \ldots, x_2]^T = \begin{bmatrix} x_{11} & x_{12} \\ x_{21} & x_{22} \\ \vdots & \vdots \\ x_{n1} & x_{n2} \end{bmatrix} \quad (1)$$

$$g = [g_1, \ldots, g_n] \quad (2)$$

where upper script T denotes the transpose. In the Mamdani fuzzy model, both the antecedent and consequent are fuzzy propositions. A general form of linguistic fuzzy if-then rule is given as Eq. (3).

$$R_i : \text{if x is } A_i \text{ then y is } B_i;\ i = 1,\ 2,\ldots,K \quad (3)$$

where Ri is the rule number, Ai and Bi are the fuzzy sets, x is the antecedent variable representing the input in the fuzzy system, and y is the consequent variable related to the output of the fuzzy system [10].

In this study, numerical parameters of input and output variables were fuzzificated as linguistic variables: very very low (L_1), very low (L_2), low (L_3), negative medium (L_4), medium (L_5), positive medium (L_6), high (L_7), very high (L_8) and very very high (L_9) linguistic classes (Fig.3).

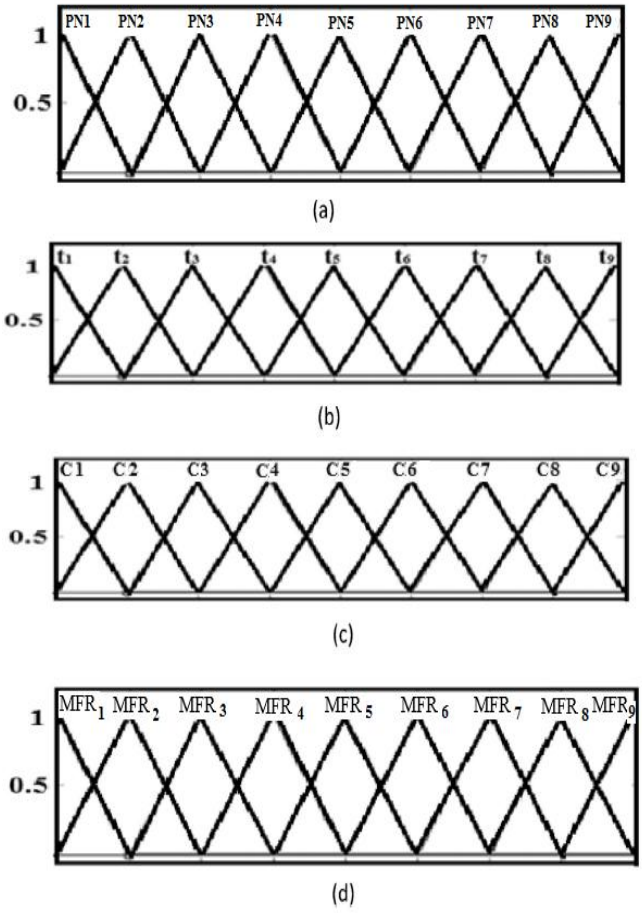


Fig. 3. *Fuzzy membership functions for three input variables and one output variable: (a) PN fuzzy set graphic, (b) t fuzzy set graphic, (c) C fuzzy set graphic, (d) MFR fuzzy set graphic*

3. Results and Discussion

HHO gas has substantial advantages when compared to the gasoline due to its high diffusivity. First two of these advantages is rate of formation of homogenous mixture is greater since HHO diffuses faster in mixture. Secondly, HHO can dilute quite fast under circumstances of leakage. Several researches show that 1866 litres of HHO gas is obtained from 1 liter of water, after ignition, the HHO gas returns to original volume after combustion [11, 12].

The HHO dry cell with 12x12 plate was tested in this study for temperature, current, mass flow rate (Figs. 4-6). According to the experimental results;

- The highest temperature value was found at 5 minutes in the 12-9 plate combination.
- The highest temperature value was measured as 25.5 ^{o}C.
- The highest temperature value occurred at 1.01 A.
- The temperature increased when the current increased.
- The mass flow rate increased when time increases.
- The highest value of the mass flow rate was 0.261 x 10^{-3} kg /h. This value was measured in a 9 plate combination and on the 1st minute.

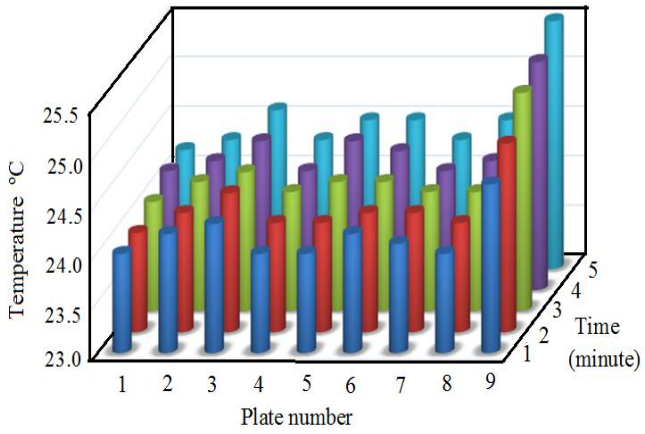


Fig.4. *The temperature values for time*

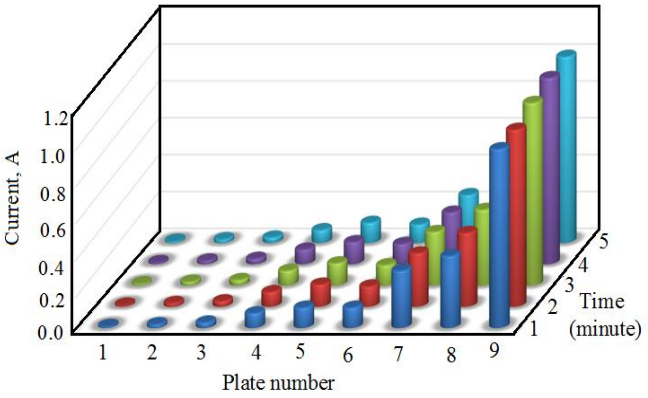


Fig.5. *The current values for time*

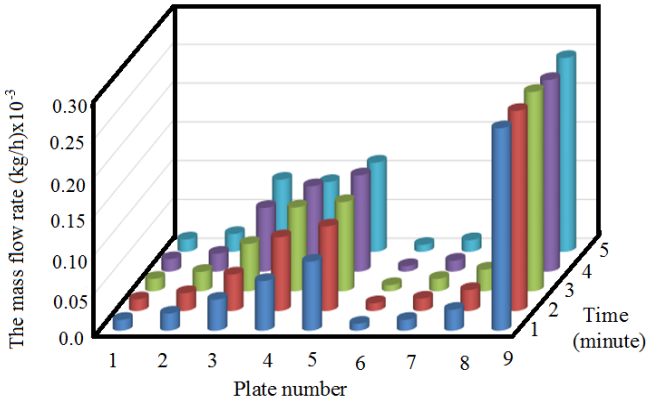


Fig.6. *The mass flow rate values for time*

The purpose of this study is to model the performance of the HHO dry cell using experimental data by the RBMTF modeling technique. The performance parameter is mass flow rate. In Table 1 shows the comparison of experimental data with RBMTF for the mass flow rate.

Table 1. *Comparison of experimental (EXP.) data with RBMTF for the variation of time with mass flow rate (MFR) for plate number (PN)*

Time (min.)	MFR (kg/h)	MFR (kg/h)	MFR (kg/h)		MFR (kg/h)	MFR (kg/h)	Debi (kg/h)
	PN = 1 (EXP.)	PN = 2 (EXP.)	PN=3 (EXP.)		PN=1 RBMTF	PN=2 RBMTF	PN=3 BMTF
1	0.014 x 10^{-3}	0.022 x 10^{-3}	0.04 x 10^{-3}		0.015 x 10^{-3}	0.021 x 10^{-3}	0.05 x 10^{-3}
2	0.015 x 10^{-3}	0.023 x 10^{-3}	0.047 x 10^{-3}		0.016 x 10^{-3}	0.024 x 10^{-3}	0.048 x 10^{-3}
3	0.016 x 10^{-3}	0.025 x 10^{-3}	0.061 x 10^{-3}		0.017 x 10^{-3}	0.026 x 10^{-3}	0.062 x 10^{-3}
4	0.016 x 10^{-3}	0.023 x 10^{-3}	0.082 x 10^{-3}		0.017 x 10^{-3}	0.024 x 10^{-3}	0.084 x 10^{-3}
5	0.016 x 10^{-3}	0.023 x 10^{-3}	0.093 x 10^{-3}		0.018 x 10^{-3}	0.024 x 10^{-3}	0.095 x 10^{-3}
Time (min.)	MFR (kg/h)	MFR (kg/h)	MFR (kg/h)		MFR (kg/h)	MFR (kg/h)	MFR (kg/h)
	PN=4 (EXP.)	PN=5 (EXP.)	PN=6 (EXP.)		PN=4 RBMTF	PN=5 RBMTF	PN=6 BMTF
1	0.064 x 10^{-3}	0.089 x 10^{-3}	0.009 x 10^{-3}		0.065 x 10^{-3}	0.09 x 10^{-3}	0.010 x 10^{-3}
2	0.095 x 10^{-3}	0.109 x 10^{-3}	0.01 x 10^{-3}		0.093 x 10^{-3}	0.119 x 10^{-3}	0.012 x 10^{-3}
3	0.108 x 10^{-3}	0.115 x 10^{-3}	0.008 x 10^{-3}		0.109 x 10^{-3}	0.125 x 10^{-3}	0.009 x 10^{-3}
4	0.11 x 10^{-3}	0.124 x 10^{-3}	0.007 x 10^{-3}		0.12 x 10^{-3}	0.124 x 10^{-3}	0.008 x 10^{-3}
5	0.09 x 10^{-3}	0.115 x 10^{-3}	0.009 x 10^{-3}		0.10 x 10^{-3}	0.116 x 10^{-3}	0.0011 x 10^{-3}
Time (min.)	MFR (kg/h)	MFR (kg/h)	MFR (kg/h)		MFR (kg/h)	MFR (kg/h)	MFR (kg/h)
	PN=7 (EXP.)	PN=8 (EXP.)	PN=9 (EXP.)		PN=7 RBMTF	PN=8 RBMTF	PN=9RBMTF
1	0.14 x 10^{-3}	0.027 x 10^{-3}	0.261 x 10^{-3}		0.15 x 10^{-3}	0.0278	0.263 x 10^{-3}
2	0.16 x 10^{-3}	0.027 x 10^{-3}	0.258 x 10^{-3}		0.17 x 10^{-3}	0.027x 10^{-3}	0.259 x 10^{-3}
3	0.16 x 10^{-3}	0.028 x 10^{-3}	0.257 x 10^{-3}		0.17 x 10^{-3}	0.029x 10^{-3}	0.258 x 10^{-3}
4	0.14 x 10^{-3}	0.026 x 10^{-3}	0.247 x 10^{-3}		0.15 x 10^{-3}	0.027 x 10^{-3}	0.248 x 10^{-3}
5	0.15 x 10^{-3}	0.027 x 10^{-3}	0.25 x 10^{-3}		0.16 x 10^{-3}	0.028 x 10^{-3}	0.26 10^{-3}

4.Conclusions

In this study, a HHO dry cell with 12x12 plate was investigated experimentally and modeled by RBMTF. According to the experimental results; the highest value of the mass flow rate is 0.261 x 10^{-3} (kg /h). This value was measured in a 12-9 plate combination and on the 1st minute.

The comparison between experimental data and fuzzy logic is done using statistical methods such as the R^2 are defined as follows (Eq.1),

$$R^2 = 1 - \frac{\sum_{m=1}^{n}(t_{m,m} - y_{p,m})^2}{\sum_{m=1}^{n}(t_{m,m} - \bar{t}_{m,m})^2} \quad (4)$$

where n is the number of data patterns, $y_{p,m}$ indicates the predicted, $t_{m,m}$ is the actual value of one data point m, and $\bar{t}_{m,m}$ is the mean value of all actual data points [13].In this study, the R^2=98.5 is for the mass flow rate and RBMTF can be successfully used in HHO dry cell with 12x12 plate combination.

Acknowledgment

Financial support of experimental study from the research fund of the Selcuk University under Grant No. BAP 17402018 is gratefully acknowledged.

5. References

concrete panels used in residential buildings in Turkey, Expert Systems with Applications 38 (2011) 5553–5560.

[1] https://www.renewableenergyworld.com/hydrogen/tech.html.

[2] R. Cameron, Effects of on-board HHO and water injection in a diesel generator, Bachelor of Engineering Research Project, University of Southern Queensland Faculty of Engineering and Surveying, 2012.

[3] S. Yadav Milind, S.M. Sawant, Investigations on oxyhydrogen gas and producer gas as alterntive fuels on the performance of twin cylinder diesel engine, International Journal of Mechanical Engineering and Technology (IJMET), vol.2, pp.85-93, 2011.

[4] Abdullah Işıktaş, Kevser Dincer, Ali Verim, Osman Türkmen, Sadık Ata, Experimental Investigation and Fuzzy Logic Modelling of Performance Hydroxy Dry Cell with Different Plate Combination, International Journal of Intelligent Systems and Applications in Engineering, IJISAE, 2016, 4 (Special Issue), 18–22, 2016.

[5] Shakhawat, C., Tahir, H., & Neil, B. (2006). Fuzzy rule-based modelling for human health risk from naturally occurring radioactive materials in produced water, Journal of Environmental Radioactivity, 89, 1–17.

[6] M. Tosun, K. Dincer, S. Baskaya, Rule-based Mamdani-type fuzzy modelling of thermal performance of multi-layer precast ignition engine, International Journal of Innovative Research in Science, Engineering and Technology, vol.2, pp. 393-404, 2013.

[7] K. Dincer , S. Tasdemir , S. Baskaya , I. Ucgul & B. Z. Uysal, Fuzzy Modeling of Performance of Counter flow Ranque-Hilsch Vortex Tubes with Different, Geometric Constructions, Numerical Heat Transfer, Part B, 54: 499–517, 2008.

[8] E. Leelakrishnan, N. Lokesh, H. Suriyan, Performance and emission characteristics of Brown's gas enriched air in spark

[9] M. Bölgen, Fuzzy logic and data mining technıques in evaluating of credit risks of companies, Master Thesis, Graduate School of Natural and Applied Sciences of Dokuz Eylül University, Turkey, 2010.

[10] Sadık Ata, Kevser Dincer, Fuzzy logic modeling of performance proton exchange membrane fuel cell with spin method coated with carbon nanotube, international journal of hydrogen energy 42 (2017) 2626-2635.

[11] Sakthıvel, S., 2014, An Experimental Assessment of Performance and Exhaust Emission Characteristics by Addition of Hydroxy (HHO) Gas in Twin Cylinder C.I. Engine, International Journal of Innovative Research in Science, Engineering and Technology, Vol. 3(2), pp. 60-65.

[12] Yusuf YILMAZ, Sadık ATA, Gürol ÖNAL, Abdullah IŞIKTAŞ, Kevser DINCER, A Fuzzy Logıc Approach For The Estımatıon Of Performance Hydroxy Dry Cell With Different Plate Combınatıon, Selcuk Univ. J. Eng. Sci. Tech., v.6, n.1, pp. 70-87, 2018.

[13] Onal, G., Dincer, K., Yayla, S., Yılmaz, Y., Ersoyoğlu, A.S. Pt/C Coating for Proton Exchange Membrane Fuel Cell (PEMFC) and Rule-Based Mamdani-Type Fuzzy Modeling of PEMFC Performance, International Journal of Mining, Metallurgy & Mechanical Engineering, 3(3), 122-128, 2015.

ADHESION AND PHYSICO-MECHANICAL CHARACTERISTICS OF COATINGS OF CHROMIUM CARBONITRIDE, GENERATED ON STEEL SUBSTRATES

АДГЕЗИОННЫЕ И ФИЗИКО-МЕХАНИЧЕСКИЕ ХАРАКТЕРИСТИКИ ПОКРЫТИЙ КАРБОНИТРИДА ХРОМА, СФОРМИРОВАННЫХ НА СТАЛЬНЫХ СУБСТРАТАХ

Phd Chekan N.M.[1], Ass.prof, dr.Eng. Auchynnikau Y.V.[2], Phd Akula I.P.[1], Ass.prof. Phd Eisymont Y.I.[2], Pinchuk T.I.[3]
Physicotechnical Institute, National Academy of Sciences of the Republic of Belarus[1], Yanka Kupala State University of Grodno,Grodno, Belarus[2,] Institute of Powder Metallurgy of the National Academy of Sciences of the Republic of Belarus[3]
e-mail: pec@bas-net.by,ovchin_1967@mail.ru

Abstract. *In the present work, the adhesion and physico-mechanical characteristics of heat-resistant vacuum coatings formed on steel substrates are investigated. An increase in the values of adhesion and physico-mechanical parameters of coatings formed from multicomponent compounds is established. The tribotechnical characteristics of coatings based on chromium carbonitride have been studied.*
KEYWORDS: adhesion, coating, morphology, friction, microhardness

1. Introduction

Chrome coatings are widely used to create antifriction anti-adhesion layers for various functional purposes. Wide distribution found coatings on the basis of electrolytic chromium in the manufacture of various types of products of automotive and automotive tractors. In works [1-3] it was shown that the use of composite coatings based on chromium modified with ultradisperse clusters of synthetic carbon (UDD) is an effective direction of increasing the life of friction units of automobile shock absorbers. Such coatings have a higher hardness (by 23-40%), wear resistance (1.6-2.2 times) compared with base chromium and can be applied in one cycle without additional grinding and polishing of the parts. This allows to significantly reduce the thickness of the working layer (up to 5-10 microns) while maintaining the main performance characteristics. At the same time, when applying composite chromium coatings of small thickness, the role of microdefects caused by the presence of aggregates of the solid phase modifier (UDD) in the electrolyte solution increases substantially. Therefore, the corrosion resistance of modified UDD coatings decreases significantly with decreasing thickness, which significantly reduces the efficiency of their use in engineering. Coating with a thickness of more than 5-10 microns from the modified chromium is economically expedient, so it allows to significantly increase the wear resistance of the modified products, even despite the rather high cost of UDD (1, -1, 5 US dollars per carat of the modifier). In [4-5], it was proposed to apply the Foleoks fluorine-containing oligomers F-1, F-8 and F-14 to the working surface when creating electrolytic coatings, which provides not only a significant increase in the wear resistance of the interface, but also a corrosive durability of coatings. After 150 hours of soaking in salt fog at 600 °C, the test samples have no visible traces of corrosion damage, while the samples with a base coating after 48 hours of testing have a significant number of local corrosion sites. At the same time, the microhardness of the coating and its hydrophobicity increase substantially. The use of composite coatings will not only significantly increase the service life of shock absorbers, but also significantly reduce their energy intensity [4-6].

A promising area in the field of creating chrome coatings and compositions based on it is the use of vacuum technologies. One of the promising types of these coatings is chromium nitride (CrN), which is a new alternative in the field of protective high-temperature layers. Coatings of CrN, CrCN have good thermal stability, low deposition temperature, high wear resistance and corrosion resistance. The disadvantage is the lack of precise information for the formation of these coatings, which affects the porosity of the coating and, as a consequence, reduces the corrosion resistance and tribological properties. Further development of studies on the characteristics of vacuum coatings was the creation of two-layer systems Cr-CrN, Cr-CrCN. These coatings are characterized by increased wear resistance, low coefficient of friction and high microhardness in comparison with CrN coatings. Usually this system is obtained by magnetron sputtering. This method gives advantages in deposition rate and low content of impurities. In addition, this method allows the creation of thin films with different variations in the crystallographic structure and morphology of the structure [7]. Multilayer coatings of Cr-CrN, CrCN are formed by changing the deposition parameters of the coating, which makes it possible to obtain composite that are gradient in structure, that is, a layer close to the substrate exhibits increased crystallinity and the upper layers are amorphous [8-9]. One of the main parameters determining the physical and mechanical characteristics of surface layers, coatings, and films are surface energy. By surface energy is meant an excess of energy in the surface layer at the interface of two phases in comparison with energy in the volume of two phases [10].

According to established ideas, the surface layers of solids, whose size does not exceed the action of the radius of molecular forces, have a structure different from the structure of the bulk phase of the condensed body. In the structure of a solid body, boundary, transition layers are distinguished, which can have a significant effect on the values of the surface energy determined experimentally. One of the methods for determining the surface energy of solid substrates is to measure the contact angles of the polar and non-polar liquids wetting [11]. Based on the values of the contact angle, it is possible to calculate the value of the surface energy. In the scientific literature there are works showing the relationship between the value of surface energy and physical characteristics, so in [12] it is proposed to consider surface energy as an additional tool for providing in space the constancy of positioning, i.e. stationary state of the two contacting parts. This arrangement is recommended to receive with the help of such a phenomenon as setting effect. To create a certain energy state of the contacting parts, in which connections (bridging bridges) arise, it is proposed to

use the technological process. Thus, the process of formation of the energy state of the surface layer of two (and more) parts with predetermined physico-mechanical properties is controlled [12].

The purpose of this work was to study the adhesion and physico-mechanical characteristics of chromium carbonitride coatings formed on steel substrates

2. Research methodology.

Adhesion characteristics were studied by the scratch analysis method. Standard equipment used for indenting uses a module for measuring scoring, research of wear and profilometry. A feedback system is used to control the applied load, the force acting on the sample, which does not depend on the topography of the surface. The pre-scan procedure allows you to measure the actual penetration depth for a scratch test to characterize the elastic recovery using the post-scan procedure [13]. Scratch testers are equipped with an easy-to-use software package that allows the user to perform a scratch test in a wide variety of test modes, including simple scratching, an extended scratch test (with pre-scanning and post scan), simple scratch mapping, scratch mapping with different modes, defined by the user.

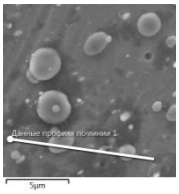
Morphological features of coatings formed on the basis of refractory metals after determining the adhesion characteristics were studied by scanning electron microscopy.

Scanning electron microscope is a device with great possibilities, which allow to characterize heterogeneous materials and surfaces at such a high level. In the scanning electron microscope (SEM), the surface under investigation is irradiated by a thin-focused electron beam, which can either rest or unfold in a raster over the surface of the sample. As a result of the interaction, secondary electrons, reflected electrons, characteristic X-ray radiation, Auger electrons and photons of different energies arise. They are produced in certain volumes (generation areas within the sample) and are used to measure many of its characteristics (composition, surface topography, crystallographic orientation, etc.).

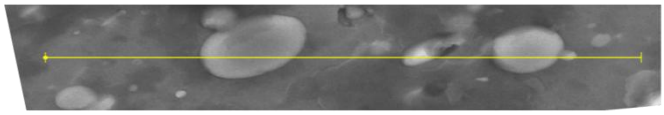
The scanning electron microscope is one of the most versatile instruments for studying and analyzing the microstructural characteristics of solids. The main reason for the wide use of SEM is the high resolution in the study of massive objects, reaching today 10-15 nm (100-150 Å). One of the important features of SEM is that it allows you to observe the topography of a solid with a resolution and depth of field that is significantly higher than the corresponding parameters of light microscopes. Information in the study of the surface is transferred by reflected secondary electrons and other simulating signals. The thickness of the sample is not particularly important, as is the case in transmission electron microscopy, where information is transferred by transmitted electrons that penetrate the sample by no more than 0.1 μm. Dielectric materials are particularly difficult to investigate in SEM. When an electron probe hits a dielectric, its absorbed electrons accumulate on its surface because of the absence of a charge flowing to the ground. The accumulation of electrons leads to the appearance of charged regions on the surface of the sample, which during subsequent scanning can irregularly deflect the primary beam, leading to serious distortions. In addition, the presence of a surface charge greatly changes the secondary electron emission. From the charging effect, you can get rid of the conductive coating on the surface of the sample. The criterion for choosing the material for deposition is usually the production of the maximum number of secondary electrons. Based on the consideration of the physical aspects of secondary electron emission, it was concluded that a 15-nm gold coating should give optimal secondary electron emission. In the "Sputter coater" installation, the conductive layer is created by cathode sputtering of gold. The prepared samples are placed in a scanning electron microscope and imaged at different magnifications. Acceleration voltage is one of the main parameters of shooting in EMS. Samples were sampled at an accelerating voltage of 20 kV. The morphology of the samples was studied using a high-resolution scanning electron microscope "Mira" from Tescan (Czech Republic). The microscope is equipped with secondary electron (SE) detectors and back-reflected electrons (BSE), which allow for the study of samples in two modes. When shooting samples in the secondary electron (SE) mode, the contrast in the image is created by reflecting the electron beam from the sample surface. In the case of an inverse-reflected electron (BSE) detector, the contrast in the picture is created by the atomic number of the sample elements. The type of detector used, the magnification and other shooting parameters are indicated in the information line at the bottom of each frame. The elemental composition was investigated using an INCA 350 microspectral analyzer from Oxford Instruments (UK). Defined elements from B to U. The minimum detection limit of an element is 0.5%. The error of the method is 5-15 relative percent.

3. Research results.

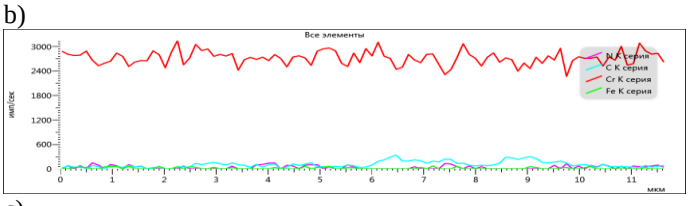
According to the data presented in Fig. 1a, chromium carbonitride coatings formed by plasma-chemical methods are composite coatings. There is a matrix in which globular formations with increased nitrogen concentration and a reduced carbon concentration are included with respect to the content of these chemical elements in the coating matrix.



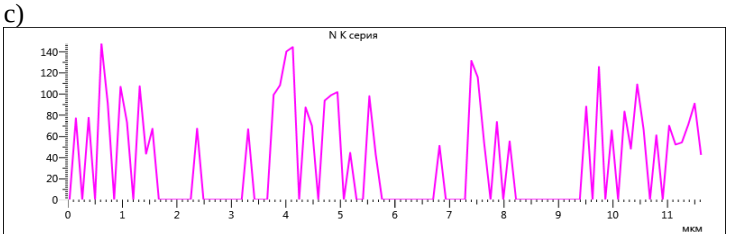
a)



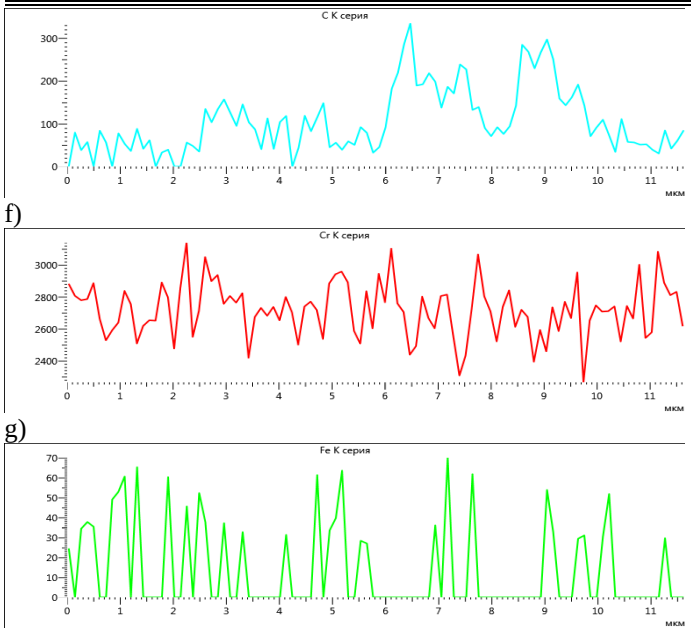
b)



c)



d)



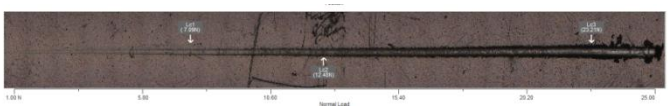
f)

g)

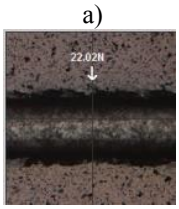
h)

Figure 1 *Dependence of the distribution of chemical elements in the coatings of chromium carbonitride: a-coating of chromium carbonitride; b-surface area of the coating for which the content of the chemical elements was measured, c-the total distribution of the chemical elements in the CrCN coating, d - the nitrogen distribution in the CrCN coating, f - the carbon distribution in the CrCN coating, g - the chromium distribution in the CrCN coating, h -iron in the coating of CrCN.*

The presence of iron in CrCN coatings is due to the fact that the thickness of the coating is on the order of 2-5 μm and does not completely shield the steel substrate. The structure and chemical composition of the coating have a significant effect on the adhesion and physico-mechanical characteristics of the coatings.



a)



b)

Figure 2 *- Type of scratch on the CrCN coating obtained by the scratch analysis method. a - a shape of a scratch, b - a fragment of a scratch where there is a full peeling of a covering from a substrate*

Coatings of CrCN begin to peel off at values that are in the region of 12 - 13 N. The complete peeling of the coating from the substrate is observed at values of ~ 23 N. These values are 1.8-2 times higher than the adhesion characteristics of vacuum chrome coatings. According to the data of [14-15], the effect of the load on the coefficient of friction depends on the type of contact interaction - elastic or plastic. In the general case, the function f (N) is nonmonotonic and is determined by a quadratic function (Figure 2). It is believed that the position of the minimum of this curve depends on the ratio of the molecular and mechanical components. In the case where the ratio of the coefficient of friction responsible for the molecular component to the friction coefficient responsible for the mechanical component is greater than unity, the minimum of the curve f (N) is shifted to the region of smaller values of N. In the region of small loads, the plastic contact [14-15] f is determined mainly by the molecular component of friction.

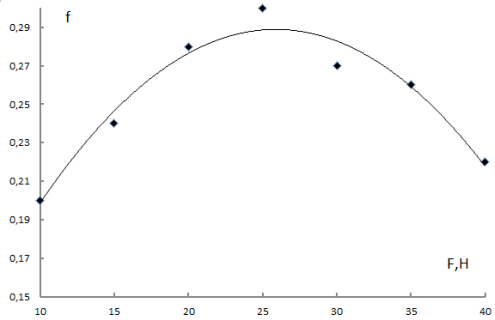


Figure 3 *- Dependence of the friction coefficient of the pair "CrCN-ShKh 15" from the load*

The decrease in the coefficient of friction with increasing N is due to the fact that N increases faster than the increase in the area of the actual contact caused by this increase, and, as a consequence of the frictional force. That is, an increase in the load by n times entails an increase in the number of frictional bonds and their dimensions, and, consequently, an increase in the total shear resistance by a smaller number of times. After reaching the f minimum a plastic contact is realized in the main. The position of the minimum of the curve depends on the ratio of the molecular and mechanical components. In the course of tribological tests of diamond-like coatings, the reverse effect is observed. At low loads, the friction coefficient of the CrCN coating over steel increases. Then, under loads in the region of 25-30 N, an extremum point is observed. Further increase in the values of the normal load is accompanied by a significant decrease in the coefficient of friction. Thus, the behavior of the tribotechnical characteristics of chrome coatings differ from the classical views when the normal load changes.

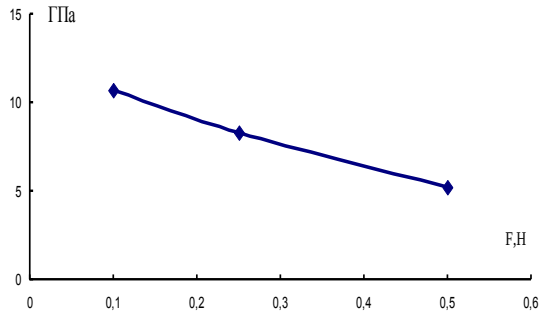


Figure 4 *- Dependence of the change in the microhardness of the CrCN coating formed on 40X steel from the applied load on the pyramid*

This dependence of the friction coefficient on the load for these coatings is explained by the fact that in the structure of CrCN there is a carbon with a high concentration in comparison with the base chrome coating. The increase in load promotes the diffusion of carbon into the friction zone and the formation of a separation film with low shear stress

values, which is expressed by a decrease in the friction coefficient with increasing load. Determination of the microhardness of CrCN coatings by the Vickers method leads monotonic decrease in values with increasing load on the indenter. The microhardness parameters of the coatings are reduced three times with the load increasing from 0.1 to 0.5 N. Thus, at loads of 0.25-0.5 N, the coating is impressed into the material of the steel substrate. However, carrying out measurements with these loads makes it possible to establish a modifying effect of high-hard coatings, since the microhardness of the steel substrate is no more than 2-3 GPa.

4. Conclusion.

Based on the obtained data, it is established that the microhardness values of steel substrates are in the range from 2,400 to 3,000 MPa and do not depend on the load on the diamond pyramid. The microhardness values of chromium carbonitride coatings decrease monotonically with increasing load on the diamond pyramid. This effect is due to the indentation of the coating in the structure of the steel substrate material. The adhesion characteristics of CrCN coatings are 1.8-2 times higher than the adhesive characteristics of vacuum chrome ones. The tribological characteristics of CrCN coatings are investigated. It is shown that diffusion of carbon into the friction zone and formation of a separation film with low shear stresses is possible, which is expressed by a decrease in the friction coefficient with increasing load.

Bibliography:

1. Novye materialy i tekhnologii, primeniaemye pri proizvodstve kardannykh peredach [Tekst]/ V. I. Kravchenko, V. A. Struk, G. A. Kostiukovich, E. V. Ovchinnikov // Vestnik Belorussko-Rossiiskogo universiteta. – 2006. – № 4 (13). – S. 91-99.
2. Kompozitsionnye pokrytiia na osnove elektroliticheskogo khroma, modifitsirovannogo ul'tradispersnym uglerodom / S.D. Leshchik, A.I. Mamonchik, V.A. Struk, E.V. Ovchinnikov // Problemy i puti realizatsii nauchno-tekhnicheskogo potentsiala voenno-promyshlennogo kompleksa: Tezisy dokladov mezhdunarodnoi konferentsii, Kiev, 15-17 marta 2000 g. Kiev, 2000. – S. 98 - 99.3 .
3. Funktsional'nye nanokompozitsionnye materialy dlia konstruktsii kardan-nykh peredach [Tekst] / V. I. Kravchenko, G. A. Kostiukovich, V. A. Struk, E. V. Ovchinnikov // Trans and motoauto'04: Proceedings of International conference, Plovdiv, 14 – 17 oct. 2004. / Scientific-technical union of mechanical engineering of Bulgaria; editor: D. Damianov. – Sofia, 2004. – Vol. 2. – rr. 66-67.
4. Metallopolimernye pokrytiia na osnove modifitsirovannogo khroma i ftorsoderzhashchikh oligomerov / A.I. Mamonchik, E.V. Ovchinnikov, S.D. Leshchik, A.F. Sen'ko // Materialy. Tekhnologii. Instrumenty. - 1998. – T.3, №2. – S.101
5. Tribotekhnicheskie kharakteristiki kompozitsionnykh mnogosloinykh pokrytii [Tekst] / E. V. Ovchinnikov, S. D. Leshchik, V. A. Struk, O. V. Kholodilov, D. I. Fedorov // Trenie i iznos. – 2000. – T. 21, № 2. – C. 147-155.
6. Ovchinnikov, E. V. Tonkie plenki ftorsoderzhashchikh oligomerov: osnovy sinteza, svoistva i primenenie [Tekst] / E. V. Ovchinnikov, V. A. Struk, V. A. Gubanov. – Grodno: GGAU, 2007. – 326 s.
7. Kelly PJ, Arnell RD (2000)Magnetron sputtering: a review of recent developments and applications. Vacuum 56:159–172
8. Majzoobi GH, Hojjati R, NematianM, Zalnejad E, Ahmadkhani AR, Hanifepoor E (2010) A new device for fretting fatigue testing. Trans Indian Inst Metals 63(2–3):493–497
9. Chunyan Y, Linhai T, Yinghui W, Shebin W, Tianbao L, Bingshe X (2009) The effect of substrate bias voltages on impact resistance of CrAlN coatings deposited by modified ion beam enhanced magnetron sputtering. Appl Surf Sci 255:4033–4038
10. .Khimicheskii entsiklopedicheskii slovar'. - Pod red. Knuniants I.L. - M.: Sovetstkaia entsiklopediia, 1983. – s.793.
11. Akhmatov A.S. Molekuliarnaia fizika granichnogo treniia. – M.: «Fizmatgiz», 1963, 472 s.
12. Musokhranov M. V., Antoniuk F. I. , Kalmykov V. V. Poverkhnostnaia energiia i protsess skhvatyvaniia kontaktiruiushchikh poverkhnostei Nauka i Obrazovanie. MGTU im. N.E. Baumana. Elektron. zhurn. 2014. № 11. S. 45–51.
13. 1. CSM INSTRUMENTS. Tekhnicheskoe opisanie. Mikro Skretch Tester (MST 2) [Elektronnyi resurs] / OOO «Nienshants-Saintifik». – Rezhim dostupa: http://lab-nnz.ru/wp-content/uploads/02-MST2_Technical-Features_2011-RUS.pdf. – Data dostupa: 29.11.2016.
14. Tribotekhnicheskii mekhanizm deistviia epilamov pri trenii. 2. Tribotekhnicheskie kharakteristiki epilamirovannykh materialov / I.I. Garbar [i dr.] // Trenie i iznos. − 1990. − T. 11. − №6. − S. 987-996.
15. Poplevich, V.I. Zashchitnaia effektivnost' ftorirovannykh karbonovykh kislot / V.I. Poplevich // Khimiia i tekhnologiia topliv i masel. - 1990.- №8. – S. 22-23.